



UNIVERSITÄT ZU LÜBECK

Aus dem

Institut für systemische Entzündungsforschung

der Universität zu Lübeck

Direktor: Prof. Dr. med. Jörg Köhl

**Der Einfluss zirkadianer Rhythmen auf die
Entwicklung des experimentellen allergischen
Asthmas**

Inauguraldissertation

zur Erlangung der Doktorwürde

der Universität zu Lübeck

- Aus der Sektion Medizin -

vorgelegt von

Julia Kilian

aus Altdöbern

Lübeck 2021

1. Berichterstatter: Prof. Dr. med. Jörg Köhl

2. Berichterstatter: Priv.-Doz. Dr. med. Christian Rose

Tag der mündlichen Prüfung: 7.6.2022

Zum Druck genehmigt. Lübeck, den 7.6.2022

- Promotionskommission der Sektion Medizin -

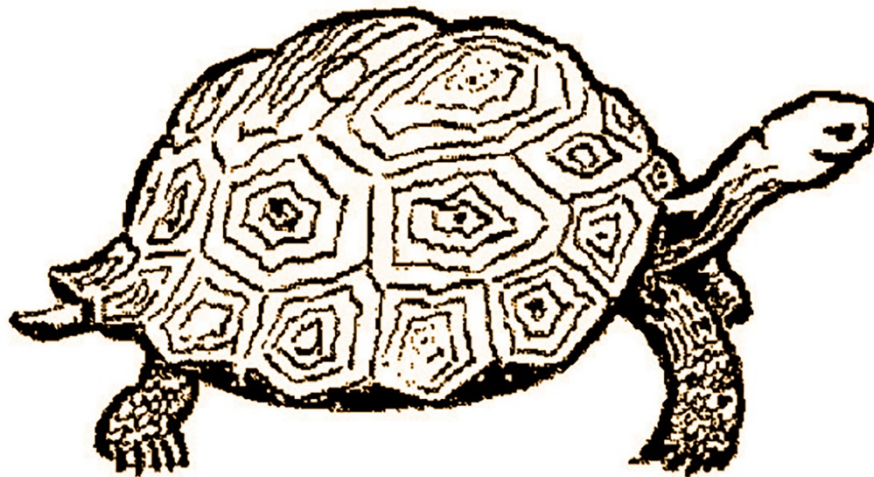
Declaration of Authorship

I hereby declare that I have authored this thesis independently, that I have not used other than the declared sources/resources, and that I have explicitly marked all material that has been quoted either literally or by content from the used sources. According to my knowledge, the content or parts of this thesis have not been presented to any other examination authority and have not been published.

Copenhagen, 10 August 2021

.....

Julia Kilian



„Es gibt ein großes und doch ganz alltägliches Geheimnis. Alle Menschen haben daran teil, jeder kennt es, aber die wenigsten denken je darüber nach. Die meisten Leute nehmen es einfach so hin und wundern sich kein bisschen darüber. Dieses Geheimnis ist die Zeit.“

aus ‚Momo‘

Michael Ende ^{1,2}

Table of Contents

1	Abstract	1
1.1	Abstract.....	1
1.2	Zusammenfassung	3
2	Introduction.....	8
2.1	Allergic asthma.....	9
2.1.1	A short overview about asthmatic phenotypes	9
2.1.2	Definition and clinical symptoms of allergic asthma	10
2.1.3	Pathophysiology of allergic asthma	11
2.1.4	The central role of pulmonary antigen-presenting cells in allergic asthma.....	19
2.1.5	The role of complement in allergic asthma	23
2.2	Circadian rhythms	28
2.2.1	The molecular clock	28
2.2.2	Circadian rhythms in the healthy lung	30
2.2.3	Circadian rhythms in allergic asthma	31
2.3	Mouse models in allergic asthma and circadian rhythm research	
	33	
2.3.1	Mice in experimental allergic asthma	34
2.3.2	Mice in circadian experiments.....	35
2.4	Aims of the project.....	36
3	Materials and Methods.....	38
3.1	Overview of materials.....	38
3.1.1	Mice and mouse keeping	46
3.1.2	Software	48
3.2	Methods	50

3.2.1	Activity analysis by infrared scan analysis	50
3.2.2	Induction of the asthmatic phenotype	52
3.2.3	Lung function measurement (AHR)	54
3.2.4	Mouse preparation and cell isolation.....	55
3.2.5	Flow cytometry	57
3.2.6	Analyzing the cytokine profile.....	66
3.2.7	Histology	68
3.2.8	Statistical analysis	70
4	Results.....	73
4.1	The circadian rhythm regulates the steady-state distribution of pulmonary APCs.....	73
4.1.1	Pulmonary macrophages and cDC2s fluctuate inversely in steady-state conditions	74
4.1.2	Impact of C5aR1-deficiency on circadian activity.....	75
4.1.3	The C5a/C5aR1 axis drives the circadian oscillations of pulmonary APCs	77
4.2	The time of allergen sensitization impacts on the immune cell recruitment into the airways and the lung.....	79
4.2.1	Allergen sensitization at ZT15 results in a strong recruitment of neutrophils into the airways	80
4.2.2	Impact of allergen sensitization during the resting or activity phase on the production of cytokines in the airways	81
4.2.3	Impact of one-time HDM immunization at ZT3 or ZT15 on pulmonary immune cells.....	83
4.2.4	Naïve and memory T cell migration into the lungs increases after HDM administration at ZT3	83
4.3	The impact of repeated HDM immunization during the resting or activity phase on the development of the allergic phenotype	86

4.3.1	Repeated HDM administration at ZT15 enhances the activity level and reduces it when given at ZT3.....	86
4.3.2	The airway resistance increases after immunization at ZT3 and ZT15.....	93
4.3.3	Strong airway inflammation in response to repeated HDM immunization at ZT3 and ZT15.....	94
4.3.4	Repeated HDM immunization at ZT3 results in higher numbers of pulmonary macrophages and neutrophils as compared to immunization at ZT15	96
4.3.5	Similar pulmonary migration of T cells at ZT3 and ZT15..	96
4.3.6	Increased number of T cells in the draining lymph nodes after repeated HDM immunization at ZT3.....	97
4.3.7	Increased frequencies of Th2, Th17 and Treg cells upon HDM immunization at ZT3 and/or ZT15.....	102
4.3.8	Increased pulmonary IL-13, IL-17 and IFN- γ production in response to HDM treatment at ZT3	104
4.3.9	Minor production of Th2 cytokines in the airways after HDM treatment at ZT3 and ZT15.....	105
4.3.10	Increased mucus production in response to HDM treatment at ZT3	106
5	Discussion	108
5.1	The circadian rhythm regulates immune cell distribution in the lungs at steady state	109
5.1.1	The C5a/C5aR1 axis contributes to circadian-driven pulmonary sensitivity	113
5.1.2	The time of allergen sensitization impacts on the development of airway and pulmonary inflammation	116

5.1.3	The allergic phenotype in response to repeated allergen exposure during the sleeping phase is stronger as compared with exposure during the activity phase.....	121
5.2	Allergic asthma interrupts the regular sleep-wake cycle.....	127
6	References	131
7	Appendix.....	155
7.1	Supplementary material.....	155
7.2	List of abbreviations	166
7.3	List of figures	170
7.4	List of tables	172
8	Acknowledgments.....	174
9	Curriculum vitæ.....	176

1 Abstract

1.1 Abstract

The worsening of asthmatic symptoms in the early morning is well appreciated. Recently, the molecular basis for circadian rhythms were discovered. Since then, inner clock-driven rhythms became the focus also in immunological research. In this thesis, I have investigated the impact of circadian rhythms on immune cell migration and function in the course of allergic asthma in a mouse model as a first step to better understand the circadian fluctuation in asthmatic symptoms in humans.

First, changes in the number of antigen-presenting cells in the airways and the lung of naïve mice were investigated. I found an inverse fluctuation of pulmonary macrophages and migratory CD11b⁺ conventional dendritic (cDC2) cells with macrophages peaking during the activity phase and the cDC subset during the resting phase. This immune cell pattern might be of great importance for the immune response in response to allergen exposure. Interestingly, I also observed a significant impact of the complement cleavage fragment, the C5a anaphylatoxin, on steady-state fluctuation of immune cells.

In a house dust mice-induced asthma model, I examined the influence of allergen exposure during the resting or activity phase on the sensitization and effector phase of allergic asthma. During sensitization, T cell numbers in the lung increased following allergen administration during the resting time. Further, the eosinophil-attracting cytokine IL-5 and the neutrophil-attractor CXCL1 increased in the airways.

Repeated allergen exposure during the resting phase resulted in a more severe phenotype as compared with allergen administration during the activity phase as evidenced by a stronger mucus production and increased airway hyperresponsiveness. Assessing the physical activity, I found physical exhaustion predominantly in mice immunized during the resting phase. At the cellular level, I found a higher frequency of different

1 Abstract

T cell subsets in the draining lymph nodes but not in the lung after allergen exposure during the resting as compared with the activity phase. Pulmonary T cells after HDM-immunization were mainly Th2, Th17 and T_{reg} cells. Of note, pulmonary IL-13, IL-17 and IFN- γ production was much higher after HDM exposure during the resting as compared with the activity phase.

In summary, my findings demonstrate a circadian rhythm of immune cells that is regulated, at least in part, by the C5a/C5aR1 axis. Allergen exposure during the activity or resting phase has a distinct impact on the development of the allergic phenotype. My findings suggest that exposure during the resting phase results in a stronger allergic phenotype than allergen contact during the activity phase. Thus, reduction of repeated allergen exposure during the nighttime sleep may help to reduce the development of allergic asthma in genetically susceptible individuals, provided that the findings in the mouse model can be transferred to the human situation.

1.2 Zusammenfassung

Schon seit vielen Jahren sind Tag-Nacht-Schwankungen in den Kardinalsymptomen des allergischen Asthmas bekannt. Hierbei handelt es sich um eine chronisch-entzündliche Atemwegserkrankung, bei der es zu einer reversiblen Obstruktion des Bronchialsystems durch Allergene kommt. Die Kardinalsymptome sind Bronchospasmus, vermehrte Produktion von zähem Schleim, Becherzellhyperplasie sowie Hypertrophie der glatten Muskelzellen. Hinzu kommen wiederkehrende Beschwerden mit Giemen und Brummen, Husten sowie Luftnot. Für eben diese wurde eine deutliche Zunahme in den frühen Morgenstunden schon seit langer Zeit beobachtet. In den letzten Jahren wurde hierzu intensiv Forschung betrieben, nachdem die molekulare Grundlage für biologische Rhythmen festgeschrieben im zellulären Genom nachgewiesen werden konnte. Eine zentrale innere Uhr im ventralen Teil des Hypothalamus, dem sog. suprachiasmatischen Kern, stellt hierbei die übergeordnete Organisationseinheit dar. Im Laufe der letzten Jahre konnten zudem immer mehr lokale, organ- oder zellbezogene, sog. periphere Uhren nachgewiesen werden. Die bisher beobachteten Tag-Nacht-Schwankungen in Krankheitssymptomen schienen somit nicht länger nur von Hormonschwankungen oder Lichtverhältnissen abzuhängen, vielmehr gab es auf molekularer Ebene Kreisläufe, die für eine Anpassung an sog. zirkadiane, also 24-Stunden-Rhythmen sorgen. Auch im allergischen Asthma wurden mehr und mehr solcher zirkadianen Rhythmen nachgewiesen. Ziel dieser Arbeit war, ein besseres Verständnis zu erlangen bezüglich der zirkadianen Fluktuation von Immunzellen in den Atemwegen, der Lunge und den drainierenden Lymphknoten und dem möglichen Einfluss dieser zirkadianen Rhythmik der Immunzellen auf die Entwicklung des allergischen Phänotyps nach einmaliger oder mehrmaliger pulmonaler Exposition mit dem Hausstaubmilben-Allergen. Ein bewährtes Model in der Asthmaforschung als auch der Chronobiologie ist der Mausorganismus, welcher auch in dieser Arbeit genutzt wurde.

1 Abstract

Hierbei können die durchgeführten Versuche in drei große Blöcke unterteilt werden. Zuerst habe ich die grundlegenden Rhythmen von Immunzellen in den Atemwegen und im Lungengewebe im Abstand von sechs Stunden (*circadian time* (CT) 3, 9, 15 und 21) mittels Durchflusszytometrie untersucht. Um sämtlichen Einfluss sog. äußerer Taktgeber wie Licht und Geräusche zu vermeiden, fand dieses Experiment in kompletter Dunkelheit statt. In einem weiteren Schritt habe ich den Einfluss des Komplementsystems auf die zirkadiane Rhythmik der Immunzellen untersucht, da dieses System eine wichtige Rolle bei der Entwicklung des allergischen Asthmas spielt und zudem einer zirkadianen Rhythmik folgt. Im zweiten und dritten experimentellen Block wurden die Mäuse dann mit Hausstaubmilbenextrakt immunisiert, wobei es sich hier um ein etabliertes Verfahren zur Induktion von allergischem Asthma in Modellorganismen handelt. Diese Experimente wurden in geregelten Hell-Dunkel-Bedingungen durchgeführt. Es wurden die zwei Zeitpunkte gewählt, bei welchen die deutlichsten Unterschiede in Bezug auf die zirkadiane Fluktuation von Immunzellen festgestellt wurden (*Zeitgeber time* (ZT) 3 und 15). Zunächst erfolgte zur Analyse der Sensibilisierungsphase eine einmalige Immunisierung, wonach Lungengewebe und die bronchoalveoläre Lavage-Flüssigkeit mittels Durchflusszytometrie untersucht wurden. Zudem habe ich die Zytokinproduktion in den Atemwegen untersucht. Im dritten Experimentalblock erfolgte die viermalige Immunisierung mit Hausstaubmilbenextrakt, wodurch sich ein starker asthmatischer Phänotyp entwickelte. Es erfolgte eine Lungenfunktionsmessung der Versuchs- und Kontrollgruppen, wonach Lungen- und Lymphgewebe sowie bronchoalveoläre Flüssigkeit erneut mittels Durchflusszytometrie näher untersucht wurden. Um ein genaueres Bild der adaptiven Immunantwort zu erhalten, habe ich T Effektorzellen einer intrazellulären Färbung unterzogen, und die Bildung spezifischer Th1, Th2, Th17 und T_{reg} Zytokine und Transkriptionsfaktoren bestimmt. Zudem wurde die Produktion von Th1, Th2 und Th17 Zytokinen in den Atemwegen und im

1 Abstract

Lungengewebe untersucht. Zuletzt habe ich in Lungengewebeproben mittels Periodsäure-Schiff-Färbung die Mukusproduktion analysiert. Über das gesamte Experiment erfolgte ebenfalls eine infrarottechnische Überwachung des Bewegungsprofils der Versuchstiere, um mögliche Wechselwirkung zwischen der Entwicklung eines asthmatischen Phänotyps und dem Schlaf-Wach-Rhythmus der Mäuse aufzudecken.

Die hier durchgeführten Versuche zeigten einen deutlichen chronobiologischen Einfluss in der Entstehung und Ausprägung des allergischen Asthmas. Bereits im Grundzustand konnte ich zirkadiane Schwankungen von pulmonalen antigen-präsentierenden Zellen nachweisen. Es zeigte sich eine gegenläufige Fluktuation von pulmonalen Makrophagen und CD11b⁺ konventionellen dendritischen Zellen (cDC2). Interessanterweise zeigten die Makrophagen einen starken Anstieg zum Zeitpunkt CT15 in der frühen Aktivitätsphase; im Gegensatz dazu war die Anzahl an cDC2s in der frühen Ruhephase (CT3) am höchsten. cDC2 sind ein Subtyp der dendritischen Zellen, welcher besonders für die asthmaspezifische Initiierung einer Th2-Immunantwort nach Allergenkontakt in den Lymphknoten wichtig ist, während Makrophagen eine mehr allgemeine immunologische Abwehreinheit darstellen und beim allergischen Asthma eine eher regulatorische Rolle wahrnehmen. Die zirkadiane Rhythmik der Makrophagen wird über das Komplementsystem, genauer, das Anaphylatoxin C5a reguliert, da C5aR1-*Knock out*-Mäuse keine rhythmischen Schwankungen der Makrophagen zeigten. Auffallend war, dass in diesen Tieren eine Fluktuation von eosinophilen Granulozyten zu messen waren mit hohen Zellzahlen während der Ruhephase zu den Zeitpunkten CT3 und CT9. Das Fluktuationmuster der cDC2s wurde etwas verschoben und ihr Maximum war nun gegen Ende der Ruhephase zum Zeitpunkt CT9 nachweisbar.

Im zweiten Versuchsblock konnte ich Unterschiede in der Immunantwort nach einmaliger Allergenexposition während der Ruhe- bzw. der Aktivitätsphase der Mäuse feststellen. In den Atemwegen fand ich eine deutliche neutrophile Immunantwort ausschließlich nach

1 Abstract

Allergenexposition in der Aktivitätsphase zum Zeitpunkt ZT15. Hingegen zeigte sich eine verstärkte Produktion des Th2 Zytokins IL-5 sowie des Neutrophilen-Chemoattractants CXCL1 vor allem nach Allergenstimulation während der Ruhephase (ZT3). Zudem fand ich eine höhere Anzahl pulmonaler eosinophiler Granulozyten und verschiedener T Zell Subsets nach Immunisierung während der Ruhephase (ZT3). Diese Befunde legen eine zeitabhängige Initiation der Immunantwort während der initialen Allergensensibilisierung nahe.

Im abschließenden Experimentalblock habe ich dann den Einfluss der wiederholten Allergenexposition während der Ruhe- oder Aktivitätsphase auf die Ausbildung des allergischen Phänotyps untersucht. Hierbei zeigte sich eine signifikant stärkere Atemwegshyperreagibilität nach Exposition während der Ruhephase. Auch zeigten histologische Analysen eine deutlich erhöhte Mukusproduktion in den Alveolen. Auf zellulärer Ebene fand ich eine verstärkte neutrophile Immunantwort in den Atemwegen und der Lunge nach Allergenexposition in der Ruhephase, entgegengesetzt zu den Beobachtungen nach einmaligem Allergenkontakt. Zudem kam es zu einer deutlich vermehrten Einwanderung verschiedener T Zell Subsets in die mediastinalen Lymphknoten nach wiederholter pulmonaler Allergenstimulation in der Ruhephase im Vergleich zur Aktivitätsphase. In der Lunge konnte ich eine erhöhte Frequenz von Th2, Th17 und Treg Zellen nach wiederholter Allergenexposition beobachten, die allerdings unabhängig vom Zeitpunkt der Immunisierung war. Interessanterweise fand ich eine deutlich vermehrte pulmonale Zytokinproduktion der Th2 Zytokine IL-13 und IL-17 sowie des Th1 Zytokins IFN- γ nach Allergenstimulation in der Ruhephase. Auch in den Atemwegen wurden nach wiederholter Allergenexposition vermehrt die Th2 Zytokine IL-5 und IL-10 gebildet, wobei die IL-10-, nicht jedoch die IL-5 Konzentrationen nach Exposition in der Ruhephase höher waren als in der Aktivitätsphase. Zudem zeigten sich hohe Level an CXCL1, die tendenziell höher waren nach Allergenexposition in der Ruhephase. Diese Unterschiede im

1 Abstract

asthmatischen Phänotyp nach Allergenexposition während der Ruhe- oder Aktivitätsphase waren assoziiert mit deutlich veränderten Aktivitätsmustern der untersuchten Individuen. Versuchstiere, welche während ihrer Ruhephase mit Allergenen in Kontakt kamen, entwickelten ein deutlich reduziertes Aktivitätspotential, während die andere Versuchsgruppe, immunisiert während ihrer Aktivitätsphase, deutlich verstärkte Bewegungsmuster zeigten. In beiden Gruppen wurde ebenfalls deutlich, dass die eigentliche Ruhephase im Vergleich zum Zeitraum vor dem allerersten Allergenkontakt viel häufiger durch vermehrtes Aufwachen unterbrochen wurde.

Zusammenfassend haben die von mir durchgeführten Experimente gezeigt, dass es in der Pathophysiologie des allergischen Asthmas eine direkte Verbindung zwischen dem Zeitpunkt des Allergenkontaktes und dem entstehenden Phänotyp gibt. Diesem Phänomen scheinen zirkadiane Schwankungen in der Anzahl verschiedener Immunzellen des angeborenen sowie adaptiven Immunsystems in den Atemwegen und dem Lungengewebe zugrunde zu liegen. Meine Daten legen nahe, dass ein Antigen auf unterschiedlich suszeptibles Immunsystem mit einem mehr oder minder stark ausgeprägten allergischen Potential trifft, je nachdem zu welchem Zeitpunkt das Allergen inhaliert wird. Diese neuen Erkenntnisse zur zirkadianen Rhythmik von Immunzellen und deren Auswirkung auf die Entwicklung eines allergischen Phänotyps könnten evtl. helfen, die Allergensensibilisierung in suszeptiblem Patienten zu reduzieren. Zudem bietet diese Arbeit Ansatzpunkte für zukünftige Forschung, in der weitere, durch die innere Uhr kontrollierte Mechanismen in der Pathophysiologie des allergischen Asthmas aufgedeckt werden können.

2 Introduction

Over the past decades, allergic asthma became more and more prevalent in our society with severe health and economic consequences. Around 10 million people under the age of 40 years are diagnosed with asthma in Europe, leading to estimated €72 billion health care costs every year ³. In Germany, the lifetime prevalence of asthma is about 8.6% with an increase of 3% within 10 years ⁴. In light of intense research, morbidity and mortality rates were reduced over the last years. There are effective therapeutics, e.g. β_2 -sympathomimetics and glucocorticoids that prevent and stop asthmatic symptoms, such as wheezing or shortness of breath, and reduce airway swelling, which causes the life-threatening asthma attacks. The medication depends on the disease severity, which is classified into four levels. Less severe cases are treated with short-lasting emergency medication in the case of acute attacks, so-called relievers. More severe cases receive medication with a long-lasting effect on a daily basis, so-called controllers, on top. Here, the frequency of night attacks is an important read-out to check the grade of asthma control with or without asthma medication ⁵.

Over 75% of asthmatic patients wake up at night due to coughing or dyspnea at least once per week, while 40% have these symptoms on a daily basis ⁶. In line with these data, Gervais and colleagues described a 24h rhythm in bronchial hyperreactivity upon challenge with house dust mite (HDM) extract. The FEV₁ describing the allergen's effect on bronchial construction peaked at 11 p.m. and reached its trough at 8 a.m. ⁷. Intense research in the field of chronobiology within the last decades helped to understand the molecular mechanisms underlying circadian rhythms in the human body. Recent findings even suggest a central role for the circadian clock in the regulation of allergic reactions ⁸.

2.1 Allergic asthma

Our immune system defends the body against potentially dangerous microbes, bacteria, viruses and parasites. It comprises humoral and cellular systems that protect the body from the pathogen invasion by a range of defense mechanisms. These pathways are highly regulated to avoid overreactions against autologous cells or harmless substances. If this regulation is disturbed, autoimmune diseases can develop, in which defective self-tolerance results in cell and organ destruction, or allergies, where harmless molecules can activate the defense machinery ^{9,10}.

2.1.1 A short overview about asthmatic phenotypes

Historically, asthma has been subdivided into two variants: allergic (extrinsic) and non-allergic (intrinsic) asthma ¹¹. Extrinsic asthma was defined by the occurrence of specific serum immunoglobulin (Ig) E and the direct relation between asthma symptoms and allergen contact. Furthermore, extrinsic asthma developed at young age ¹². In contrast, neither specific IgE levels nor the influence of allergens was seen in intrinsic asthma. Also, it first developed mainly in people older than 40. It turned out that the division into two groups was way too simple, as increasing evidence was found suggesting similar pathophysiological pathways ¹³. For example, Humbert et al. measured increased levels of the IgE-promoting cytokine IL-4 and the eosinophil-mobilizing cytokine IL-5 in asthmatic individuals, irrespective of the presence of allergies or not.

Today, scientists and clinicians have defined a more detailed classification system that helps to better understand origin, symptoms and improve therapy strategies. The current understanding of the different asthmatic phenotypes in light of clinical and physiological features, pathobiology and biomarkers, genetics and therapy targets are outlined in Table 2-1 ^{12,14}. It is well appreciated, that these phenotypes are altered by

2 Introduction

confounders describing independent risk factors that worsen or improve the asthmatic course ¹⁵. They include active and passive smoking ¹⁶, female sex hormones ¹⁷, viral and bacterial contact ^{18,19} and occupational compounds ²⁰.

	Natural history	Clinical and physiological features	Pathobiology and biomarkers	Genetics	Response to therapy
Early-onset allergic	Early onset; mild to severe	Allergic symptoms and other diseases	Specific IgE; T _H 2 cytokines; thick SBM	17q12; T _H 2-related genes	Corticosteroid-responsive; T _H 2-targeted
Late-onset eosinophilic	Adult onset; often severe	Sinusitis; less allergic	Corticosteroid-refractory eosinophilia; IL-5	?	Responsive to antibody to IL-5 and cysteinyl leukotriene modifiers; corticosteroid-refractory
Exercise-induced		Mild; intermittent with exercise	Mast-cell activation; T _H 2 cytokines; cysteinyl leukotrienes	?	Responsive to cysteinyl leukotriene modifiers, beta agonists and antibody to IL-9
Obesity-related	Adult onset	Women are primarily affected; very symptomatic; airway hyperresponsiveness less clear	Lack of T _H 2 biomarkers; oxidative stress	?	Responsive to weight loss, antioxidants and possibly to hormonal therapy
Neutrophilic		Low FEV1; more air trapping	Sputum neutrophilia; T _H 17 pathways; IL-8	?	Possibly responsive to macrolide antibiotics

Table 2-1: Asthma phenotypes

This overview outlines the current knowledge about asthma phenotypes. They are divided into early-onset allergic, late-onset eosinophilic, exercise-induced, obesity-related and neutrophilic asthma. To each phenotype, the natural history, clinical and physiological features, pathobiology and biomarkers, known genetics as well as therapeutic targets are summarized. SBM = subepithelial basement membrane, FEV1 = forced expiratory volume in 1 second, ? = not finally clarified. Republished and modified with permission of Springer Nature from 'Asthma phenotypes: the evolution from clinical to molecular approaches' ¹²; permission conveyed through Copyright Clearance Center, Inc.

2.1.2 Definition and clinical symptoms of allergic asthma

Allergic asthma is an example of an inappropriate, overactive immune response. It is a chronic inflammation of the airways, marked by airway hyperreactivity (AHR), mucus overproduction and recurrent episodes of wheezing, coughing, breathlessness and chest tightness, as well as airway remodeling ⁵. Allergic asthma is clinically defined by the presence of specific serum immunoglobulin E (IgE) and/or a positive skin-prick test to the major airborne allergen (e.g. HDM or pollen) as typical characters of atopy, a 'genetically determined stage of hypersensitivity to environmental allergens' ^{21,22}.

2.1.3 Pathophysiology of allergic asthma

Allergic asthma originates from an inappropriate Th2/Th17 immune response after contact to harmless environmental proteins in genetically susceptible individuals²³. For a better understanding, the disease development can be divided into the sensitization and effector phase, in which both, innate and adaptive immune responses occur. In the following, these two distinct phases are explained in detail with house-dust mite (HDM) as the allergen trigger.

2.1.3.1 Sensitization phase

When airborne allergen such as the HDM allergen enters the airways in genetically susceptible individuals, they meet the airways epithelial layer first (Figure 2-1, p. 12). It was shown, that the epithelial layer in asthmatic individuals suffers from dysfunctional tight and adherent junctions which facilitates the intrusion of allergens²⁴. The dysfunction of the epithelial cell layer might result from previous damage through respiratory viruses²⁵ or tobacco smoke that also downregulate tight and adherent junctions. Further, such insults induce the production of reactive oxygen species^{26,27}. Additionally, the allergen's own protease activity is able to disrupt the epithelial barrier through the activation of Protease-activated receptor-2 (PAR-2)²⁸ and of pattern-recognition receptors, notably Toll-like receptor (TLR) 4^{22,23}. Thereby, damaged epithelial cells release alarmins, cytokines and chemokines, in particular thymic stromal lymphopoietin (TSLP), IL-25 and IL-33 that activate the innate immune cell network³¹. TSLP upregulates OX40L expression on DCs, a costimulatory molecule that enhances Th2 differentiation by supporting DC and T cell interaction³². IL-25 enhances the production and function of Th2 cytokines³³. During allergen sensitization, IL-33 mobilizes and activates type 2 innate lymphoid cells (ILC2) which increases the immune response³⁴. Macrophages, ILC2 as well as pulmonary dendritic cells (DC) are recruited to the airways via local chemokine production (e.g. CC-chemokine ligand (CCL) 20) by the epithelial cells. Here, the DCs play a

major role, as they bridge the innate with the adaptive immune response. They take up and process antigens to present them via their major histocompatibility complex (MHC) II to naïve T cells³⁵. In which direction the naïve CD4⁺ T cell develops depends on the type of allergen as well as the cytokine milieu established in the draining lymph nodes. Recently, a pivotal role of the ILC2 has been uncovered. These cells respond antigen-independent to environmental antigens and secrete a range of cytokines. Interestingly, they are able to transform into other ILC subsets depending on the cytokine milieu established by antigen-presenting cells (APC) and epithelial cells. Through IL-5 and IL-13 production at an early time point, before Th2 development, they induce a proinflammatory Th2 environment³⁶.

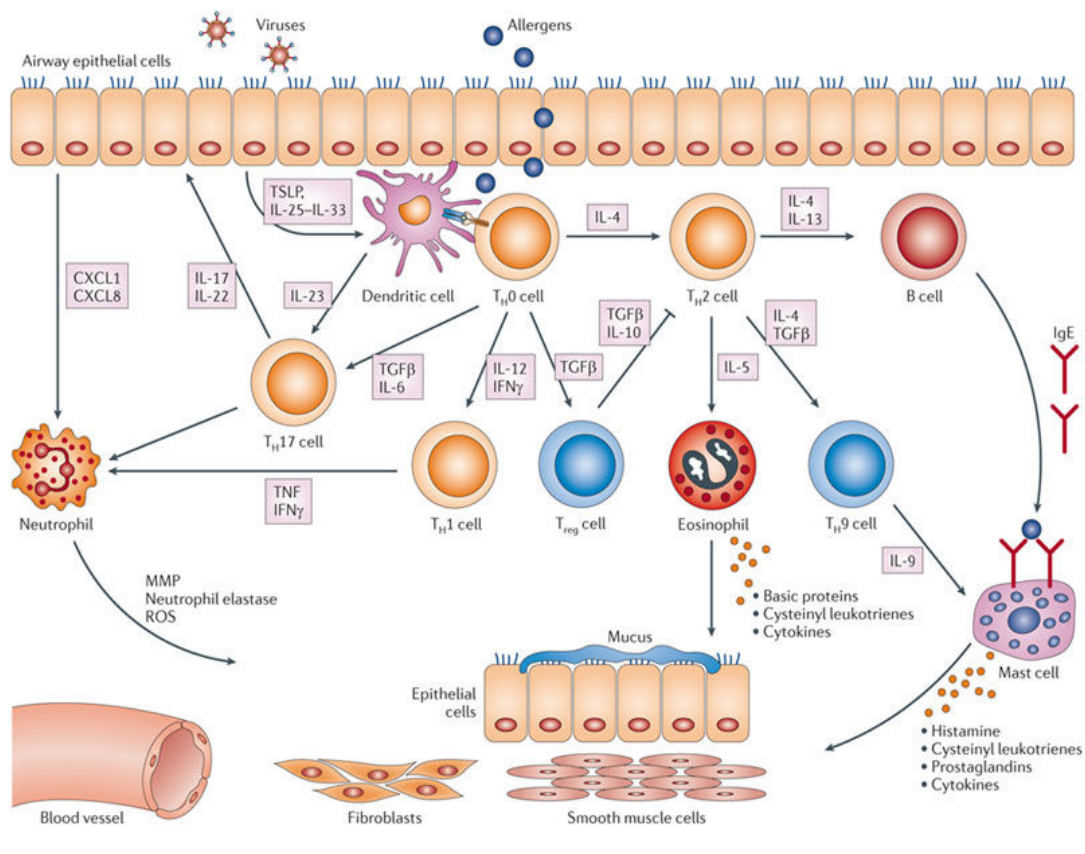


Figure 2-1: Immunopathology of allergic asthma

This figure depicts the immune response in the lung driving the allergic asthma phenotype. First, allergens enter the airways and pass the epithelial cells due to their proteolytic activity. They are recognized by APCs, especially DCs that promote the differentiation of naïve T cells into four different subsets: Th17, Th1, Th2 and T_{reg} cells. Th17 cells recruit and activate neutrophils and epithelial cells through the release of IL-17 and IL-22. Th1 cells modulate the allergic inflammation by TNF- α and

2 Introduction

IFN- γ release regulating neutrophils. Th2 cells are most important, as they drive the inflammation through the release of pro-inflammatory cytokines such as IL-4 and IL-13, which activate the antibody switch into IgE-producing B cells. IL-5 mobilizes and activates eosinophils; IL-4 and TGF β indirectly drive mast cell activation. The T_{reg} cells can suppress Th2 cell activation through IL-10 and TGF β release. Together these immune responses result in thickening of smooth muscle cells, growth of myofibroblasts and mucus overproduction, leading to the asthmatic phenotype. See text for further details. Republished with permission of Springer Nature from 'The potential of biologics for the treatment of asthma'³⁷; permission conveyed through Copyright Clearance Center, Inc.

2.1.3.2 Effector phase in allergic asthma

Once HDM has been processed by pulmonary DCs, it is finally presented to naïve T cells. The epithelium-derived cytokines TSLP, IL-25 and IL-33 also support the effector phase as they boost the function of basophils, eosinophils and mast cells as well as help to establish a Th2 memory³⁸. In the following section, I will provide a detailed overview about important T cell subsets in allergic asthma that is summarized in Figure 2-2, p. 15.

Th2 differentiation

The cytokine IL-4 is required to polarize Th2 cell differentiation. After initial activation, IL-4 is locally produced by the T cell itself and amplifies the signal transducer and activator of transcription 6 (Stat6) and the transcription factor GATA3 driving Th2 differentiation^{39,40}. However, there are no DC equivalents known that produce IL-4 and thereby initiate Th2 differentiation. Stephen Holgate introduced the following concepts of IL-4 origin³⁸. First, a cytokine milieu leaking the presence of IL-12 and IFN- γ may induce Th2 differentiation (so-called default program)⁴¹. IL-12 can be generated by macrophages, monocytes, neutrophils and DCs. It is a critical driver of IFN- γ production that consecutively induces the expression of the T-box transcription factor TBX21 T-bet and Stat4, which in turn lead to Th1 cell differentiation⁴²⁻⁴⁴. Second, IL-4 might originate from basophils, as experiments with helminths showed that basophils act as APCs during the initial allergen contact and produce high levels of IL-4⁴⁵. This was later disproven and DCs were found to initiate Th2

responses whereas basophils enhance Th2 differentiation ⁴⁶. Even today, the primary origin of IL-4 still remains elusive.

Th17 differentiation

In severe cases of asthma with strong neutrophilic response, there is also an activation of Th17 cells, a third effector T cell subset besides Th1 and Th2 cells. Their differentiation is initially driven through the presence of IL-6, produced by cells from the innate immune system, and TGF- β , mainly produced by T cells and T_{reg} cells by DC induction, that activate Stat3 ⁴⁷⁻⁴⁹. Stat3 in turn induces the Th17 cell master regulator ROR γ t ⁵⁰. Th17 cells produce IL-21 that in turn propagates its own differentiation ⁵¹ and IL-23, which stabilizes Th17 responses ⁴⁷.

Th22 differentiation

When naïve effector T cells interact with plasmacytoid DCs, the first step is done to develop into Th22 cells. This recently discovered subset produces IL-22, but not IL-17 or IFN- γ ⁵². In the local environment of tumor necrosis factor (TNF) and IL-6, CD4⁺ T cells differentiation is driven into the Th22 direction. Concerning the individual transcription factors that drive Th2 commitment, basonuclin (BNC) 2 and forkhead box protein O (FOXO) 4 have been identified ^{53,54}.

Th9 differentiation

Another asthma-related subtype originating from naïve T cells are Th9 cells. In the presence of IL-4 and TGF β , a range of transcriptional factors including STAT6, interferon regulator factor (IRF) 4 and GATA3 become activated and induce Th9 development ⁵⁵. The transcription factor PU.1 is of major importance as it represses Th2 development and enhances *IL9* promoter expression ^{46,47,48}.

2 Introduction

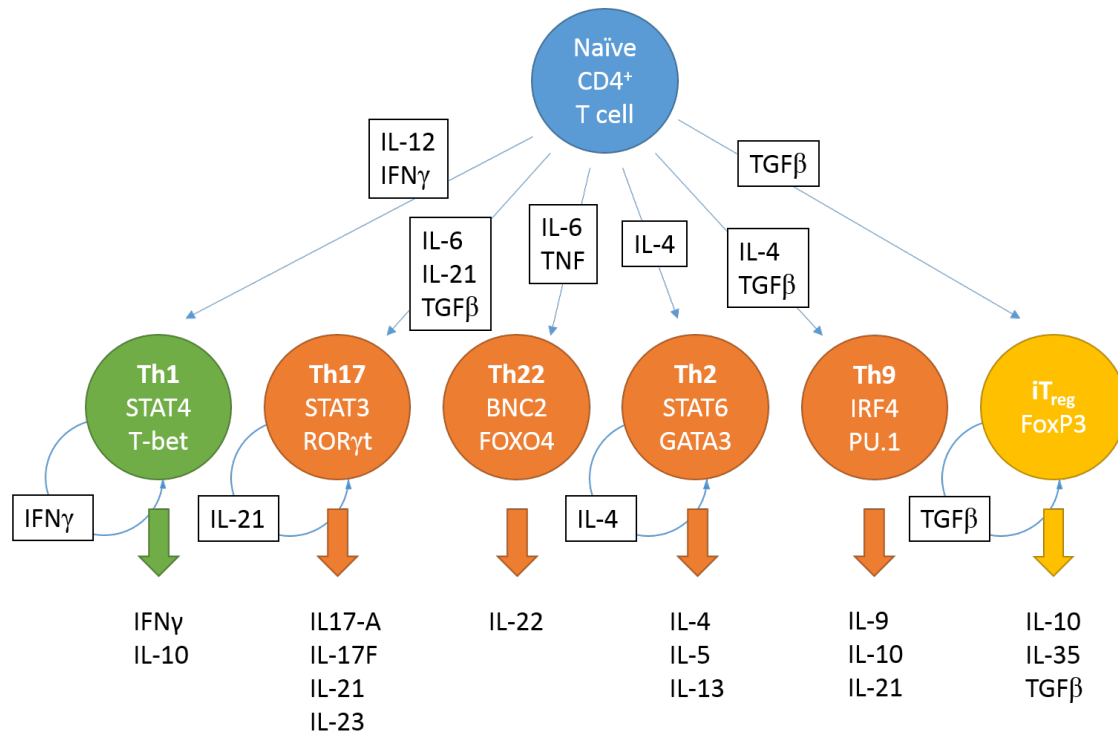


Figure 2-2: Differentiation of CD4⁺ T cells

The cartoon gives an overview about T cell differentiation in the course of allergic asthma. Originating from naïve CD4⁺ T cell, a defined set of cytokines induces (first arrow) the development defined T cell subsets. The circles show the different Th subsets and the transcription factors that drive their differentiation. Some of them drive their own development by autocrine effects of signature cytokines, highlighted by circular arrows. For each T cell subset, the produced major important cytokines are given below. For detailed information see text. Green = pro- and anti-inflammatory effect, red = predominantly proinflammatory, yellow = predominantly anti-inflammatory

Cytokine milieu at the site of inflammation

While T cells are primed in the lymph nodes, pulmonary DCs release the chemoattractants CCL17 and CCL22 which attract T cells to the inflamed airways⁵⁹. There, the several T cell subsets orchestrate the immune response through cell-specific cytokine release.

Th2 cells produce mainly IL-4, IL-5 and IL-13, which are responsible for the establishment of the asthmatic phenotype⁶⁰. As described earlier, IL-4 is of major importance for the initiation of the asthmatic phenotype by driving Th2 differentiation, however, it also stimulates IgE synthesis in B cells⁶¹. IL-5 drives not only B cell development and differentiation, it also is the main factor for mobilization, maturation and differentiation of eosinophils⁶². However, IL-5 is not only produced by Th2 cells but by the

2 Introduction

recently discovered ILC2 which also produce local eotaxin to promote eosinophil accumulation ⁶³. IL-13 is the most important cytokine during the effector phase. It induces AHR and mucus production by the induction of epithelial genes (e.g. MUC5AC and periostin resulting in mucus plugging), smooth muscle thickness by increasing sensitivity to contractile agents (e.g. acetylcholine) and rising calcium release leading to contractions, and finally sub-epithelial fibrosis by driving TGF β production in monocytes and epithelial cells that enhance fibroblast's activity ⁶¹.

Th17 cells can produce IL-17A, IL-17F as well as IL-22 in the course of severe allergic asthma leading to the recruitment of neutrophils ³⁸. IL-17A induces CXCL1 and CXCL8 secretion by binding to the IL-17R complex on epithelial cells resulting in neutrophil attraction ⁶⁴. IL-17F induces IL-6 production in smooth muscle cells and together with IL-17A and IL-22 increases airway remodeling ⁶⁴⁻⁶⁶. IL-22 is produced by a range of effector T cells, for instance Th22 cells, and has immune modulatory properties in the course of allergic asthma. It reduces eosinophilic inflammation, mucus hyperplasia, AHR and Th2 cytokine production in the lungs without influencing the systemic immune production, e.g. IFN- γ , IL-4 or IL-13 release in the spleen ⁶⁷. Supporting its proinflammatory properties, it was shown that high IL-22 levels go in line with increased IgE serum levels in asthmatic patients ⁶⁸.

Another mediating cytokine is IL-9 that is produced by Th9 cells. It has a wide-ranging impact on target cells in asthma. These include mast cell production of histamine and proteases, increased eosinophil survival, enhancement of Th2 cytokine production, broncho-constriction and goblet cell metaplasia ⁵⁵.

Finally, Th1-produced IFN γ has to be taken into account. IFN- γ is produced by natural killer (NK) and invariant natural killer T cells (NKT) during innate immune responses, as well as during the adaptive immune response by CD8⁺ cytotoxic T cells in addition to Th1 cells ⁶⁹. It was shown

that IFN- γ , despite regulating asthma development (discussed later) also enhances pro-inflammatory functions driving the chronic state. Mast cells express IFN- γ receptors whose activation enhance neutrophil and eosinophil responses, airway remodeling and asthma-related cytokine release ⁷⁰.

The humoral response

In humans, activated Th2 cells stimulate in the presence of IL-4 and IL-13 B cells to undergo a class-switch from immunoglobulin (Ig) M towards allergen-specific IgE production. Clonal B cells mature into plasma cells and produce large IgE amounts. Via binding to the high-affinity Fc ϵ receptor 1 (Fc ϵ R1), mast cell degranulation occurs in the presence of antigen ³⁸. In addition to mast cells, this high-affinity receptor is also expressed on DCs, where direct allergen contact can boost and aggravate the Th2 response ⁷¹. Mast cells are the main source of histamine and other proinflammatory molecules that are responsible for the mentioned allergic symptoms. In the early phase, they induce vasodilatation and the increased vascular permeability. Further, they stimulate bronchial remodeling and enhance mucus production through their direct impact on epithelial and vascular cells, myofibroblasts and smooth muscle cells. In response to ongoing inflammation, the epithelium is finally destroyed and collagen degraded ⁷².

Memory T cells in allergic asthma

To complete the picture about the role of T cells in allergic asthma, CD4⁺ memory T cells need to be considered. Memory T cells comprise different subsets including central memory cells, residing in the secondary lymphoid tissue, effector memory T cells, migrating between peripheral tissue, blood and spleen, as well as tissue-resident memory cells, which increase the immune system's efficacy ^{73,74}. After allergen contact, CCR7⁻ tissue-resident memory cells and CCR7⁺ central memory cells are formed and reside in the lung parenchyma and the mediastinal lymph nodes ⁷⁵. CCR7 is important to guide memory cells through lymphoid tissues.

Interestingly, CCR7⁺ central memory cells compared to their CCR7⁻ counterparts show higher proliferation and plasticity suggesting that they might be of greater importance in driving the allergic response ⁷⁵.

2.1.3.3 The anti-inflammatory immune response in allergic asthma

During the allergic response of Th2 cells, also anti-inflammatory T_{reg} cells are activated. T_{reg} cells belong to the group of CD4⁺ T cells and their main task is to protect the body from uncontrolled effector T cell activation, e.g. in autoimmune diseases ⁷⁶. They require transcription factor Forkhead Box 3 (FoxP3) for their differentiation, which is induced by TGFβ ^{77,78}. Two distinct subsets of T_{reg} cells exist: natural thymus-derived nT_{reg}, and induced, extra-thymically derived iT_{reg} cells. The nT_{reg} is important for self-tolerance while the latter controls inflammation, e.g. during chronic pulmonary and gastrointestinal diseases ⁷⁶. In inflammatory conditions, they produce IL-10, IL-35 and TGF-β that block naïve T cell differentiation into Th2 cells. The receptor protein cytotoxic T-lymphocyte-associated protein (CTLA) 4 expression and TGF-β production suppresses IgE production by inducing IgG class switch ⁷⁹. Furthermore, T_{reg} cells induce T cell apoptosis by granzyme production, inhibit IL-12 production and by that downregulate DC activation ⁸⁰. Unfortunately, their regulatory function is often limited and their numbers are reduced in allergic asthma-suffering individuals resulting in disease aggravation ⁸¹. Interestingly, recent research pointed towards a pathogenic T_{reg} response in chronic inflammation. It was shown that a polymorphic IL-4R in T_{reg} cells was reprogrammed towards 'Th17-like' T_{reg} cells by Stat3 and Stat6 activation, resulting in RORγt expression and IL-17 production ⁸².

In addition to regulatory T cells, anti-inflammatory IL-10 is also produced by Th1 cells, Th9 cells as well as by monocytes and macrophages ⁸³. The interaction of IL-10 with DCs is essential for tolerance induction and IL-10 receptor deficiency on DCs lead to excessive neutrophilic activation ⁸⁴.

Finally, the anti-inflammatory properties of IFN- γ shall be pointed out in the context of allergic asthma. This cytokine promotes Th1 and suppresses Th2 responses. They reduce eosinophil mobilization from the bone marrow, eosinophil migration to the lungs and can reduce AHR. Furthermore, IFN- γ might reduce mucus overproduction via direct effects on the epithelial cells ⁶⁸. Together with IL-4, IFN- γ may also suppress Th17 differentiation ³⁸.

2.1.4 The central role of pulmonary antigen-presenting cells in allergic asthma

Every cell in the body is able to present antigens via the MHC I receptor to cytotoxic CD8⁺ T cells. However, there are specialized antigen-presenting cells (APC), which present antigens via MHC II receptors to CD4⁺ T cells and activate these cells thereby bridging innate and adaptive immunity. In humans and mice, DCs and macrophages are important cell subsets for antigen presentation ⁸⁵. In the following section, the focus will be on pulmonary APC subsets in mice and their roles for the development of allergic asthma.

2.1.4.1 Dendritic cells

DCs play the major role in the development of maladaptive Th2/Th17 immune responses by bridging innate and adaptive immunity. Pulmonary DCs are phenotypically and functionally sub-specialized. Some DCs reside in the lungs in steady state, while others migrate upon inflammation. Up to now, four subsets have been described, distinguished by their specific surface marker expression: CD11b⁺ conventional DCs (cDC2), CD103⁺ cDCs (cDC1), plasmacytoid DCs (pDC) and monocyte-derived DCs (moDC) that migrate into the lungs upon inflammation. DC activation is regulated by their interaction with lung epithelial cells through cytokine release by epithelial cells (EC) after allergen contact ⁸⁶.

2 Introduction

The cDC subsets are the most important in allergen uptake, processing and presentation to naïve CD4⁺ T cells. Here, the cDC1 subset is localized directly under the pulmonary epithelium, where they spread their dendrites into the alveolar lumen through the epithelial layer and express high amounts of tight junction proteins, e.g. Claudin-1 and -7, to stabilize interconnections (Figure 2-3, p. 21) ^{23,87}. cDC2s seem to be widely distributed in the pulmonary tissue, perivascular and around the airways ⁸¹.

Concerning their roles in allergic asthma, the available data suggest that cDC1s are more relevant in sampling allergens due to their ability to build tight junctions with the airway epithelium ⁸⁷. Previously, it was reported that cDC1s drive Th2 responses efficiently by antigen uptake and migration towards lymph nodes in a murine model for OVA-sensitized allergic asthma ⁸⁹. Controversially, Platinga et al. found that cDC1s have a minor importance in antigen uptake using an HDM-model for allergic asthma ⁹⁰. Furthermore, cDC1s release high amounts of the chemokines CCL17 and CCL22, suggesting that they contribute to the homing of activated T cells to the lungs ^{89,91}. They may also drive Th1-responses ⁹² and can to induce tolerance through the induction of T_{reg} cells ⁹³.

cDC2s play the major role in the development of the Th2 response in allergic asthma. cDC2s take up antigens efficiently and migrate fast to the lymph nodes, where they induce Th cell differentiation into Th2 and Th17 cells ^{90,94}. Here, TSLP, IL-25 and IL-33 released by the epithelial layer orchestrate cDC2 function. In this context TSLP drives the expression of OX40L to promote Th2 cell differentiation ⁹⁵.

Pulmonary pDCs play a major role in viral infections, where they lead the antiviral response by TLR7-triggered Type I IFN- γ production, also in the course of asthma ^{96,97}. Their role in the development of allergic asthma is controversial. They are not as efficient in allergen uptake as cDC2s and less effective in T_{reg} induction compared to cDC1s ^{98,99}. However, pDCs act tolerogenic by driving the T_{reg} cell differentiation, when airborne

allergens enter the airways ⁹⁸. It was shown recently that pDCs also might modulate cDC function. The presence of Flt3L results in an increase in the pDC/cDC ratio, leading towards a strong anti-inflammatory response after allergen challenge ¹⁰⁰.

MoDCs derive from monocytic precursors in the bone marrow; differentiate into short-lived Ly6c^{hi} or long-lived Ly6c^{lo} moDCs to migrate to the lungs or the lymph nodes without differentiating ²⁰. They are located at the interface between airways and blood vessels in steady state in a little amount and are recruited by epithelial-derived CCL2/CCR2 signaling to the lungs during allergic inflammation ^{101,102}. The moDCs can be discriminated from cDC2s by the expression of CD64 ⁹⁰. They support cDC2s in antigen uptake and also drive Th cell differentiation into Th2 and Th17 cells. Importantly, they produce large amounts of eosinophil- and monocyte-attracting and -activating chemokines as CCL24, CCL2 or CCL4 ⁹⁰.

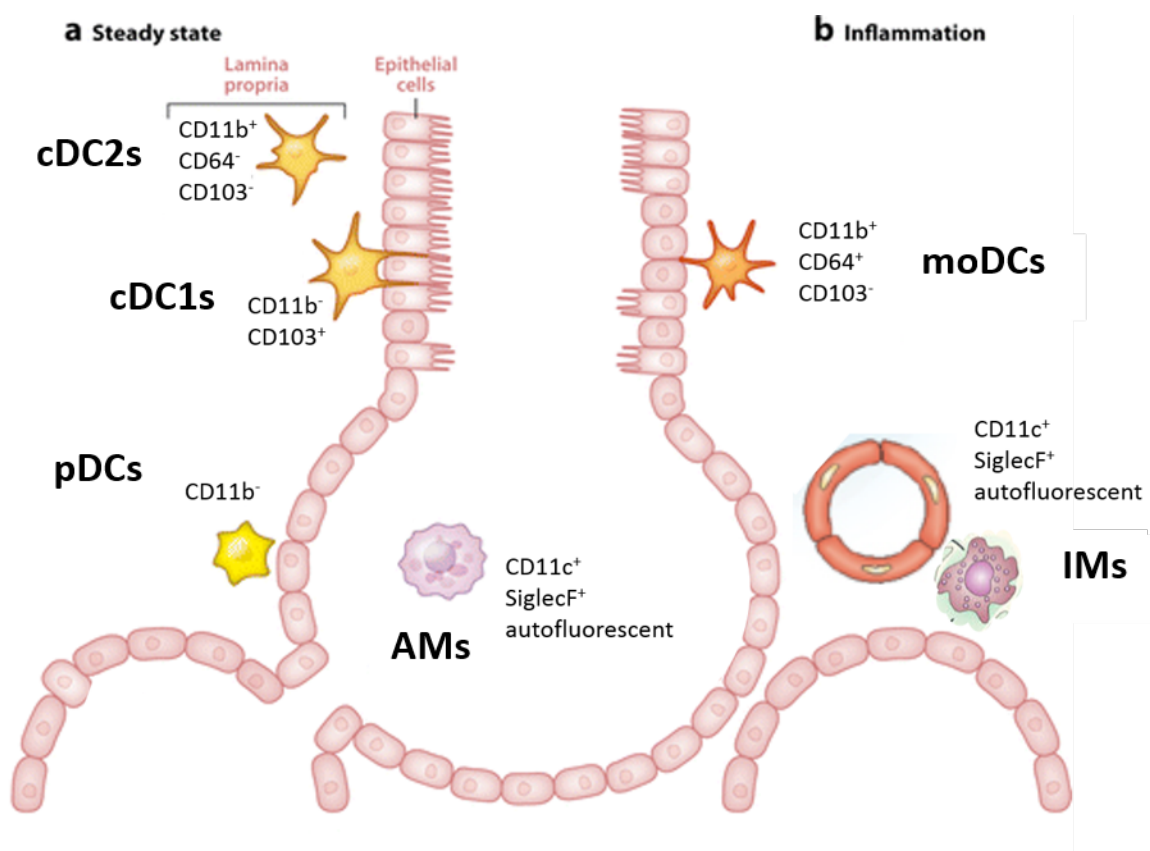


Figure 2-3: Distribution of pulmonary APCs

The figure depicts the distribution of the several pulmonary dendritic cell (DC) and macrophage subsets and their expressed cluster of differentiations (CD), which were used in the following experiments for identification. A) In steady state, CD11b⁺

2 Introduction

conventional DCs (cDC2s), CD103⁺ cDCs (cDC1s) and plasmacytoid DCs (pDCs) are present in the pulmonary interstitium. Alveolar macrophages are situated in the alveolar space. B) During inflammation, monocyte-derived DCs (moDCs) as well as interstitial macrophages (IM) enter the pulmonary tissue. Republished and modified with permission of Annual Reviews, Inc. from 'Lung dendritic cells in respiratory viral infection and asthma'⁸⁶; permission conveyed through Copyright Clearance Center, Inc.

To sum up, pulmonary DCs exert a critical role in allergic sensitization in the lungs as they drive the inflammatory response towards an asthmatic phenotype. Also, they contribute to airway remodeling, the chronic state of allergic asthma. Here, TSLP secreted by the epithelial cells and TGF- β produced by fibroblasts, stimulate and modulate DC activity, which in turn leads to the resolution of airway inflammation through airway remodeling^{103,104}.

2.1.4.2 Macrophages

Pulmonary macrophages comprise two subsets (Figure 2-3, p. 21): alveolar macrophages (AM) residing in the airways and the alveolar space¹⁰⁵, and interstitial macrophages (IM), which are located close to DCs in the alveolar interstitium¹⁰⁶. Their roles in allergic asthma are still not clear. Yolk-sac derived AMs descend from fetal monocytes, populate the lung around birth and are able to self-maintain their local numbers throughout lifetime²³. They have pro- and anti-inflammatory properties in the course of allergic asthma. In the beginning, their anti-inflammatory potential predominates by suppressing chemokine expression and neutrophil recruitment¹⁰⁷. AMs further suppress DC-driven antigen presentation and inflammation during allergen sensitization²³. When allergen exposure continues, AMs lose their anti-inflammatory potential, become so-called M2-macrophages and produce the proallergic cytokines IL-4 and IL-13^{108,109}. This dual role of AMs could result from IL-12, a Th1-activating cytokine produced by monocytes, macrophages, neutrophils and DCs¹¹⁰. Interestingly, the percentage of IL-10⁺ AMs is high in healthy individuals pointing towards an asthma-suppressing role¹⁰⁸.

In regard of non-alveolar IMs, there is not much known about their role in allergic asthma. Recent findings suggest IMs have different backgrounds: some originate from yolk-sac-derived pre-macrophages, populate the lung and are maintained as non-active IMs in submesothelial and perivascular regions. Others develop postnatal in the bone marrow and populate the lung tissue later in life ¹¹¹. These monocyte-derived cells sustain lung homeostasis and produce IL-10 at steady state, which suppresses DC function ¹⁰⁶.

2.1.5 The role of complement in allergic asthma

The complement system is an important humoral part of innate immunity. It consists of more than 50 proteins and cleavage products, partly soluble, partly bounded to cell membranes, which in perfect interaction lead to attack and destruction of pathogens. They are mainly produced in liver cells, however, local complement production has been reported in a variety of cells of the whole body ^{112,113}. As a part of the ancient pattern-recognition systems, the complement cascade is activated by conserved exogenous or endogenous danger-associated molecular patterns (DAMP).

There are three different activation pathways known (Figure 2-4a, p. 25). The first is the classical, often called 'antibody-dependent' pathway. Here, the pattern recognition molecule (PRM) C1q recognizes the Fc segment of immunoglobulin M or G (IgM or IgG), however, it gets also activated by endogenous c-reactive protein (CRP) or specific structures on the microbial surface ¹¹⁴. Activated C1q binds to the serin proteases C1r and C1s, together forming the C1 complex. Its proteolytic activity cleaves C2 and C4 whose cleaving products generate the C3 convertase C4b2a ¹¹⁴.

The same C3 convertase is generated during the so-called lectin pathway. Here, the PRMs mannose-binding lectin (MBL) and ficolins recognize carbohydrate molecules on the bacterial surface. After recognition, the molecules bind to MBL-associated serine proteases (MASP), similar to the

2 Introduction

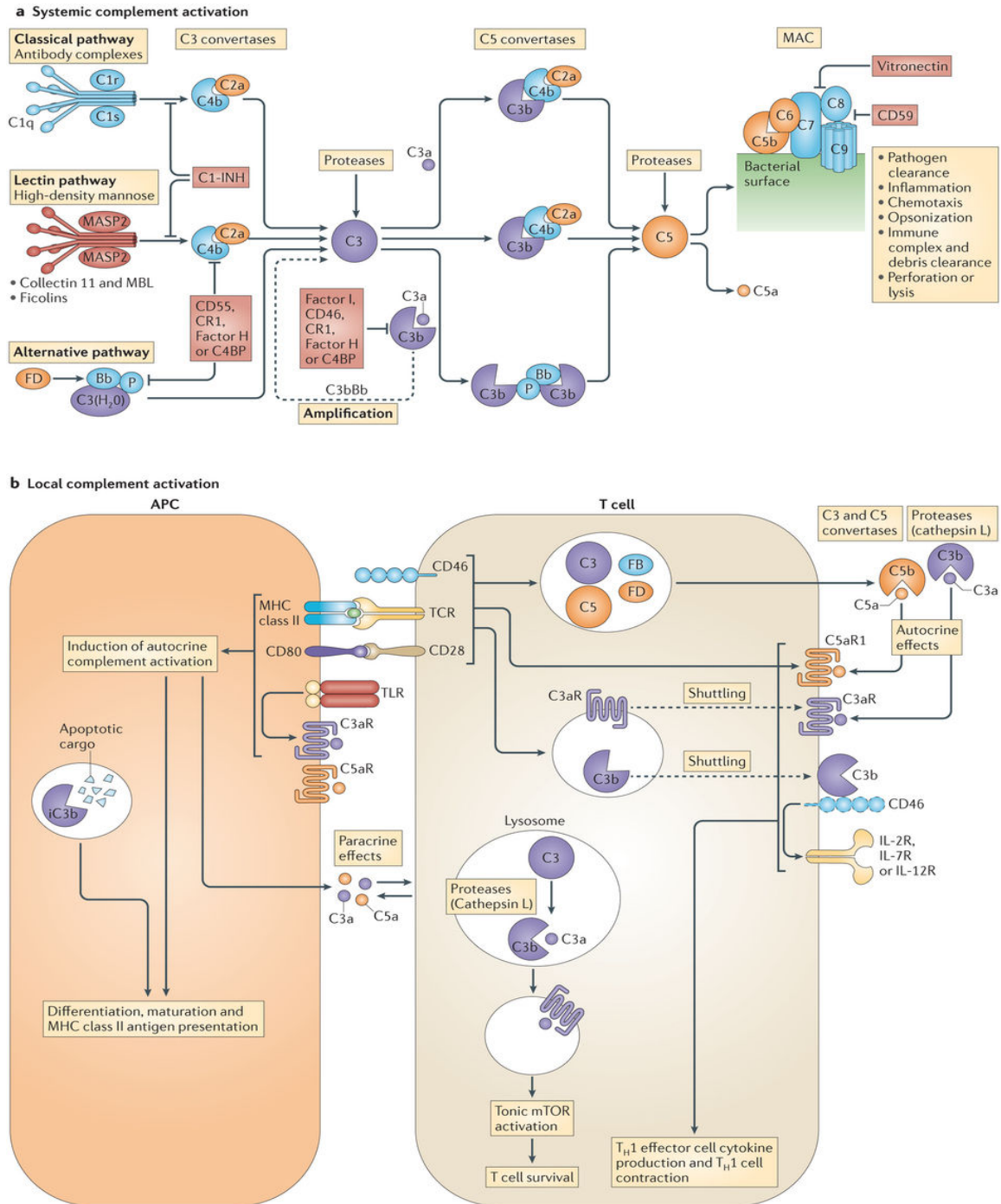
previous C1r/C1s activation. In the following, the MASP-2 cleaves C2 and C4 and by that generates the same C3 convertase C4b2a ¹¹⁴.

The third option is the alternative pathway combining three different possibilities of C3 cleavage together with factor B. First, a so-called 'tick-over mechanism' is able to sense foreign cells in the body. C3 contains a hydrolyzed fraction C3_{H2O} that binds to factor B protease when recognizing foreign particles. After cleavage by the protease factor D, a soluble C3 convertase is formed, called C3_{H2O}Bb. Secondly, C3 convertase assembly may also be initiated by a properdin-dependent way. The PRM properdin is able to sense PAMPs and DAMPS on foreign and apoptotic cells. After recognition, it attracts soluble C3b to form and stabilize C3 convertase, e.g. C3bBbP. Third, the surface-bound C3 convertase is able to amplify C3 cleavage via C3 activation and by that increase complement activation dramatically ¹¹⁴.

All three pathways converge at the level of C3 activation that dissociates in a large C3b part, an opsonin, and a smaller C3a unit, called the C3a anaphylatoxin (AT). C3b forms together with the respective cleavage products different types of C5 convertases, resulting in C5 cleavage with the side product C5a, a second AT. The large fragment C5b associates with C6 and C7 to insert into the cell membrane. By binding to C8 and C9, the membrane attack complex (MAC) is formed resulting in cell lysis ¹¹⁴⁻¹¹⁶.

Recently, the expression of complement receptors on nearly every cell of the body could be proven ¹¹⁷. The asthma-relevant macrophages, epithelial cells as well as fibroblasts are able to produce C1q and M-ficolin, two substances activating the complement cascade, and also the complement factors B, D and C3 ¹¹⁸. Furthermore, stimulation of the complement receptors C3aR and C5aR1 on T cells influences their maturation and activation; and modulate APC function (Figure 2-4b, p. 25) ¹¹⁹.

2 Introduction



Nature Reviews | Immunology

Figure 2-4: The complement cascade

A) The complement cascade can be activated through three different pathways, the lectin, the classical, as well as the alternative pathway. For detailed information see above. B) In addition, local activation of complement occurs in antigen presenting cells (APC) and T cells. These immune cell subsets express the complement receptors C3aR and C5aR1 that are activated by local cleavage of C3 and C5 convertases. The cleavage products C3a and C5a in turn activate their respective AT receptors on T cells and APCs. I.e., C3a uptake activates resting CD4⁺ T cells, by that upregulate growth factors and interleukins and finally enhance effector T cell function. Republished with permission of Springer Nature from 'Complement – tapping into new sites and effector systems'¹¹²; permission conveyed through Copyright Clearance Center, Inc.

2.1.5.1 The dual role of the anaphylatoxin C5a in the course of allergic asthma

The AT C5a exerts proinflammatory and immunoregulatory properties that are central for the development and maintenance of allergic asthma. C5a levels increase significantly after allergen challenge in the bronchoalveolar fluid compared to basal amounts ¹²⁰. Moreover, direct C5 cleavage into C5a and C5b occurs in response to HDM-associated protease Derp3 ¹²¹. Proteases of activated AMs also stimulate C5 cleavage ¹²².

C5a itself attracts inflammatory cells including eosinophils and mast cells to the lung and activates mast cells and basophils to release histamine upon airway inflammation ¹²³. C5a also induces airway remodeling by inducing matrix metalloproteinase (MMP) 9 release from neutrophils ¹²⁴. Further, it regulates Th1/Th2 responses by regulating IL-12 production ^{123,125}.

There exist two distinct AT receptors mediating C5a function: the G-protein coupled receptor C5aR1 and the G-protein independent receptor C5aR2 (former C5a receptor-like 2 (C5L2) with opposing roles in allergy regulation ¹²⁶. C5aR1 is expressed on several pulmonary cell subsets, including bronchial epithelial and smooth muscle cells ¹²⁷, as well as on AMs, cDC2s, eosinophils and neutrophils in steady state conditions and on moDCs during inflammation ¹²⁸. C5aR1 is not expressed on cDC1s, B cells or T cells during the allergic effector phase ¹²⁸. C5aR1 has a regulatory function during allergen sensitization, but obtains a proallergic role during the effector phase. It has been demonstrated that C5aR1 signaling regulates the cDC/pDC ratio during sensitization. This is of major importance in asthma development as C5a might induce tolerance to airborne allergens ¹¹⁸. In fact, a disrupted C5a/C5aR1 axis results in increased T cell proliferation and thus allergic inflammation ¹¹⁸. Recently, it was proven that the C5a/C5aR1 axis promotes tolerance by downregulating CD40 expression on cDC2s upon HDM/OVA sensitization

2 Introduction

resulting in reduced T cell priming ¹²⁹. C5aR1 activation also regulates AM numbers in steady state and drives neutrophil recruitment from pulmonary tissue towards the airways ¹³⁰. Contrarily, C5aR1 promotes the allergic asthma phenotype during the effector phase as it was shown that pharmacological targeting reduces inflammatory cell and cytokine responses in an OVA-driven asthma model ¹³¹. Here, an overall reduction in Th2 responses was detectable when C5 was blocked by an antibody, however, ILC2 proliferation and differentiation were not affected ¹³².

Contrarily, C5aR2 seems to exert an anti-allergic role in asthma development. As it is not directly coupled to a G protein, C5aR2 was first assumed to work as a decoy receptor to modulate C5a function and by that limiting allergic inflammation ¹³³. However, C5aR2 can also directly interfere with C5aR1 and by that convert proallergic into anti-inflammatory signaling ¹³⁴. Contrarily, it was shown that C5aR2-knock out mice did not develop allergic asthma upon HDM stimulation ¹³⁵. However, further analyses showed little evidence for direct influence of C5aR2 on C5aR1 signaling and rather found an inhibitory role for C5aR2 on other PRRs ¹³⁶.

Interestingly, a circadian pattern of complement factors and the AT C3a has been observed in the circulation. C3 and C4 plasma levels were fluctuating with a peak during daytime hours followed by a decrease during the night without any influence of sleep. Contrarily, C3a plasma levels oscillated with a maximum at nighttime with a strict sleep-wake-cycle. C5a levels could not be measured due to rapid clearance from circulation. C3aR and C5aR1 numbers on human monocytes did not follow a circadian rhythm ¹³⁷. The circadian rhythm of C3, C4 and C3a and of asthma symptoms may point toward a link between the intensity of complement activation during the night and the development of asthma symptoms.

2.2 Circadian rhythms

Due to the rotation of the earth around its own axis, life on earth had to adopt to the 24h-lasting change of light and darkness, according to day and night. Animals and plants had to learn to live with these changes and developed mechanisms to use accessible resources as effective as possible ¹³⁸. Most animals became diurnal, which means that they are active during daytime when the sun is shining and adopted rhythmicity to the sunlight. Later, such changes during day and night could be assigned to an internal biological clock, controlling and organizing the so-called circadian rhythms (from the Latin *circa diem* = around a day) at the molecular level, which synchronizes to outer Zeitgeber as light or food intake and consequently lead to a well-adopted behavior.

2.2.1 The molecular clock

The molecular clock is built up hierarchically with the suprachiasmatic nucleus (SCN) as the central pacemaker. This part of the brain is the only region in the body, where photic information is received and transformed. First, the photosensitive pigment melanopsin absorbs light information in the retina of the eye, which is connected with the SCN via the retinohypothalamic tract. Here, the photic input adjusts the molecular clock ¹³⁹. In addition to the light, which is the main important Zeitgeber, temperature, food-intake as well as other parameters help to adapt the central clock to the environment ¹⁴⁰.

The role of the SCN as the master clock and central pacemaker has been widely discussed. Recent findings suggest that its main role is to orchestrate and synchronize the peripheral clocks, as these cannot receive photic information from the periphery ¹⁴¹. These peripheral clocks are existing ubiquitously, are self-sustained and autonomous, and control organ-specific functions in nearly every cell in a circadian matter ^{142,143}. They are adjusted by the SCN through direct autonomic nerve and

humoral signals (e.g. glucocorticoids), or indirectly by timed sleep-wake-cycles, feeding or body temperature ¹⁴⁴.

Central and peripheral clocks have the same molecular basis: they consist of interconnected transcriptional-translational feedback loops of so-called clock genes, which generate protein products in circadian oscillating amounts (Figure 2-5, p. 29).

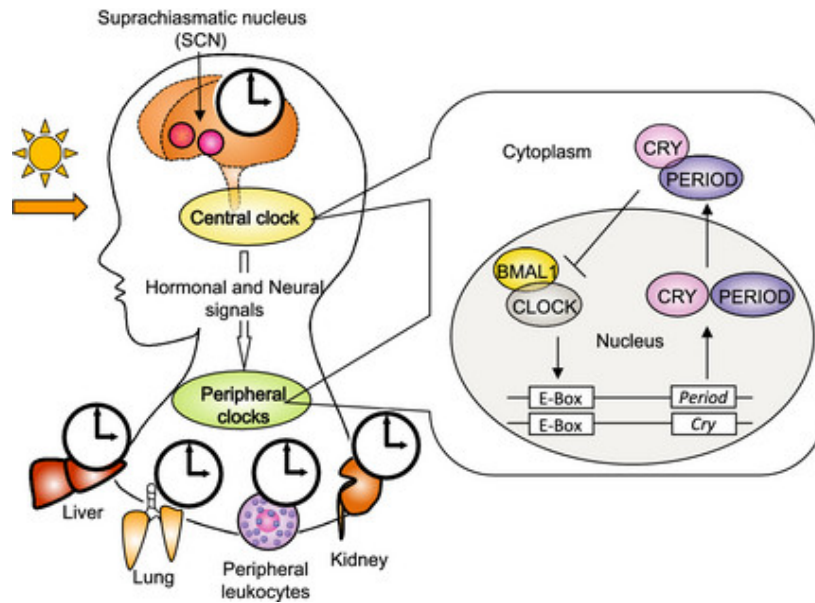


Figure 2-5: The mammalian molecular clock.

The central clock is located in the suprachiasmatic nucleus in the hypothalamus, where light input from the retina entrains the peripheral clocks through modulating hormonal and neural signals. The molecular basis of the central as well as the peripheral clocks are the same: the heterodimer BMAL1/CLOCK activates the transcription of cryptochrome (CRY) and period (PER) genes. These proteins associate and thereby inhibit their own expression by suppressing the CLOCK/BMAL1 activity. Like a range of other clock-related genes, 24h-lasting oscillations of protein levels occur and regulate behavior and physiology of the organism. This network is much more complicated than depicted here ¹⁴¹, however this figure shows in a simplistic way the underlying concept of circadian rhythms in mammals. Republished with permission of John Wiley and Sons from 'The circadian clock functions as a potent regulator of allergic reaction' ⁸; permission conveyed through Copyright Clearance Center, Inc.

The molecular clock modulates immune responses

Recently, the circadian clock was described as a basic element of the innate and adaptive immunity e.g., the core proteins BMAL1 and CLOCK regulate toll-like receptor 9 (TLR9) expression ¹⁴⁵, an important pattern recognition receptor (PRR) within antigen-presenting cells. During the

adaptive immune response, cytokine release is directly linked to the expression of clock genes, as human CD4⁺ T cells produce IFN- γ , IL-2 and IL-4 in a circadian manner ^{146,147}. Furthermore, Kraft and colleagues could show that CD4⁺ T cell numbers in the lungs fluctuate during day and night. They examined patients with nocturnal and non-nocturnal asthma by bronchoscopy to compare T cell and eosinophil numbers at day and night. Interestingly, they found increased CD4⁺ T cell numbers in the alveolar tissue in patients with nocturnal asthma during the night, which correlated inversely with the lung function ¹⁴⁸.

2.2.2 Circadian rhythms in the healthy lung

Physicians recognized rhythms in the lung physiology already a long time ago. Using improved methods, these could be analyzed in detail in the last decades. Taking advantage of the spirometer technology, precise measurements of the airway resistance became possible. Already years ago, significant day-night differences were observed regarding the forced expiratory volume in one second (FEV1) and the peak expiratory flow (PEF), two hallmarks that describe the airway caliber. Measurements in healthy humans showed that the airways were tightest in the early morning hours just before waking up ¹⁴⁹.

A second, circadian-driven mechanism has been observed in response to hypercapnia. In the early morning hours, humans show the highest tolerance towards accumulation of CO₂ in the blood. This might be part of the body's division of energy, as reduced CO₂-sensitivity results in reduced work of breathing ¹⁵⁰.

In addition to differences in lung physiology, differences in the lung's immune function have been shown during day cycle. Depending on the time of day, a different allergen dose was needed to trigger acute bronchospasm with the lowest dose needed during resting phase. It was also seen that a late asthmatic response with ongoing AHR and lymphocytic infiltration appeared rhythmically in the nights following

allergen exposure¹⁵⁰. Lately, the molecular mechanisms underlying these circadian changes have been investigated¹⁵¹.

2.2.3 Circadian rhythms in allergic asthma

As described above, it is widely appreciated that allergic asthma depends on the circadian clock expressed in immune and epithelial cells (Figure 2-6, p. 33). Exemplary, bronchoalveolar lavages of asthmatics were taken at different times of the day to investigate the lymphocyte and cytokine status. Researchers found an association between the number of CD4⁺ T cells and IL-5 levels regarding the time of lavage with a peak at nighttime¹⁵². This discovery is in line with fluctuations in the eosinophil number in the airways¹⁵³. BMAL1 expression in the bronchial secretory cells (Clara cells) in the epithelium was found to contribute to this circadian rhythm^{154,155}. BMAL1 regulates the circadian expression of CXCL5, a neutrophil-recruiting chemokine, independent of rhythmic glucocorticoid signaling¹⁵⁶. Zaslona and colleagues demonstrated the importance of circadian regulation in asthma using a mouse model in which Bmal1 was absent in myeloid cells (Bmal1-LysM^{-/-} mice)¹⁵⁷. These mice developed a more severe phenotype with a much higher increase in IL-5 and eosinophil numbers than in WT mice in an ovalbumin-driven asthma model. They suggested a negative-regulating role for the central clock protein Bmal1 in allergic asthma.

Recently, it was shown that these Bmal1-related effects in circadian control of pulmonary inflammation were mediated by the orphan nuclear receptor REV-ERB α linking the pulmonary clock to the innate immune response¹⁵⁸. REV-ERB α serves as a downstream transcription factor in the molecular clock network and has furthermore the capacity to directly interfere with DNA molecules¹⁵⁹. Mutated REV-ERB α in murine bronchial epithelial cells enhanced the neutrophilic response towards inhaled LPS and abrogated the circadian immune response. Beyond that, Pariollaud et al. described a homeostatic function of REV-ERB α suppressing

2 Introduction

inflammation in steady state. In contrast, REV-ERB α degradation increases upon inflammatory signaling leading to time-dependent variations in chronic inflammatory diseases ¹⁵⁸.

Overall, leucocyte trafficking in asthma might result from an interplay of circadian clock-driven mechanisms in the leucocytes themselves and in the epithelial cell network ¹⁶⁰. In the last decades, the expression of molecular clock genes has been demonstrated in several murine immune cells such as splenic macrophages, DCs and B cells, intestinal mast cells, blood eosinophils and monocytes as well as in T cells ¹⁶¹⁻¹⁶⁷. However, it is still unclear whether the varying availability of leucocytes is the main driver for lung phagocytic capacity, or to what extent intrinsic clock-driven mechanisms interfere to provide a time-dependent surveillance for pathogens ¹⁵⁰.

Recently, blood samples from asthmatic children were examined for the expression of single nucleotide polymorphisms (SNP) in central clock genes (CLOCK, BMAL1, Per3 and TIMELESS). For the first time, three polymorphisms in the TIMELESS gene were identified as associated with childhood asthma. The data suggest that central clock genes may serve as direct regulators of disease development ¹⁶⁸. However, the precise role of TIMELESS as a regulator of the human molecular clock is still under intense research. Lately, it was shown that TIMELESS binds the central clock proteins PER2 and CRY2 and could thereby contribute to regulate minor phase shifts to maintain circadian rhythmicity ¹⁶⁹.

Together, the available data suggest that circadian mechanisms drive the pathophysiology of allergic asthma in experimental and clinical allergy. Importantly, chronotherapy has been used in asthma therapy for many years. Depending on the type of treatment, it was proven to be most efficient when given in the afternoon (e.g. prednisolone) or early evening (e.g. montelukast or bambuterol) in reducing night symptoms ¹⁷⁰.

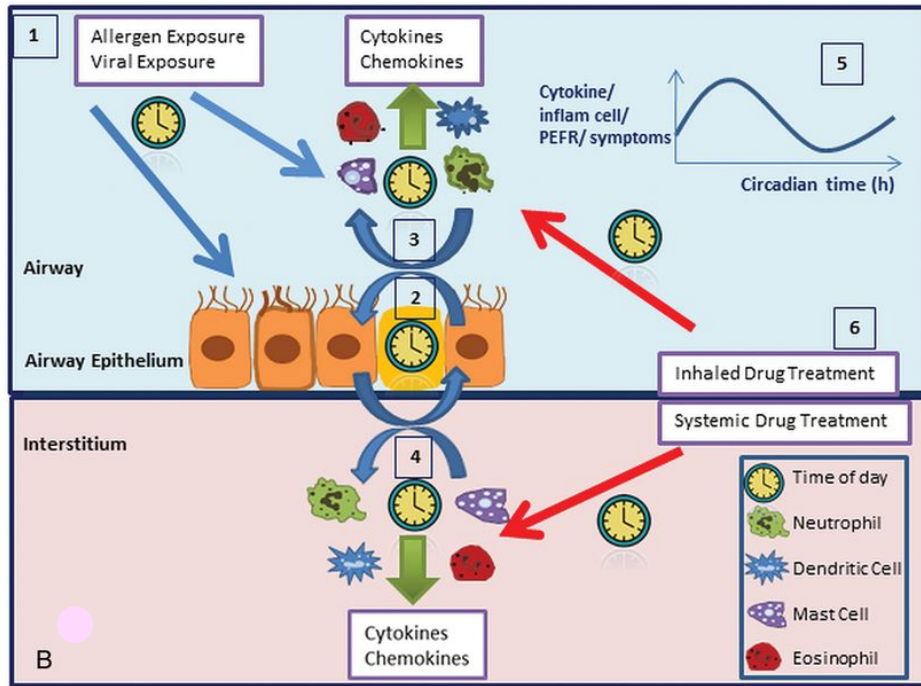


Figure 2-6: The molecular clock in asthma development.

The time of day has a substantial influence on the severity of the allergic reaction after allergen exposure. (1) The peripheral clocks exist in the pulmonary Clara cells leading to time-dependent allergen sensibility. (2) The epithelial clock interacts with peripheral clocks expressed in immune cells. (3, 4) This leads to a circadian expression of inflammatory cytokines and chemokines in the airways and the interstitium. (5) Due to these circadian fluctuations, the asthmatic sensitivity and symptoms change during the 24h cycle. (6) By timing medical treatment, asthma symptoms can efficiently get reduced. Republished with permission of BMJ Publishing Group Lt. from 'The circadian clock and asthma'¹⁷¹; permission conveyed through Copyright Clearance Center, Inc.

2.3 Mouse models in allergic asthma and circadian rhythm research

The house mouse (*mus musculus*) is a common used model organism to examine the mechanisms underlying human diseases. Thus, mice are commonly used in scientific research. Mouse keeping is simple and cheap, and nutritional requirements are low. Mice have a very short generation time of 18-21 days and breed during the whole year with a litter size roughly from 6-12. They tolerate inbreeding and can be easily genetically manipulated to delete and modify defined genes. Finally, mice and humans have a high genetic concordance; less than 1% of the mouse

genes are without any human homologue ¹⁷². Anatomic similarity simplifies the transfer of research results to the human organism. That being said, there are still differences between both species and translation of experimental results needs to be done with caution ¹⁷³.

2.3.1 Mice in experimental allergic asthma

Especially in lung research, the mouse is the preferred animal model. The murine immune system has been analyzed in detail over the last decades, inflammatory lung reactions are well studied and a broad spectrum of technical instruments have been developed ¹⁵⁰. Especially allergic asthma has been studied intensively in the mouse model and our current understanding is largely based on the pathophysiology unveiled in the mouse system ¹⁷⁵.

However, the lung anatomy of mice and humans shows several differences. The mouse lung consists of a single left and 4 right (a cranial, a middle, a caudal and an accessory) lung lobes. The human lung comprises 2 left (upper and lower) and 3 right (upper, middle and lower) lung lobes. Furthermore, there is no cartilage tissue around the bronchial tubes distal from the main bronchi in mice, and they are smaller than those in humans. Further, the number of mucous and serous epithelial cells in mice is lower than in humans. Also, they lack submucosal glands. Functionally seen, mice are obligate nose breathers as they have a very large glottis, while humans breathe through both mouth and nose ^{176,177}. It is important to keep such details in mind in experimental mouse models of allergic asthma.

Several immunization strategies have been developed to reproduce the features of allergic asthma in mice. The most common strategies include ovalbumin and HDM as antigens and use BALB/c mice, as they develop as strong and long-lasting allergic airway inflammation, AHR, mucous production, maladaptive Th2 and often Th17 responses including the production of allergen-specific IgG1 and IgE antibodies. In this project, I

have used the well-established HDM model ¹⁷⁸, as HDM is an important aeroallergen in humans. Repeated intratracheal administration without additional adjuvant induces a strong asthmatic phenotype. I used female BALB/c mice, which show a more consistent development of the allergic phenotype than male mice.

2.3.2 Mice in circadian experiments

Mice are frequently used to study circadian rhythms. However, several things need to be considered.

First, the mouse is, as many other rodents, a nocturnal animal due to predation pressure by their natural enemies. Thus, they are active in the dark and rest during daytime. When mice are housed in a standard animal facility, they are entrained by the outer Zeitgeber light. Light input is strictly regulated by external factors such as the working hours of the animal keepers. This is problematic, as it results in frequent disturbance of the animals during their regular resting period, as the animal keepers clean and change cages and the scientists perform their experiments during daytime. To avoid such disruption of the regular sleep cycle, mice have to be housed in special sound- and lightproof boxes for circadian experiments, where they are not disturbed during their resting period and can sleep without interruption. Light in the boxes can be regulated precisely and the laboratory has established dim red light (<1.5 lux) to reduce external disturbance to a minimum when performing an experiment during their activity period ^{179,180}.

When using a 12:12h LD cycle, there are exactly 12h of light and 12h of darkness. The mice adopt to this outer Zeitgeber. Zeitgeber time 0 (ZT0) is defined as light on, and ZT12 as light off. However, to define the impact of the inner clock on immune functions in allergic asthma, it is necessary to keep the mice in total darkness (DD). Only then, statements about the molecular clock system are possible. When switching from LD- to DD-conditions, mice need to adopt at least 2 days until the experiment can

start ¹⁸¹. BALB/c mice have in DD conditions a shorter day lasting only 22.94 ± 0.06 h, which does not affect short-time protocols very much ¹⁸². For circadian experiments, male mice are typically used to reduce the influence of hormonal cycles, i.e. estrogen, that affects general activity ¹⁸¹. The free-running experiments in DD conditions were performed with both male and female mice; however, only female mice were used for immunization protocols due to experimental limitations.

2.4 Aims of the project

Fluctuation of pulmonary immune cells that follow a circadian rhythm were detected already years ago. In particular, circadian immune cell regulation has been recognized in pulmonary epithelial cells (see chapter 2.2.3, p.31). So far, the focus in circadian rhythm research was on clock gene expression in defined immune cell subsets. However, how circadian mechanisms regulate the distribution of pulmonary immune cells remains elusive. Also, the impact of diurnal changes on the activation of immune cells contributing to the development of allergic asthma are poorly understood. As antigen-presenting cells are the key instructors of the maladaptive immune response, these cell subsets are of major interest in this context. The hypothesis underlying this thesis was: (i) that immune cells in the airways and the lung follow a circadian rhythm; and that (ii) such circadian fluctuations in immune cells impact on the development of experimental allergic asthma in mice immunized with house dust mite at the sensitization and the effector phase.

To test these hypotheses, I pursued the following specific aims:

Specific aim 1. Delineate the impact of circadian rhythm on the distribution of airway and pulmonary immune cells in wild type (WT) mice in steady state.

- H₁: The total number of pulmonary immune cells in the lungs and the airways vary during the 24h cycle, i.e. the number of alveolar macrophages, pulmonary macrophages, cDC1s, cDC2s, and eosinophils.

Specific aim 2. Determine the influence of the C5a/C5aR1 axis activation on the distribution of pulmonary immune cells in steady state.

- H_{2a}: The immune cells in C5aR1-knock out mice show an activity pattern that is different from WT mice in DD conditions.
- H_{2b}: The total number of pulmonary immune cells in the lungs and the airways is fluctuating during the night and day cycle in C5ar1^{-/-} mice, i.e. the number of alveolar macrophages, pulmonary macrophages, cDC1s, cDC2s, and eosinophils fluctuates.
- H_{2c}: The number of immune cells in the lung and the airways of WT and C5ar1^{-/-} mice shows a different circadian fluctuation pattern.

Specific aim 3. Define the impact of allergen exposure at day or nighttime on the development of the allergic phenotype in experimental allergic asthma.

- H_{3a}: The strength of the early allergic phenotype after initial allergen sensitization is dependent on the time of allergen sensitization.
- H_{3b}: The allergen-induced Th2 and Th17 differentiation depends on the time of the initial allergen contact.

Specific aim 4. Delineate the influence of the time of allergen contact on the development of the effector phase of experimental allergic asthma.

- H_{4a}: The strength of the airway hyperresponsiveness and mucus production depends on the time of allergen contact.
- H_{4b}: The time of allergen exposure influences the distribution of immune cells in the airways, the lung and the mediastinal lymph nodes in the effector phase of experimental allergic asthma.
- H_{4c}: T cell priming and migration towards the lungs is affected by the time of allergen exposure.
- H_{4d}: The production of pro- and anti-inflammatory cytokines in the lungs and the airways depends on the time of allergen contact.

Specific aim 5. Determine the impact of repeated HDM immunization on the circadian rhythm.

- H₅: The four-week HDM-treatment during the resting or the activity phase affects the sleep-wake pattern of WT mice.

3 Materials and Methods

3.1 Overview of materials

Table 3-1: Chemicals

Name	Manufacturer
Acetyl- β -methyl-choline 100 mg/mL	Sigma-Aldrich Chemie GmbH, Steinheim
AutoMACS-Rinsing Solution	Miltenyi Biotex GmbH, Bergisch Gladbach
Bathocuproine (BCP)	Sigma-Aldrich Chemie GmbH, Steinheim
BD Cytofix/Cytoperm	BD Biosciences Europe, Erembodegem, Belgium
BD FACS Flow Sheath Fluid	BD Biosciences Europe, Erembodegem, Belgium
β -Mercaptoethanol	Sigma-Aldrich Chemie GmbH, Steinheim
Bovine Serum Albumin (BSA)	Thermo Fisher Scientific, Waltham, USA
Brefeldin	BD Biosciences Europe, Erembodegem, Belgium
Calcium ionophore (ionomycin)	Millex/Merck Millipore, Darmstadt
CompBeads Anti-Rat/Anti- hamster	BD Biosciences Europe, Erembodegem, Belgium
Dimethyl amiloride hydrochloride	Sigma-Aldrich Chemie GmbH, Steinheim
Disodium hydrogen phosphate	Sigma-Aldrich Chemie GmbH, Steinheim
Dulbecco's Phosphate buffered Saline (PBS)	GE Healthcare Europe GmbH, Wien, Austria
Dulbecco's modified Eagle's Medium (DMEM)	GE Healthcare Europe GmbH, Wien, Austria
Dulbecco's modified Eagle's Medium (DMEM) colorless	GE Healthcare Europe GmbH, Wien, Austria

3 Materials and Methods

Esmeron (Rocuroniumbromid) 10 mg/mL	Organon Teknika, Eppelheim
Ethanol, 70% denatured	Th. Geyer GmbH & Co. KG, Renningen
Ethanol, 96% denatured	Th. Geyer GmbH & Co. KG, Renningen
Ethylene diamine tetra acetic acid (EDTA) 50 mM	Thermo Fisher Scientific, Waltham, USA
Fetal bovine serum (FBS)	GE Healthcare Europe GmbH, Wien, Austria
Formaldehyde solution, 37%	Sigma-Aldrich Chemie GmbH, Steinheim
FoxP3-staining buffer	BD Biosciences Europe, Erembodegem, Belgium
GM-CSF, mouse recombinant	Peprotech Corporation, Rocky Hill, USA
House dust mite extract	Greerlabs Laboratories Inc., Lenoir, USA
HEPES-buffer 1M	GE Healthcare Europe GmbH, Wien, Austria
Isopropanol	Pfizer Deutschland GmbH, Wien, Austria
Ketavet 100 mg/mL	Pfizer Deutschland GmbH, Wien, Austria
L-glutamine 200 mM	Life technologies Corporation, Carlsbad, USA
Liberase TL Research Grade	F. Hoffmann-La Roche AG, Basel, Schweiz
Lucifer Potassium Salt	Thermo fisher Scientific, Waltham, USA
Monensin	BD Biosciences Europe, Erembodegem, Belgium
Penicillin/streptomycin	Life technologies Corporation, Carlsbad, USA
Phorbol 12-myristate 13- acetate (PMA)	Sigma-Aldrich Chemie GmbH, Steinheim
RNA-free water	Thermo Fisher Scientific, Waltham, USA
Rompun vet.	Bayer AG, Leverkusen
RPMI 1640	GE Healthcare Europe GmbH, Wien, Austria
Sodium chloride	Carl Roth GmbH & Co. KG, Karlsruhe
Sodium carbonate	Sigma-Aldrich Chemie GmbH, Steinheim

3 Materials and Methods

Sodium dihydrogen phosphate	Sigma-Aldrich Chemie GmbH, Steinheim
Sodium hydrogen phosphate	Sigma-Aldrich Chemie GmbH, Steinheim
Sodium pyruvate	Life technologies Corporation, Carlsbad, USA
Trypan blue	Life technologies Corporation, Carlsbad, USA

Table 3-2: Antibodies used in flow cytometry and cell sorting.

Antibodies and reagents used for flow cytometry and cell sorting. All the antibodies were stored at 4°C. APC = Allophycocyanin, BV = brilliant violet, Cy7 = Cyanine 7, eF = eFluor, FITC = Fluoresceinisothiocyanat, PE = Phycoerythrin, PercP = Peridinin chlorophyll protein, V450 = BD Horizon™ V450.

Epi-tope	Conju-gate	Manufacturer	Clone	Host species	Stock con-centration
CD3	FITC/AF488	eBioscience	17A2	Rat	0.5 mg/mL
CD3e	V450	eBioscience	145-2C11	Syrian gold hamster	0.5 mg/mL
CD4	PeCy7	eBioscience	RM4-5	Rat	0.2 mg/mL
CD11b	BV510	Biologend	M1/70	Rat	0.2 mg/mL
CD11c	APC	eBioscience	N418	Armenian hamster	0.2 mg/mL
CD19	eF450	eBioscience	1D3	Rat	0.2 mg/mL
CD44	BV421	Biologend	IM7	Rat	0.2 mg/mL
CD49b	V450	eBioscience	DX5	Rat	0.2 mg/mL
CD62L	APC	Biologend	MEL14	Rat	0.2 mg/mL
CD64	PE	Biologend	X54-5/7.1	Mouse IgG1	0.2 mg/mL
CD103	PercP Cy5.5	Biologend	2E7	Armenian hamster	0.2 mg/mL
CD326 (Ep-Cam)	PE	eBioscience	G8.8	Rat	0.2 mg/mL

3 Materials and Methods

FcR block (anti-CD16/32)	-	eBioscience	93	-	0.5 mg/mL
IFN- γ	APC	eBioscience	XMG1.2	Rat	0.2 mg/mL
IL-4	Pe-Cy7	eBioscience	11B11	Rat	0.2 mg/mL
IL-13	PE	eBioscience	13A	Rat	0.2 mg/mL
IL-17A	PE	eBioscience	17B7	Rat	0.2 mg/mL
Ly6G	APC	eBioscience	1A8	Rat	0.2 mg/mL
Ly6G	FITC	eBioscience	1A8	Rat	0.5 mg/mL
Ly6G	PE	eBioscience	1A8	Rat	0.2 mg/mL
Ly6G	V450	eBioscience	RB6-8C5	Rat	0.2 mg/mL
MHC Class II (I-A/I-E)	PeCy7	eBioscience	M5/114.15.2	Rat	0.2 mg/mL
SiglecF	BV421	eBioscience	E50-2440	Rat	0.2 mg/mL

Table 3-3: Kits

Name	Manufacturer
Intranuclear Staining Kit (FoxP3)	BD Biosciences Europe, Erembodegem, Belgium
RNeasy Mini Kit	QIAGEN GmbH, Hilden
Mouse IL-4 DuoSet	R&D Systems, Wiesbaden
Mouse IL-5 DuoSet	R&D Systems, Wiesbaden
Mouse IL-13 DuoSet	R&D Systems, Wiesbaden
Mouse IL-17A DuoSet	R&D Systems, Wiesbaden
Mouse IFN- γ DuoSet	R&D Systems, Wiesbaden
U-PLEX Biomarker Group 1 (Mouse) multiplex assay	Meso Scale Diagnostics, Rockville, USA

3 Materials and Methods

Table 3-4: Buffers, solutions and culture mediums

Solution	Substances	Storage
10x anesthetic	20 mg/mL Xylazine (Rompun) 50 mg/mL Ketamine (Ketavet)	4°C
1x anesthetic	PBS 2 mg/mL Xylazine (Rompun) 5 mg/mL Ketamine (Ketavet)	4°C
Fixation buffer (ICS)	1:4 dilution of Fix/Perm concentrate in diluent	4°C
Formalin solution	900 mL Aqua dest. 7.8 g Na ₂ HPO ₄ 1.87 g NaH ₂ PO ₄ 100 mL Formalin (37%)	4°C
MACS buffer	AutoMACS-rinsing solution 1% bovine serum albumin (BSA)	4°C
Permeabilization buffer (ICS)	1:10 dilution of Perm in bidest. Water	4°C
RBC lysis buffer	Aqua dest. 155 mM NH ₄ Cl 10 mM NaHCO ₃ 0.1 mM EDTA pH 7.2 – 7.4 sterile	4°C
Restimulation medium	10 % FBS, heat-inactivated 100 µg/mL Streptomycin 100 U/mL Penicillin 1% L-Glutamine (2 mM) Sodium pyruvate 50 µM β-Mercaptoethanol	4 °C
PBS buffer	Aqua dest. 13.7 mM NaCl 0.27 mM KCl	4°C

3 Materials and Methods

	0.81 mM Na ₂ HPO ₄ 0.15 mM KH ₂ PO ₄ pH 7.2 – 7.4, sterile filtered	
RPMI complete	RPMI 1640 1 mM sodium pyruvate 200 mM L-glutamine 100 µg/mL penicillin 100 µg/mL streptomycin 10% FBS	4°C

Table 3-5: Consumables

Name	Manufacturer
Aluminium foil	Carl Roth GmbH & Co. KG, Karlsruhe
Aspiration pipette, sterile	Carl Roth GmbH & Co. KG, Karlsruhe
Cannulas 20, 22, 26, 30G	BD Biosciences Europe, Erembodegem, Belgium
Cell culture plate 6-well	Sarstedt AG & Co., Nümbrecht
Cell culture plate 96-well F-bottom	Greiner BioOne GmbH, Frickenhausen
Cell culture plate 96-well U-bottom	Greiner BioOne GmbH, Frickenhausen
Cell scraper	Sarstedt Inc., Newton, USA
Cell strainer 40 µM	BD Biosciences Europe, Erembodegem, Belgium
Cover glass	Gerhard Menzel GmbH, Braunschweig
Single-use needles 20G, 26G	B. Braun Melsungen AG, Melsungen
Eppendorf reaction vessel 1.0; 2.0 mL	Eppendorf AG, Hamburg
FACS tubes 5 mL	BD Bioscience Europe, Erembodegem, Belgium
Falcon vials 15, 50 mL	Sarstedt AG & Co., Nümbrecht
ELISA panel seal	R&D-Systems GmbH, Wiesbaden
ELISA-Reservoir 25 mL	VWR International GmbH, Darmstadt

3 Materials and Methods

Embedding cassettes	Isolab Laborgeräte GmbH, Wertheim
Low retention pipette tips 10, 200, 1000 µL	Eppendorf AG, Hamburg
Microscope slide sliced, mat edge	Gerhard Menzel GmbH, Braunschweig
Pipette tips loose 10, 200, 1000 µL	Sarstedt AG & Co., Nümbrecht
Pipette tips sterile 10, 100, 200, 1000 µL	Sarstedt AG & Co., Nümbrecht
Quest nitrile gloves, powder-free	Supermax Deutschland GmbH, Gevelsberg
Scalpel	Feather Safety Razor Co. Ltd., Osaka, Japan
Single-use needles 20G, 26G	B. Braun Melsungen AG, Melsungen
Sterile filter 0.22 µM PVDF	Millex/Merck Millipore, Darmstadt
Stick pipette 10 mL	Greiner BioOne GmbH, Frickenhausen
Syringe 10 mL	BD Bioscience Europe, Erembodegem, Belgium
Tracheal cannula OD 1.2	Hugo Sachs, March-Hugstetten

Table 3-6: Devices

Description	Manufacturer
Biological Safety Cabinets	Nuaire Inc., Plymouth, USA
Cell incubator	Nuaire Inc., Plymouth, USA
Cell Sorter FACS Aria III	BD Biosciences, Germany
Centrifuge 5810R	Eppendorf AG, Hamburg
Centrifuge 5424R	Eppendorf AG, Hamburg
Cytospin centrifuge Cellspin I	Tharmac GmbH, Waldsolms
Dissection scissor	WPI Deutschland GmbH, Berlin

3 Materials and Methods

ELISA-Reader Fluostar Omega 0415	BMG Labtech GmbH, Ortenberg
FlexiVent	Scireq Scientific Respiratory Equipment Inc., Montreal, Canada
Flow Cytometer LSR II	BD Biosciences, Germany
Forceps	WPI Deutschland GmbH, Berlin
Heating plate HT200 W	Minitüb GmbH, Tiefenbach
Heating plate MR3002	Heidolph Instruments HmbH & Co. KG, Schwabach
Hot air cabinet	Memmert, Schwabach
iCycler	Bio-Rad Laboratories GmbH, München
Incubator	Heraeus, Hanau
MESO QuickPlex SQ 120	Meso Scale Diagnostics, Rockville, USA
Microscope Leica DM IL LED	Leica Microsystems GmbH, Wetzlar
Microscope camera Leica EC3	Leica Microsystems GmbH, Wetzlar
Multichannel pipette Biohit M300	Sartorius Biohit Liquid Handling Oy, Helsinki, Finland
Neubauer chamber improved	VWR International GmbH, Darmstadt
pH meter Seven easy PH S20-K	Mettler-Toledo, Schwerzenbach, Switzerland
Pipetboy	Integra Bioscience AG, Zizers, Switzerland
Pipettes (0.1-2.5 µL, 0.5-10 µL, 10-100 µL, 200-1000 µL)	Eppendorf AG, Hamburg
Scotsman AF-10/ACM55/AS	Hubbard Ice Systems, Suffolk, Great Britain
Shaker IKA works MS 3 basic	IKA works Inc. Wilmington, USA
Shaker Polymax 1040	Heidolph Instruments GmbH & Co. KG, Schwabach

Steam sterilizer E14 Hydromat	WEBECO Hygiene in Medizin und Labor GmbH & Co. KG, Selmsdorf
Vacunsafe 158310 extraction system	Integra Biosciences GmbH, Fernwald
Vortex Reax 2000	Heidolph Instruments GmbH & Co. KG, Schwabach

3.1.1 Mice and mouse keeping

Table 3-7: Used mouse strains

Used mouse strain	Breeder
BALB/c Wildtype	Charles River Laboratories, Sulzfeld
BALB/c C5ar1 ^{-/-}	In-house breeding
BALB/c Cx ₃ Cr1 ^{GFP/+} C5ar1 ^{+/+}	In-house breeding
BALB/c Cx ₃ Cr1 ^{GFP/+} C5ar1 ^{-/-}	In-house breeding

Table 3-8: Material for the mouse keeping

Material	Manufacturer
Cage changing station CS5	Tecniplast Deutschland GmbH, Hohenpeißenberg
Light- and sound-proof boxes with infrared scan measurement	Own production of the AG Chronophysiology, Prof. H. Oster
Pelletised feed Altromin 1314	Altromin Spezialfutter GmbH & Co. KG, Lage
Polysulfon-cage SealSafe PLUS Mouse (17.5x35.5x13 cm)	Texniplast Deutschland GmbH, Hohenpeißenberg
Super-touchSLIM Plus Blower Unit	Tecniplast Deutschland GmbH, Hohenpeißenberg
Wood litter Abedd LTE E-001	Abedd Lab & Vet Service GmbH, Wien, Austria

3 Materials and Methods

BALB/c wildtype (wt) mice were purchased from Charles River, unless declared otherwise, and bred in a specific pathogen-free facility in the animal facility at the University of Lübeck.

The C5ar1^{-/-} and Cx3cr1^{GFP/+} C5ar1^{-/-} and Cx3cr1^{GFP/+} C5ar1^{+/+} mice on the Balb/c background were from our own breeding. In C5ar1^{-/-} mice C5aR1 has been genetically deleted. In Cx3cr1^{GFP/+} mice, one of the alleles encoding CX3CR1 is replaced by the sequence encoding for GFP, still resulting in a fully functional CX3CR1; these mice were either positive or negative for C5aR1¹⁸³. These animals were used as the littermate control for the experiments. We have compared Cx3cr1^{GFP/+} C5ar1^{+/+} mice with Balb/c WT mice purchased from Charles River. We observed no significant differences regarding behavior, cell numbers or circadian fluctuations of the analyzed cell subsets; therefore we will refer to these mice as WT (Cx3cr1^{GFP/+} C5ar1^{+/+}) and C5ar1^{-/-} (Cx3cr1^{GFP/+} C5ar1^{-/-}).

Seven to eleven week old mice were transferred into sound- and lightproof boxes located at the Institute of Neurobiology, University of Lübeck. Mice were kept under standard laboratory conditions (23±1 °C, 55±5 % humidity) and had free access to tap water and standard mouse diet (pelletized feed). Unless stated otherwise, they were exposed to a 12:12-hours Light-Dark cycle (light phase: 250±50 lux) with lights-on at 05:00 CET. The time of lights-on is defined as Zeitgeber Time (ZT) 0, lights-off as ZT 12. Routine cage changing and stressor exposure during the dark phase were performed under dim red light (<1.5 lux). Animals were individually housed in standard polycarbonate cages, when they were monitored by infrared scan analysis (described below). When not monitored by infrared scan analysis, three mice were kept together in one cage. All mice had to stay in the boxes for at least three days before the start of the experiment to ensure the adaptation to a strict 12:12-h LD cycle. All animals were used in the age of 8-12 wks. In the baseline

experiments, male and female mice were used, while in the allergic asthma model, only female mice were included.

The approval was granted by the Federal Minister for energy transition, agriculture, environment and rural areas of Schleswig-Holstein (reference number: V312-7224.122-39(36-2/13)). The breeding and keeping of the animals took place in accordance with the guidelines of the German Law of Animal Welfare (TierSchG) and was performed by certified personnel.

3.1.2 Software

Table 3-9: Software used for analyses

Program	Company
Adobe Acrobat Reader DC	Adobe Systems Inc., San Jose, USA
BD FACSDiva Software 6.1	BD Biosciences, San Jose, USA
FlowJo v10	FlowJo LLC, USA
FlexiVent Software 5.3	Scireq Scientific Respiratory Equipment Inc., Montreal, Canada
GraphPad Prism 5.0, 8.4.3, 9.2.0	Graph Pad Software Inc., LaJolla, USA
ImageJ 1.49v Software	Wayne Rasband, National Institute of Mental Health, Bethesda, Maryland, USA
Linguee	DeepL GmbH, Köln, Germany
Microsoft Excel 2013	Microsoft Corporation, Redmond, USA
Microsoft Powerpoint 2013	Microsoft Corporation, Redmond, USA
Microsoft Word 2013	Microsoft corporation, Redmond, USA
Omega 1.30	BMG Labtech GmbH, Ortenberg

3 Materials and Methods

Zotero Standalone 4.0

Roy Rosenzweig Center for History
and New Media, USA

3.2 Methods

3.2.1 Activity analysis by infrared scan analysis

Steady state: Mice were kept in individualized sound- and lightproof boxes and monitored by infrared scan analysis. They had to adopt to a strict 12:12h LD cycle for at least 3 days, until they were kept in total darkness (DD) to exclude the light as an outer Zeitgeber. Starting from the moment when the mice were subjected to the DD conditions, the subjective time was defined as circadian time [CT]. After 48 hours in DD conditions, mice had stabilized their free-running rhythms. Then, mice were sacrificed at four different times according to CT3, CT9, CT15 and CT21 (Figure 3-1). The actograms depict the light and dark activity counts, which were statistically analyzed (Figure 3-2).



Figure 3-1: Steady-state analysis of circadian rhythms in pulmonary APCs

The experimental structure of the steady-state experiment to characterize the circadian fluctuation of pulmonary antigen-presenting cells. During the whole experiment, the infrared scan analysis was running. BALB/c WT mice were kept in strict 12:12h LD cycle for at least 3 days following 48h of DD condition. Mice were sacrificed every 6h, a bronchoalveolar lavage was taken and the lungs removed. BAL- and pulmonary cells were analyzed by flow cytometry. WT = wild type, d = days, LD = 12:12h Light dark cycle, DD = total darkness, CT = circadian time, BAL = bronchoalveolar lavage

Four-step immunization: The previous experiment was repeated in a modified mode with immunized mice over the full four-step immunization period. Here, mice were kept in strict 12:12h LD conditions (Figure 3-5). Mice were kept in the boxes for one week to define the individual baseline activity level. This baseline activity defined the correction factor for later

3 Materials and Methods

calculation of relative activity levels. The total number of activity counts were counted during every week of treatment and were divided by the respective correction factor. The resulting relative activity-curves were depicted over time and weekly activity profiles were created to depict activity levels between the different groups.

The four-step immunization protocol for activity surveillance was performed with the support of Anna Kordowski and Anna Valeska Wiese (*Institute for Systemic Inflammation Research, Lübeck*), who performed the immunization. Christiane Koch (*Institute for Neurobiology, Lübeck*) was responsible for the application of the infrared beam and mouse care in the individualized boxes.

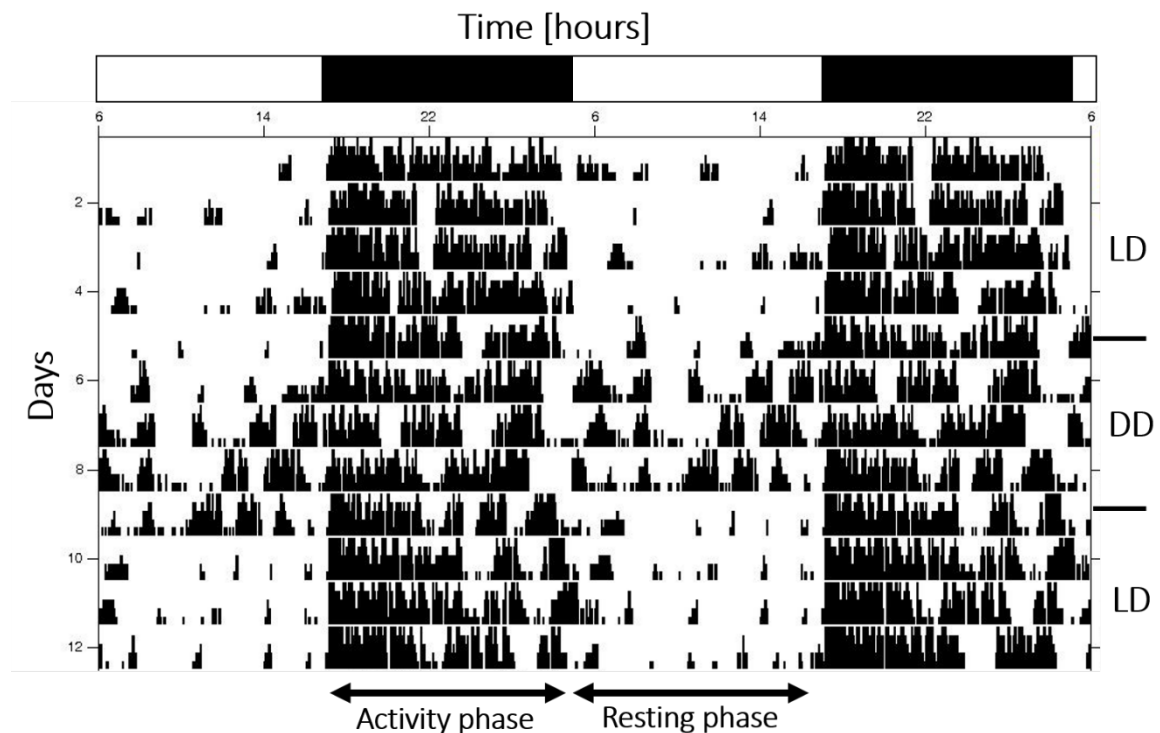


Figure 3-2: Reading an actogram

The actograms visualize the activity level of one individual mouse over a 12-day experimental period. The black vertical bars mark the activity level and are charted side-by-side, while each horizontal line describes one day. The higher an activity bar is, the more movements were detected by infrared scan. The activity and resting phases are clearly distinguishable, as many activity counts are visible during the activity phase, when the light was turned off, and only a few counts were measured during the resting phase, when the light was turned on. On day 6, the switch to DD conditions took place and the mouse showed increased activity during the resting phase. On day 9, the 12:12h LD rhythm started again and the mouse adopted again to the light-driven resting and activity periods. The exemplary actogram is representative of several analyzed mice. LD = 12:12h Light dark cycle, DD = total darkness

3.2.2 Induction of the asthmatic phenotype

To investigate the asthmatic phenotype, mice were immunized intratracheal (*i.t.*) with an HDM extract to induce the pulmonary inflammation¹⁷⁸. It is a standard method in the Köhl lab that has been evaluated and described in BALB/c WT and C5ar1^{-/-} mice^{184,185}. It is easy to perform individually at day and night.

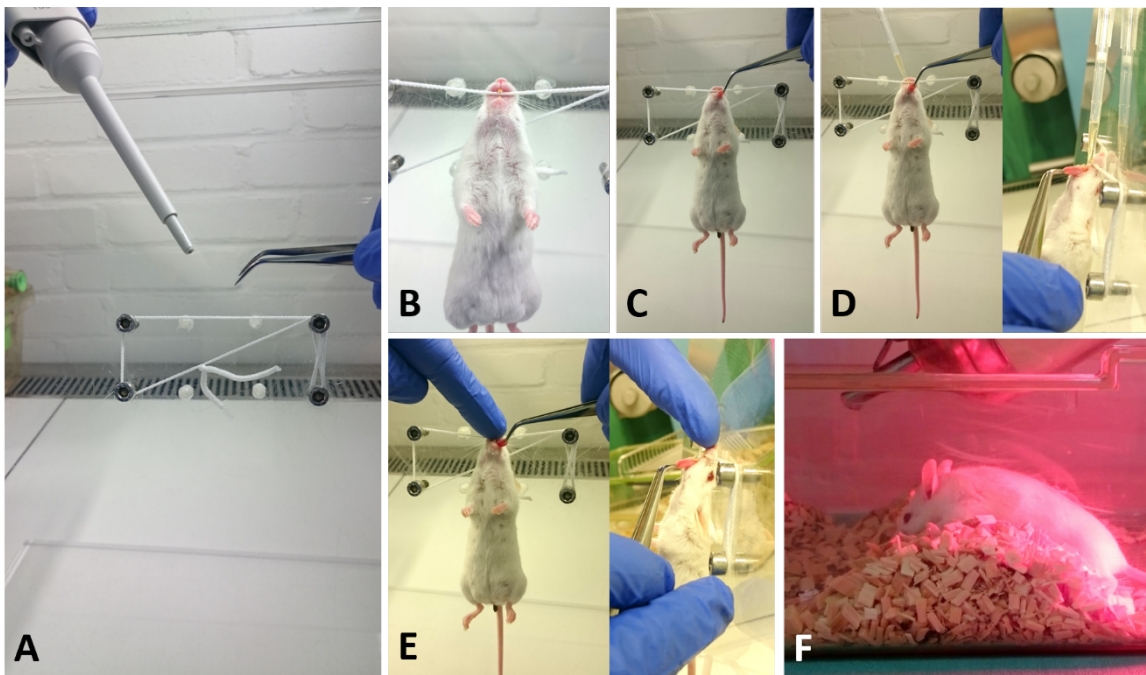


Figure 3-3: Immunization of mice

A) Experimental design for mouse fixation and HDM administration by a pipette. B) The anesthetized mouse (using 1x anesthesia) was mounted with its upper jaw teeth on the elastic rope. C) The tongue was held by a forceps and carefully pulled forward. D) The HDM/PBS solution was dropped into the mouth (frontal and side picture). E) The nose was blocked using a finger and still holding the tongue out of the mouth, until the mouse inhaled the fluid, as evidenced by a slurping sound. F) After the immunization, the sleeping mouse was placed on a litter hill in its cage to improve ventilation and stayed under a heat lamp until waking up (approximately 2h).

One-step immunization: To investigate the influence of the sensitization time on the inflammation severity, a one-step immunization model was used (Figure 3-4). Mice were anesthetized by *i.p.* injection of 300 μ L 1x anesthesia. One group was immunized at ZT 3, the other at ZT 15, as we found here the strongest cell fluctuations in the steady-state experiments (see chapter 4.1, p. 73). Recipient mice were challenged

3 Materials and Methods

once with 50 μL HDM (200 μg) extract *i.t.*; 50 μL PBS *i.t.* was given to control mice (Figure 3-3). After 24h, the corresponding group of mice was sacrificed using 150 μL 10x anesthesia and organs were removed for further analysis.

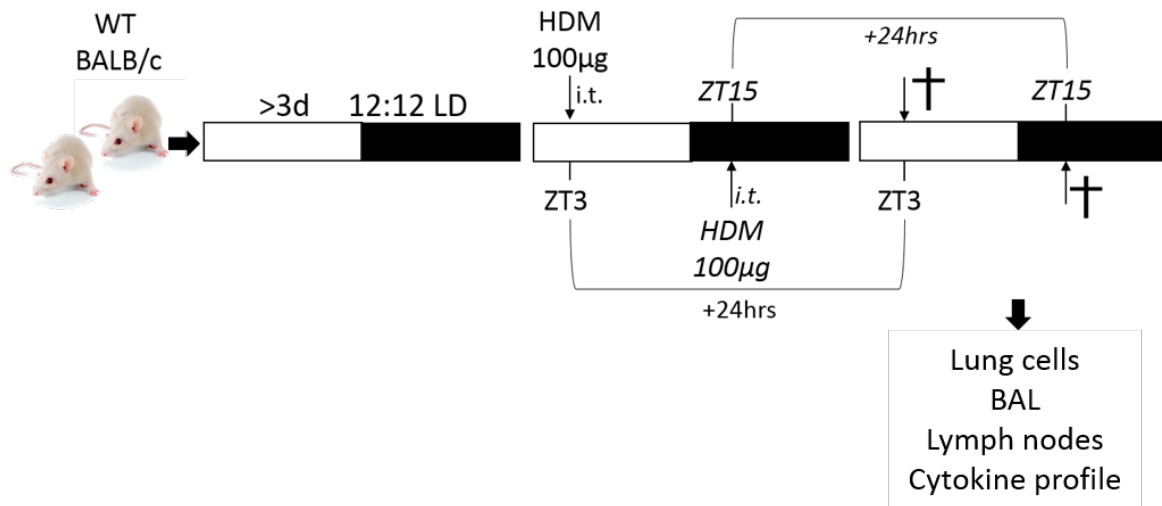


Figure 3-4: One-step immunization model

A one-step-immunization protocol was used to investigate the sensitization phase of allergic asthma in a circadian manner. Mice were kept in strict 12:12h LD conditions for at least 3 days. One group of mice was immunized with 100 μg HDM/PBS *i.t.* at ZT3, while the other was immunized at ZT15. Mice were sacrificed 24h later and organs taken. Lung cells, BALF cells and lymph node cells were analyzed by flow cytometry and the cytokine profile examined by multiplex-assay. WT = wild-type, HDM = house-dust-mite, ZT = Zeitgeber time, hrs = hours, d = days, *i.t.* = intra tracheal, BAL = bronchoalveolar lavage

Four-step immunization: To investigate the effector phase of allergic asthma depending on the circadian rhythm, recipient mice were challenged four times every seven days at precisely the same time (ZT3 resp. ZT15). Test mice received 50 μL HDM (100 μg) *i.t.* at each time point, while control mice got the same amount of PBS (Figure 3-3 and Figure 3-5). Once more, one group was immunized at ZT3, the other at ZT15. 72h after the final immunization, the AHR was determined, and organ samples were harvested for further analyses.

3 Materials and Methods

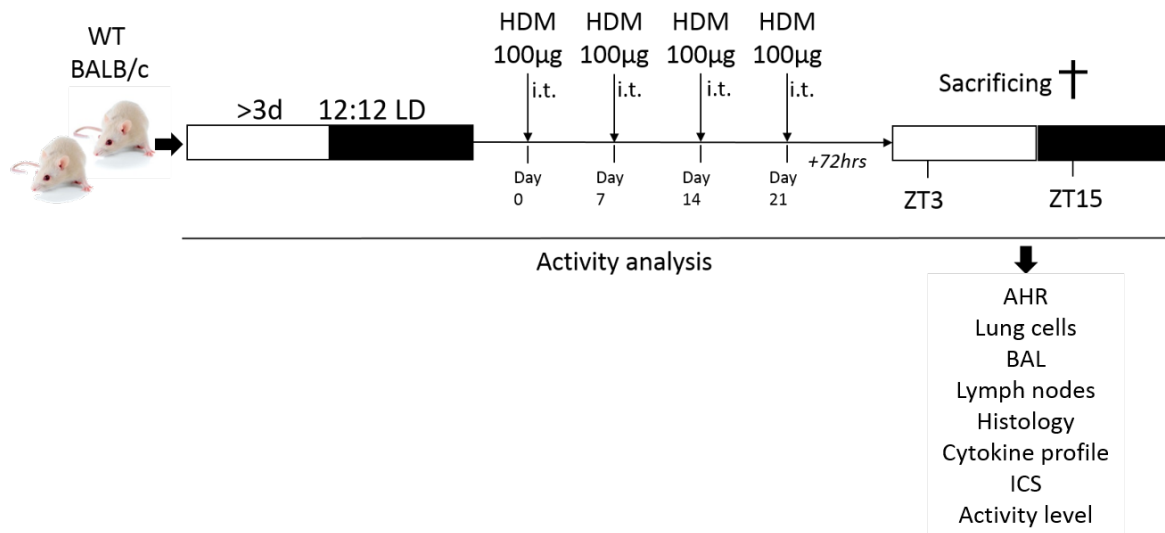


Figure 3-5: Four-step immunization model

A four-step-immunization protocol was used to investigate the effector phase of allergic asthma and the activity level. Mice were entrained for at least 3 days to a strict 12:12h LD cycle, before the first immunization with 100µg HDM *i.t.* One group of mice was immunized at ZT3, while the other group at ZT15 over 4 weeks under consequent infrared scan activity surveillance. 72h after the final immunization, mice were anesthetized and the airway hyperresponsiveness measured. Cells from the left lung lobes, the BALF and the lymph nodes were taken for flow cytometry analyses and the right lung embedded in formalin solution for histological exploration. A cytokine analysis was performed from the lung suspension and the BAL, as well as an intracellular cytokine staining in effector T cells performed. WT = wild type, d = days, hrs = hours, *i.t.* = intra tracheal, AHR = airway hyperresponsiveness, BAL = bronchoalveolar lavage, ICS = intracellular cytokine staining, LD = 12:12h light dark cycle, HDM = house-dust-mite, ZT = Zeitgeber time

3.2.3 Lung function measurement (AHR)

The airway hyperresponsiveness (AHR) is defined as an 'increased unspecific bronchial obstruction in response to pharmacological stimuli such as methacholine, histamine or serotonin'¹⁷⁷. The AHR was measured at the end of the four-step-immunization protocol, to control the successful induction of a full asthmatic phenotype as well as to investigate possible differences in severity related to the different times of immunization (ZT3 vs. ZT15).

The AHR was measured with a flexiVent™-system¹³⁵, which was calibrated following the manufacturer's instructions. Mice were anesthetized by *i.p.* injection of 50 µL 1x anesthesia. Muscle relaxation was induced by *i.p.* administration of 50 µL Esmeron. The skin and larynx muscles were dissected and the trachea exposed so that it could be

opened between two cartilage rings. The cannula of the flexiVent™-system was directly introduced into the tracheal hole and a PEEP (positive end-respiratory pressure) of 2-3 cmH₂O adjusted. The baseline was established by using nebulized PBS and measurement of the lung resistance. Then, an ultrasonic nebulizer generated aerosolized Acetyl-β-Methyl-Choline (1, 2.5, 5, 10, 25, 50, 100 mg/mL) and delivered in-line through the inhalation port for 10s. This parasympathetic substance binds the muscarinic receptors and causes a dose-dependent bronchoconstriction. After 2 minutes, the rising airway resistance was measured by eight so-called snap-shot-maneuvers. The resulting dose-response-curve was depicted as the resistance in [cm H₂O sec mL⁻¹] vs. the corresponding methacholine dose.

3.2.4 Mouse preparation and cell isolation

To investigate the pulmonary immune cell fluctuations, the BALF, the lungs, and the lymph nodes were removed and analyzed (Figure 3-6). The BALF is very sensitive for studying the acute inflammation due to the allergic immune response, as the allergen enters the lung through the airways and meets the first immune cells there. In the lungs, the resulting adaptive immune response can be studied. Activated immune cells migrate from the periphery through the blood vessels to the place of inflammation in the lung tissue. By analyzing the mediastinal lymph nodes, information about migrating immune cells can be obtained.

3 Materials and Methods

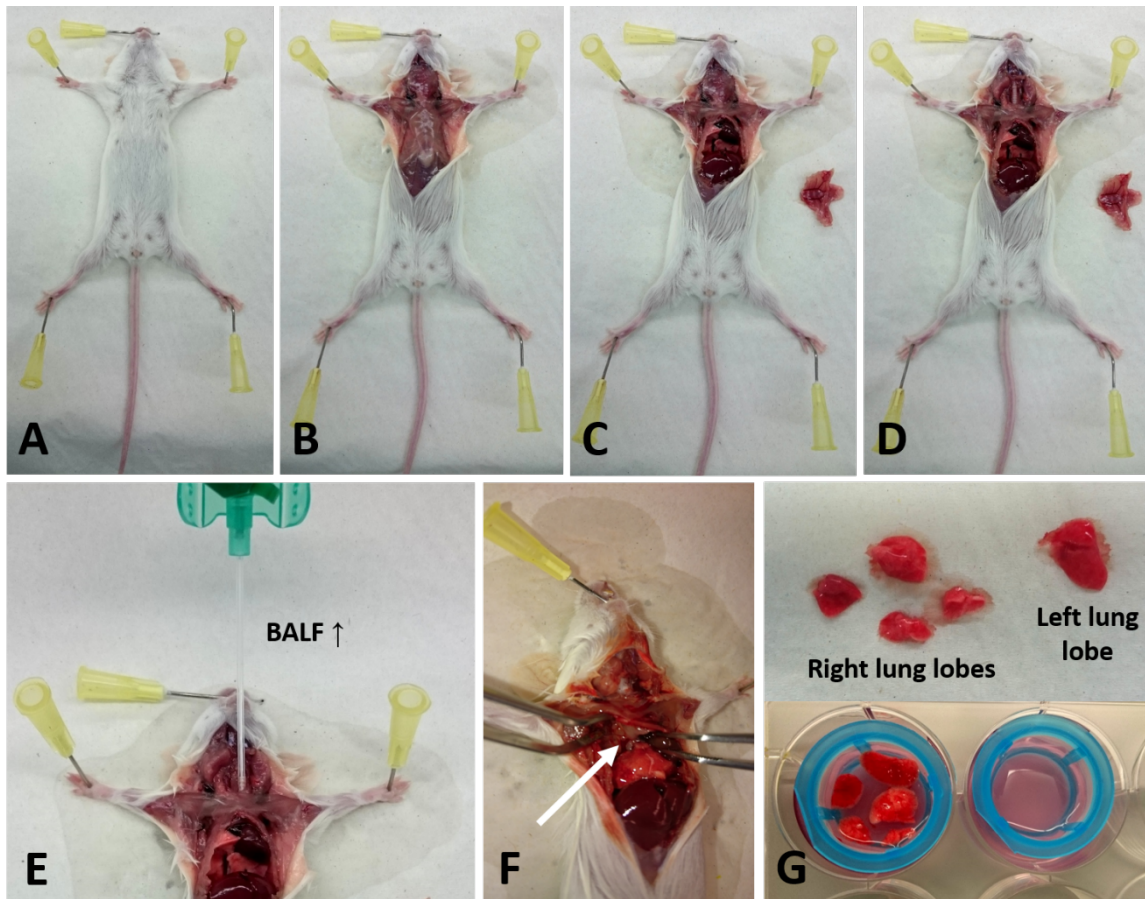


Figure 3-6: Bronchoalveolar lavage, lymph node and lung removal

A) After sacrifice, the mouse was fixed on the preparation plate and disinfected. B) The skin was opened over the chest; the thorax and larynx uncovered. C) The chest cavity was opened and the sternum removed. D) The larynx muscles were excised and the trachea opened. E) A cannula was introduced into the tracheal hole to flush the bronchial tubes and the alveoli to remove the BALF. F) The lymph nodes are located at the triangle trachea-heart-lung and visible as ca 1-2 mm big whitish shimmering spots in the mediastinum (white arrow). They were removed with a forceps and placed in RPMI-filled cell strainer (not depicted). G) Finally, the 4 right and 1 left lung lobes were removed and stored in RPMI medium.

Bronchoalveolar lavage: Mice were anesthetized using 150 μ L 10x anesthesia and the bronchoalveolar lavage fluid (BALF) was obtained by cannulating the trachea. 1.0 mL ice-cold PBS was injected, subsequently aspirated and transferred into Eppendorf tubes (Figure 3-6A-E). The tubes were centrifuged for 10 min at 250g (4°C), lysed in 100 μ L RBC lysis buffer, stopped by adding 900 μ L PBS buffer and counted under the microscope. Cell suspensions stayed in the fridge until continuing with the flow cytometry protocol.

Lymph nodes: Following the cervical dislocation, lymph nodes were removed by opening the chest cavity wide enough to lift easily the upper part from the right lung until the triangle trachea-heart-lung was identifiable. The mediastinal lymph nodes were removed by using forceps, placed on a cell strainer and stored in RPMI buffer (Figure 3-6F) until proceeding with the cell isolation. In the laboratory, the strainer was placed on a 50 mL reaction tube and the cells were isolated by mechanical disruption using a 5 mL syringe stamp. The strainer was washed with 5 mL buffer from the well and the tube centrifuged at 350 x g for 10 min (20°C). The supernatant was removed, the pellet resuspended in 1 mL PBS and the cells counted. Cell suspensions stayed in the fridge until continuing with the flow cytometry protocol.

Lung cells: For analyzing lung cells, the lung lobes were removed, placed in a cell strainer and kept in 5 mL RPMI buffer in 6-well plates (Figure 3-6G). Lung slices were cut under sterile conditions and mixed with 50 μ L Liberase TL (0.25 mg/ml final) and 25 μ L DNase I (0.5 mg/ml final), afterwards incubated at 37°C for 45 min on a shaker. Then the strainer was transferred on a 50 mL tube, the lung slides sieved through the strainer by using a 5mL syringe stamp, and washed three times with complete RPMI medium including 25 μ L DNase I/5 mL. Finally, the solution was centrifuged for 10 min at 350 x g (20°C). The supernatant was discarded, and the pellet resuspended in 3 mL RBC lysis buffer. After 3 min, the lysis was stopped by adding 27 ml PBS (+ 10% FBS to support cell survival). Then, cells were counted in a Neubauer chamber and diluted to a final number of 1×10^6 cells/mL. Cell suspensions stayed in the fridge until continuing with the flow cytometry protocol.

3.2.5 Flow cytometry

Flow cytometry was used to characterize the different cell subsets by analyzing their expressed surface molecules. After purification, the characteristic surface molecules were marked with fluorescent molecules.

Then, the cell suspension was diluted by the FACS machine until a single cell stream could pass by the laser system. This laser activated the fluorescent molecules, and a detector unit recognized the resulting fluorescence and scatter radiation. These light signals were boosted and transformed to electronic signals by a photomultiplier, which are displayed in a data file and analyzed with the FlowJo 10 software. There are two main information to gain: The side scatter (SSC) characterizes the granularity of the cells that gives information about the cell type. The forward scatter (FSC) provides information about the particle size and allows to identify damaged cells and cell debris. To analyze more than one surface molecule at a time, we used various fluorochromes for different antigens, which absorbed and emitted laser light at different wavelengths. However, it is almost impossible to avoid a spectral overlap. Therefore, a compensation is obligatory to correct mathematically the false-positive results. This compensation was performed using CompBeads following the manufacturer's recommendations.

In the following experiments, a BD LSR II flow cytometer was used to analyze BALF and LN suspensions, and a BD FACS Aria III Sorter was used for lung cells, as these were sorted afterwards to continue with subset-specific analyses.

3.2.5.1 Analysis of BAL-, lung and lymph node cells via extracellular staining

Purified and centrifuged cell suspensions were blocked with 100 μ L anti-CD16/32 (diluted 1:100 in PBS) for 20 min (4°C). Cell suspensions were spun down and resuspended in the respective 100 μ L staining solution for 20 min (4°C) (Table 3-10, Table 3-11, Table 3-12 and Table 3-13). Cells were washed once and kept in MACS buffer at 4°C in the dark until the measurement was performed.

Pulmonary and alveolar immune cells were analyzed using recently published gating strategies^{90,128}. Lymph node cells were analyzed with

3 Materials and Methods

the same DC and T cell schemes as pulmonary cells. When GFP-mice were used, the FITC-channel determined the GFP-derived fluorescence signal.

BAL panel: In the BALF (Figure 3-7B), EpCam⁺ epithelial cells were excluded first. Then, alveolar macrophages were identified as CD11c⁺SiglecF⁺ cells, and eosinophils as CD11c⁻SiglecF⁺ cells. In the SiglecF⁻ subpopulation, T cells were identified as CD4⁺Ly6G⁻, and neutrophils CD4⁻Ly6G⁺.

Neutrophil panel: Pulmonary and lymphatic neutrophils were characterized as Ly6G⁺ cells with low SiglecF expression.

T cell panel: T cells were identified as CD3⁺CD4⁺ cells, subdivided in CD44⁻CD62L⁺ naïve, CD44⁺CD62L⁺ central memory, and CD44⁺CD62L⁻ effector cells (Figure 3-7C).

DC panel: Firstly, pulmonary macrophages and lung eosinophils were excluded as SiglecF⁺ cells. Macrophages were identified as SiglecF⁺ CD11c⁺, while eosinophils were SiglecF⁺CD11c⁻ cells. In the SiglecF⁻ fraction, the lineage-positive cells were excluded. These were B cells (CD 19), T cells (CD3e), natural killer cells (CD49b) and neutrophils (Ly6G). The remaining SiglecF⁻lineage⁻ population depicted different pulmonary CD11c⁺MHCII⁺ dendritic cell (DC) subsets. These were identified and sorted using the gating strategy displayed in Figure 3-7A. There, conventional DCs (cDC) were subdivided into a CD103⁺CD11b⁻CD64⁻ (cDC1), and a CD103⁻CD11b⁺CD64⁻ (cDC2) population, and moDCs were identified as CD103⁻CD11b⁺CD64⁺cells.

Table 3-10: Antibodies used to stain BALF cells

Epitope	Conjugate	Dilution
CD4	PeCy7	1:400
Ly6G	FITC	1:400
SiglecF	BV421	1:400
CD11c	APC	1:400

3 Materials and Methods

EpCam PE 1:400

Table 3-11: Antibodies used to stain T cells in lung- and lymph node suspensions

Epitope	Conjugate	Dilution
CD3	FITC/AF488	1:400
CD4	PeCy7	1:400
CD44	BV421	1:400
CD62L	APC	1:400

Table 3-12: Antibodies used to stain neutrophils in lung- and lymph node suspensions

Epitope	Conjugate	Dilution
Ly6G	APC	1:400
SiglecF	BV421	1:400

Table 3-13: Antibodies used to stain DCs in lung- and lymph node suspensions

Epitope	Conjugate	Dilution	
CD3e	V450	1:300	} Lineage
CD19	V450	1:300	
CD49b	V450	1:300	
Ly6G	V450	1:300	
SiglecF	BV421	1:300	
MHCII (I-A/I-E)	PeCy7	1:1500	
CD11b	BV510	1:800	
CD11c	APC	1:800	
CD64	PE	1:800	
CD103	PerCb Cy5.5	1:800	

3 Materials and Methods

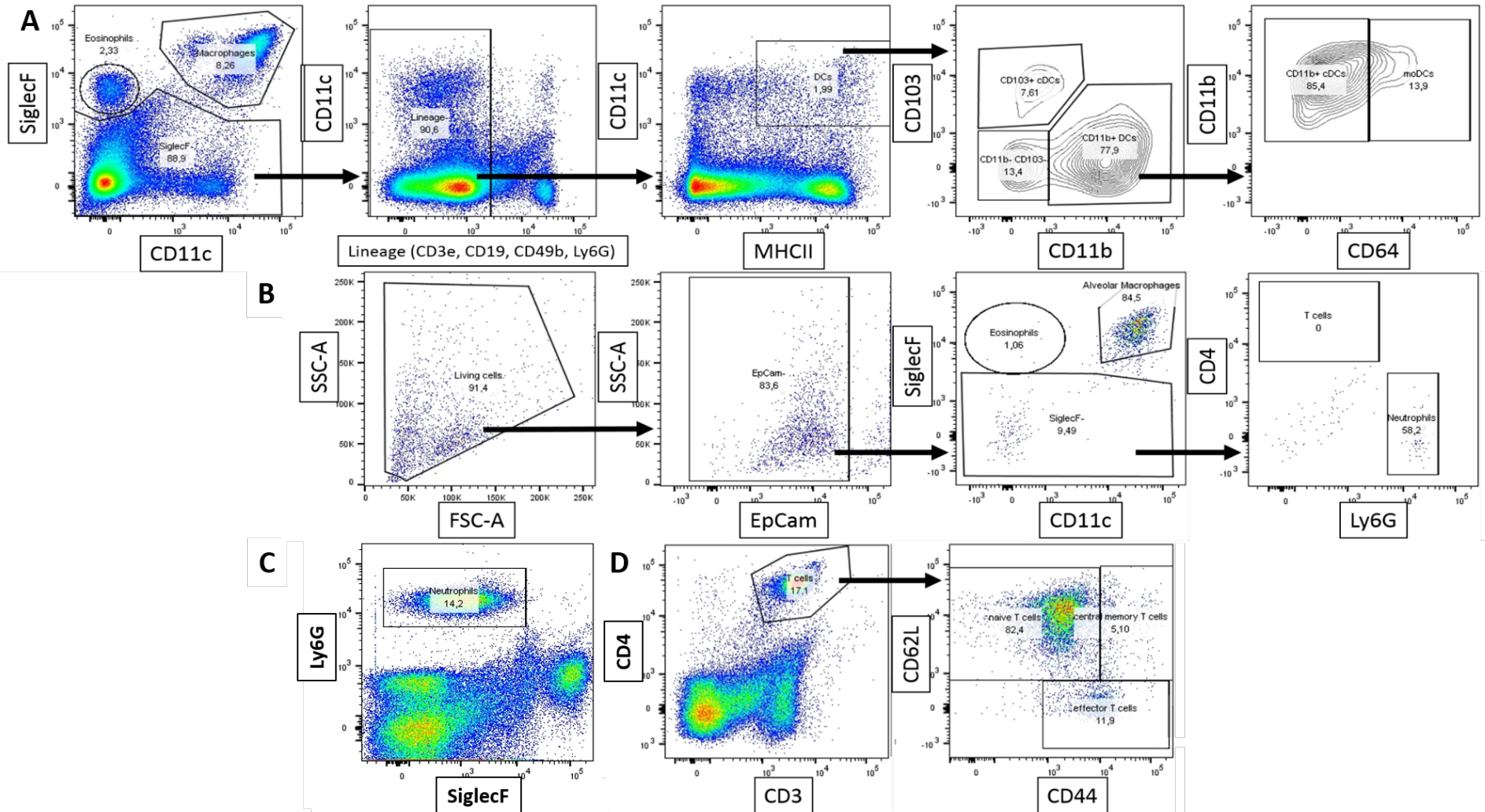


Figure 3-7: Gating strategies for lung cell and BALF suspensions

3 Materials and Methods

Cell suspensions were processed and stained for flow cytometry following the described protocols. The cells were analyzed using the presented above gating strategy. A) DC panel: Eosinophils (CD11c⁻) and macrophages (CD11c⁺) were identified as SiglecF⁺ cell subsets. The SiglecF⁻ population was analyzed for CD11c and the lineage (CD3e, CD19, CD49b, Ly6G) that excluded NK cells, B cells, T cells and lymphocytes. By using CD11c and MHCII, conventional DCs were determined. CD103 and CD11b subdivided the cDCs as CD103⁺CD11b⁻ subset, called CD103⁺ cDCs (cDC1), and a CD103⁻CD11b⁺ subset. The latter population could be subclassified in a CD11b⁺CD64⁻, called CD11b⁺ cDCs (cDC2), and a CD11b⁺CD64⁺ population, called moDCs. B) BALF panel: First, living cells were gated by a SSC-A >20K and a FSC-A >50K. Then, epithelial cells (EpCam⁺) were excluded. Macrophages (CD11c⁺) and eosinophils (CD11c⁻) were separated as SiglecF⁺ populations. The SiglecF⁻ cells were analyzed for CD4⁻ and Ly6G expression. CD4⁺ T cells are CD4⁺Ly6G⁻, while neutrophils can be described as CD4⁻Ly6G⁺. C) Neutrophil panel: Neutrophils are characterized as Ly6G⁺ with low SiglecF expression. D) T cell panel: The T cell population is characterized as CD3⁺CD4⁺ cells. By using CD62L and CD44, three subpopulations could be identified. Naïve T cells are CD62L⁺CD44⁻, central memory T cells CD62L⁺CD44⁺ and effector T cells CD62L⁻CD44^{int}. The exemplary graphs are representative for the performed flow analyses.

3.2.5.2 Intracellular cytokine staining of T cells

While flow cytometry is a common tool to identify immune cells via staining of surface molecules, it can also be used to discriminate the several T cell subsets. Using selective markers for extra- and intracellular proteins, T cell subsets can be characterized by their cytokine production and the expression of certain transcription factors (Table 3-14).

Table 3-14: Characterization of T cell subsets via extra- and intracellular cytokine staining

Republished and revised with permission of John Wiley and Sons from 'Comprehensive Phenotyping of T Cells Using Flow Cytometry' ¹⁸⁶; permission conveyed through Copyright Clearance Center, Inc.

	Th1	Th2	Th17	T_{reg}
<i>Extracellular</i>				
CD3	+	+	+	+
CD4	+	+	+	+
CD44	int	int	int	int
<i>Intracellular</i>				
FoxP3				+
<i>Intracellular upon stimulation</i>				
IFN- γ	+	-	-	
IL-4	-	+	-	
IL-10		+		+
IL-13		+		
IL-17A			+	

Boxes marked negative (-) indicate antigens, transcription factors or cytokines which are not expressed or produced by the corresponding subset. An empty box indicates that this is not used for the discrimination of a specific subset. int = intermediate

Basically, the intracellular cytokine staining (ICS) protocol consists of four steps: (1) stimulation, (2) fixation and permeabilization, (3) staining and (4) detection by flow cytometry ¹⁸⁷.

First, the digested full lung suspension was diluted in restimulation medium and seeded in 96-well plates. For each mouse lung, four wells were prepared by adding 1×10^6 cells/200 μ L each, as two wells were used for stimulated and two for unstimulated cells. Additionally, wells for Fluorescence minus one (FMO) controls and an unstained control were

3 Materials and Methods

prepared to allow precise definition of stained and unstained cell populations. The 96-well plate was stored at 4°C overnight to slow down cellular metabolism.

The next day, cytokine production was stimulated by adding phorbol 12-myristate 13-acetate (PMA) and calcium ionophore (ionomycin) only to the stimulated samples. To block cytokine secretion, the Golgi system inhibitors brefeldin A and monensin were used for stimulated and unstimulated samples (for concentration see Table 3-15). To each sample, 50 µL of the 5x mix were added and the plate was incubated for 4 h in the incubator. Then, cell suspensions were transferred from the 96-well plate into Eppendorf tubes, centrifuged for 3 min at 2600 x g, washed once with PBS, again spun down for 3 min at 2600 x g and the supernatant was discarded.

Table 3-15: Scheme for preparation of the stimulation mix

	Stock concentration	5x concentration	Working concentration
PMA	1mg/mL	250ng/mL	50ng/mL
Ionomycin	1mg/mL	2500ng/mL	500ng/mL
Monensin	1000x	5x	1x
Brefeldin	1000x	5x	1x

The second step included fixation and permeabilization. The cell pellet was resuspended in 100 µL fixation buffer and incubated for 1h at 4°C to make the cell surface permeable for antibodies to enable intracellular staining. Afterwards, 100 µL Fc-block (1:100 dilution in permeabilization buffer) were directly added to the sample and incubated for another 20 min at 4°C. Then, the tubes were spun down at 2600 x g for 6 minutes.

Due to the restriction in lasers and fluorochromes, two different mastermix solutions were prepared for the respective staining panels (Table 3-16, Table 3-17 and Table 3-18). After centrifugation,

3 Materials and Methods

supernatants were discarded, each pellet resuspended in 100 μ L mastermix and incubated for 15 min at 4°C. The staining was completed by two washing steps with permeabilization buffer and finally, the pellet was suspended in MACS buffer for flow cytometry at the BD LSR II flow cytometer.

Table 3-16: Scheme I for intracellular cytokine staining of T cells

Epitope	Conjugate	Dilution
CD3	AF488 (FITC)	1:200
CD4	PeCy7	1:300
CD44	BV421	1:300
IL-4	PE	1:200
FoxP3	APC	1:200

Table 3-17: Scheme II for intracellular cytokine staining of T cells

Epitope	Conjugate	Dilution
CD3	AF488 (FITC)	1:200
CD4	PeCy7	1:300
CD44	BV421	1:300
IL-13	PE	1:200
IL-10	APC	1:200

Table 3-18: Scheme III for intracellular cytokine staining of T cells

Epitope	Conjugate	Dilution
CD3	AF488 (FITC)	1:200
CD4	PeCy7	1:300
CD44	BV421	1:300
IL-17A	PE	1:200
IFN- γ	APC	1:200

Effector T cells were identified as CD3⁺ CD4⁺ CD44^{int}. The respective cytokine⁺ population was identified (Figure 3-8), as well as cell subset levels calculated as a percentage of effector T cells.

This experiment was performed with the support of Anna Valeska Wiese (*Institute for Systemic Inflammation Research, Lübeck*).

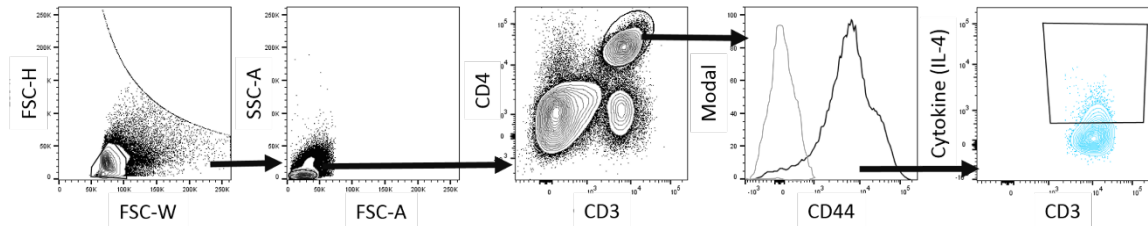


Figure 3-8: Gating strategy for intracellular stained T cells

ICS suspensions were processed and stained for flow cytometry following the described protocol. The cells were analyzed using the gating strategy presented above. First, cell doublets were excluded in the FSC-H vs. FSC-W scatter plot. Then, living cells were gated by a SSC-A >20K and a FSC-A >50K. The T cell population was identified as CD3⁺CD4⁺ cells and effector T cells by intermediate CD44 expression using histogram analysis. Finally, the cytokine of interest was plotted against CD3 and the cytokine-expressing cells analyzed. The exemplary graphs are representative for the performed flow analyses and were provided generously by Anna Valeska Wiese (*Institute for Systemic Inflammation Research, Lübeck*).

3.2.6 Analyzing the cytokine profile

The cytokine profile was investigated at the end of the one-step and four-step immunization to determine the cell activation profile. The standard enzyme-linked immunosorbent assay (ELISA) method was used to assess the cytokine production in stimulated full lung suspensions, while the multiplex assay was utilized to detect cytokine levels in the BALF.

3.2.6.1 Analyzing stimulated cell suspensions by ELISA

A sandwich ELISA is a common tool to detect and quantify cytokine levels in body fluids. First, a fixed capture antibody detects and captures the respective cytokine in the fluid. Then, a second, enzyme-coupled cytokine antibody is used to detect the same cytokine. The enzyme reacts with the substrate changing color upon activation. As light absorption depends on the color depth responding to the enzyme activity, the cytokine concentration can be determined.

To investigate cytokine levels upon four-times allergen stimulation, purified lung cell suspensions were diluted to 2.5×10^5 cells/150 μ L in restimulation buffer. Six wells of one 96-well plate (U-bottom) were filled each with 150 μ L cell suspension per mouse, while one unstimulated control per mouse was running on a separate 96-well plate. The plates were kept in the incubator at 37°C and 5% CO₂ for 24h. After 24h, the samples were restimulated with 30 μ g/mL HDM (resp. 0.45 μ L HDM per 150 μ L cell suspension) and kept in the incubator for another 72h. Afterwards, plates were centrifuged for 10 min at 350 x g and 4°C, and supernatants were analyzed for the production of IL-4, IL-5, IL-10, IL-13, IL-17A and IFN- γ using DuoSet ELISA kits, following the manufacturer's protocol. The detection limit was 16 pg/mL for IL-4 and IL-17A, 31 pg/mL for IL-5, IL-10 and IFN- γ , and 62.5 pg/mL for IL-13. This experiment was performed in cooperation with Anna Kordowski (*Institute for Systemic Inflammation Research, Lübeck*).

3.2.6.2 Analyzing the BALF cytokine profile by multiplex analysis

BALF supernatants from the one-step and four-step immunization protocol were analyzed by multi-array technology® provided by Meso Scale Diagnostics. By using the so-called multiplex assay, which is basically a sandwich immunoassay, the parallel determination of up to ten cytokine concentrations was possible. A special electrochemoluminescence detection resulted in increased sensitivity and facilitated the detection of very low cytokine levels¹⁸⁸.

To get a full picture of pro- and anti-inflammatory cytokines present in the BAL, we used an assay comprising erythropoietin (EPO), granulocyte-macrophage colony-stimulating factor (GM-CSF), keratinocyte-chemoattractant/human growth-regulated oncogene (KC/GRO, also known as CXCL1), IFN- γ , IL-1 β , IL-2, IL-4, IL-5, IL-6, IL-10, IL12p70, IL-13, TNF- α and vascular endothelial growth-factor A (VEGF-A). We followed the manufacturer's protocol¹⁸⁹ when preparing U-PLEX-plates

and analyzed these on MESO QuickPlex SQ 120 machine. The detection limits are given below (Table 3-19).

The multiplex assay of the BALF samples was performed in collaboration with Inken Schmudde (*Institute for Systemic Inflammation Research, Lübeck*).

Table 3-19: Detection levels for multiplex cytokine analysis

Cytokine	Detection limit	Cytokine	Detection limit
GM-CSF	0.16 pg/mL	CXCL1	0.40 pg/mL
VEGF	0.77 pg/mL	IFN- γ	0.16 pg/mL
IL-1 β	3.10 pg/mL	IL-2	1.10 pg/mL
IL-4	0.56 pg/mL	IL-5	0.63 pg/mL
IL-6	4.80 pg/mL	IL-10	3.80 pg/mL
IL12p70	48.00 pg/mL	IL-13	2.70 pg/mL
TNF- α	1.30 pg/mL		

3.2.7 Histology

Histologic evaluation was performed at the end of the four-step immunization protocol to visualize the pulmonary inflammation.

3.2.7.1 Embedding of lung slides in paraffin

After measuring the AHR and performing the BAL, the left lung lobes were removed, placed in a histology cassette and stored in phosphate-buffered formalin (3.7%) for 2-3h. Then, the cassettes were washed in 500 mL water in a shaker overnight to avoid formalin-induced artefacts during the following staining. Then, the cassettes were stored in 70% Isopropanol. The samples were then dehydrated in a raising ethanol-series, embedded in paraffin and finally cut into 5 μ m histologic slides with a microtome by professional staff at the department of Anatomy, University of Lübeck.

3.2.7.2 Periodic acid-Schiff (PAS) staining

The histochemical PAS staining allows to determine the amount of mucus production in the airways. It detects polysaccharides and mucous substances, e.g. glycoproteins, mucins and glycogen. PAS staining contains periodic acid, which oxidizes free hydroxyl groups of saccharides, resulting in aldehyde groups. These aldehydes react with the Schiff reagent resulting in a purple-magenta color, making mucus visible in the histologic lung slides. This step was performed by the anatomy department at Lübeck University in collaboration with Prof. Dr. med. Peter König.

Firstly, the histological samples were deparaffinized and rehydrated. Then, the first staining was performed as the samples were covered with periodic acid and washed. This step was followed by the staining with the Schiff-reagent and another washing step. To ease the detection of the PAS-stained tissue, a counterstaining was performed using hemalaun. The samples were dehydrated by increasing ethanol-series with final replacement of ethanol by xylol. Finally, the samples were mounted with entellan.

For each mouse, four slices representing different regions of the left lung were selected. In representable alveoli, the mucus-free area was calculated through the limiting mucus, and the total area by the limiting epithelium. Finally, the percentage mucus area was calculated by the ratio of the mucus and epithelial area, and the mean value of mucus producing airways of the four selected slices was calculated. Histological slides were analyzed and photos taken using the Leica microscope DM IL LED. The histological images were analyzed using the ImageJ 1.49v Software.

The analysis and calculation were performed in collaboration with PD Dr. Yves Laumonier (*Institute for Systemic Inflammation Research, Lübeck*).

3 Materials and Methods

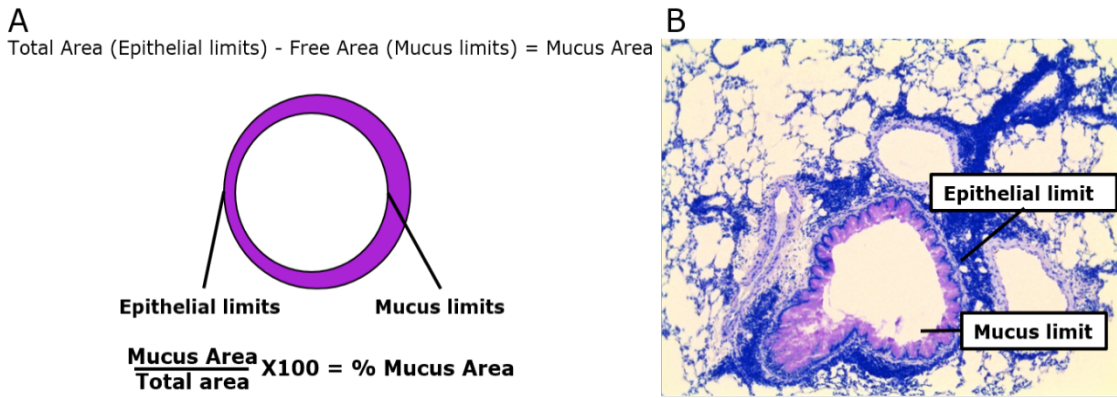


Figure 3-9: Calculation of mucus area in lung histological slides

For histological analysis, lung lobes were prepared and stained with PAS to define mucus production. A) The calculation of the mucus area was done in two steps. First, the total area limited by the surrounding epithelium was subtracted from the free alveolar area limited by the mucus. Second, a percentage calculation was performed by computing the ratio of the mucus and the total area. B) An exemplary PAS-stained histological slide of an HDM-immunized mouse lung is shown (original magnification $\times 200$). Shown is an alveolus, containing a thickened mucus layer covering the epithelium. The epithelial and mucus limits are marked.

3.2.8 Statistical analysis

Statistical analyses were performed using GraphPad Prism (versions 5.0 and 8.4.3.). The obtained data sets were trimmed for outliers using the Grubb's test¹⁹⁰ with the open source program GraphPad QuickCalcs. The cut-off was determined beyond the 95. percentile.

Overall, this work can be subdivided in three types of experiments: i) comparison of two groups with one independent variable (IV), ii) comparison of more than two groups with one variable and iii) comparison of more than two groups with two variables (Figure 3-10, p. 12). When discussing type (IV), it is categorized into variables between-subjects or variables within-subjects according to the testing strategy. Between-subject variables describe different groups for every level of the variable. Within-subjects variables test each subject on every level of the variable (Table 3-20). After choosing the respective statistical test to calculate significant differences between the group or a whole, detailed information about the compared groups was obtained by performing posttests (Tukey's post-hoc multiple comparisons test for computing

every possible comparison or Bonferroni posttest when comparing selected means ¹⁹¹).

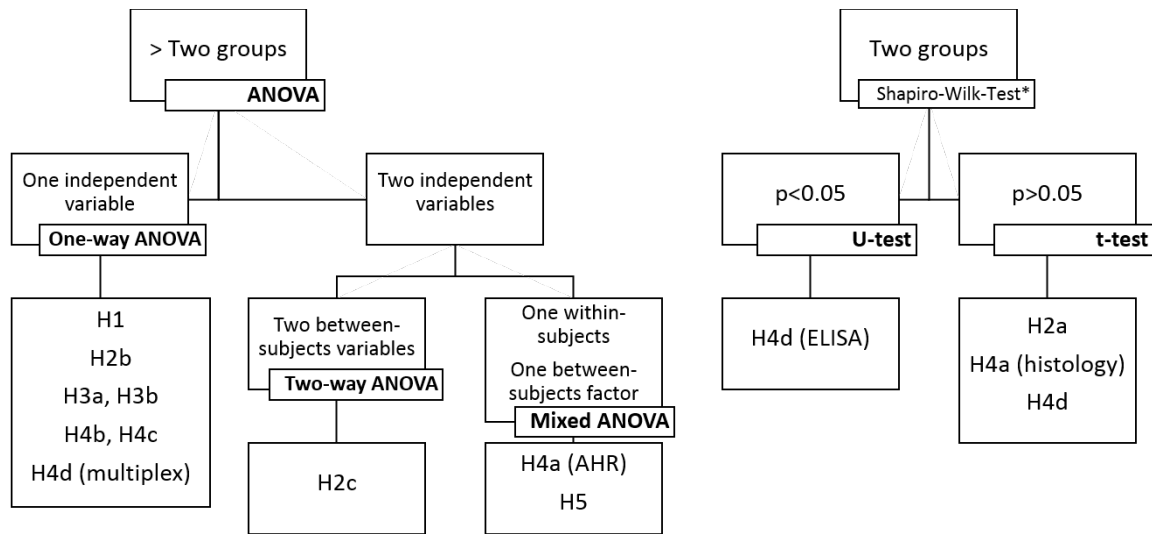


Figure 3-10: Overview about statistical methods

The graph outlines the decision tree about choosing the appropriate statistical method. To each statistical test, the respective tested hypotheses are shown in the final subtree. * test for assumption of normal distribution. H = hypothesis, ANOVA = analysis of variance, U = Wilcoxon-Mann-Whitney-U-test, t = two-tailed unpaired student's t-test, AHR = airway hyperresponsiveness, ELISA = enzyme-linked immunosorbent assay.

In general, normal distribution is a requirement when comparing different groups statistically. As the number of samples was below 30 in our study and a Gaussian distribution could not be assumed, every data set was tested first with the Shapiro-Wilk-test first ¹⁹². A significant ($p < 0.5$) Shapiro-Wilk-test defined non-normal distribution and the data set was analyzed by a non-parametric Wilcoxon-Mann-Whitney-U-test (U-test). A non-significant ($p > 0.5$) Shapiro-Wilk-test defined a normal distribution and the data set was analyzed by a two-tailed unpaired student's t-test (t-test). Concerning the analysis of variance (ANOVA), latest research results showed that one-way ANOVA is robust over for non-normal data ¹⁹³. Hence, these data sets were not tested for Gaussian distribution.

Most data sets were plotted in scatter plots depicting replicates, mean and standard error of mean (SEM); exceptions are mentioned in the respective graph descriptions.

Table 3-20: Overview about hypotheses, the related independent and dependent variables as well as performed statistical analysis

B1: between-subjects variable one, B2: between-subjects variable two, W: within-subjects variable, H: hypothesis, ANOVA = analysis of variance, U = Wilcoxon-Mann-Whitney-U-test, t = two-tailed unpaired student's t-test.

Hypothesis	Independent variable	Dependent variable	Statistical test
H1	Time of sacrifice	Total cell number, cell subset number	one-way ANOVA
H2a	Activity level	Lightening condition	t-test
	Activity level	Genotype	t-test
H2b	Time of sacrifice	Total cell number, cell subset number	one-way ANOVA
H2c	B1: Genetic background B2: Time of sacrifice	Cell subset number	two-way ANOVA
H3a	Time and type of treatment	Cell subset number	one-way ANOVA
H3b	Time and type of treatment	Cell subset number	one-way ANOVA
H4a	W: Individual mouse B: Methacholine dose	Airway hyperresponsiveness	mixed ANOVA
	Time and type of treatment	Mucus overproduction	t-test
H4b	Time and type of treatment	Cell subset number	one-way ANOVA
H4c	Time and type of treatment	Cell subset number	one-way ANOVA
H4d	Time and type of treatment	Cytokine level	U-test / t-test
H5	W: Individual mouse B: Time	Activity level	mixed ANOVA

A p value < 0.5 is shown as * or §, $p < 0.01$ as ** or §§ and $p < 0.001$ as *** or §§§. Significant p values in the data sets are shown in the respective experiments. Significant but not hypothesis-related relevant results are not shown in the respective graphs but listed together with the detailed statistical results in the appendix. Detailed information about the comparison of two groups is given in Table 7-1 (p. 155), about more than two groups with one condition in Table 7-2 (p. 156) and about more than two groups with two conditions in Table 7-3 (p. 162).

4 Results

4.1 The circadian rhythm regulates the steady-state distribution of pulmonary APCs

Self-sustained circadian rhythms were reported already in several organs, e.g. the intestine or the lung tissue ¹⁴³. Here, it could be shown that they also drive the distribution of pulmonary APCs in steady-state conditions.

The steady-state analysis was performed on DD-entrained mice to investigate the numbers of pulmonary immune cells over 24h. The outer Zeitgeber light was excluded (DD conditions), as mice were kept in total darkness 48h before sacrificing, to ensure that only inner-clock-related rhythms were detected ¹⁸¹. Simultaneously, the activity of mice was recorded to assess whether the mice showed a normal sleep-wake behavior under DD-conditions (Figure 4-1).

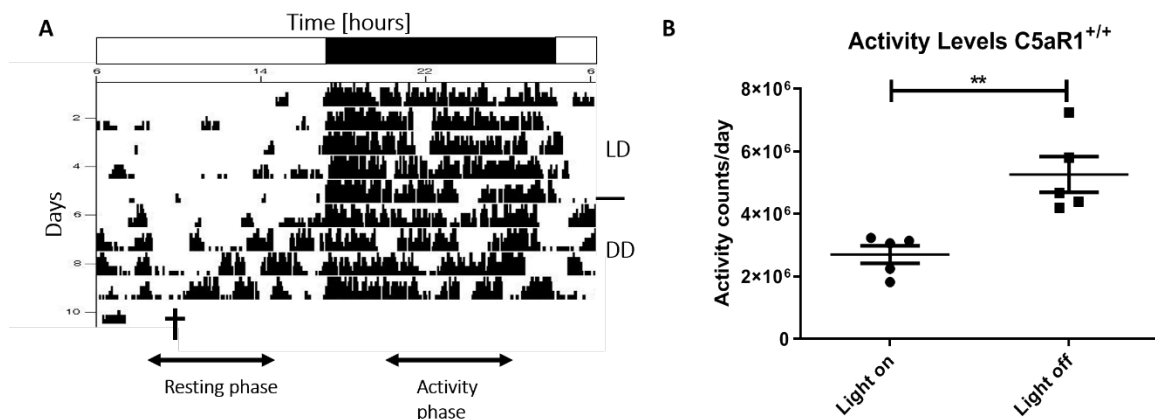


Figure 4-1: Activity levels of C5aR1^{+/+} WT mice

The actograms were analyzed following the explanations as described above, and a statistical analysis of the activity levels performed. A) Actogram of a C5aR1^{+/+} WT mouse, depicting six days in 12:12h LD condition, followed by four days of total darkness (DD). Depicted are the registered activity counts over time. Each horizontal bar describes 24h, resp. one day. The white and the black bar at top of the actogram depicts light and darkness. B) Quantification of the activity levels of C5aR1^{+/+} mice during the resting (light on) and activity phase (light off). Each dot represents the activity level of one individual mouse. n=5; data are expressed as mean \pm SD, data were analyzed by unpaired t-test; black circles = light on, black squares = light off, cross = time of sacrifice. ** p<0.01

4.1.1 Pulmonary macrophages and cDC2s fluctuate inversely in steady-state conditions

We have chosen four time points (CT3, CT9, CT15 and CT21) to obtain a comprehensive picture of the circadian cell fluctuations in the lung. After 48h entrainment to total darkness, mice were sacrificed at the indicated time, a bronchoalveolar lavage performed and the lungs were taken for cellular analyses by flow cytometry.

In the BALF, I found no significant difference in the total number of immune cells at any time point (Figure 4-2A). Further, I did not observe any significant changes in the number of alveolar macrophages, the only immune cell subset present in steady-state conditions (Figure 4-2B).

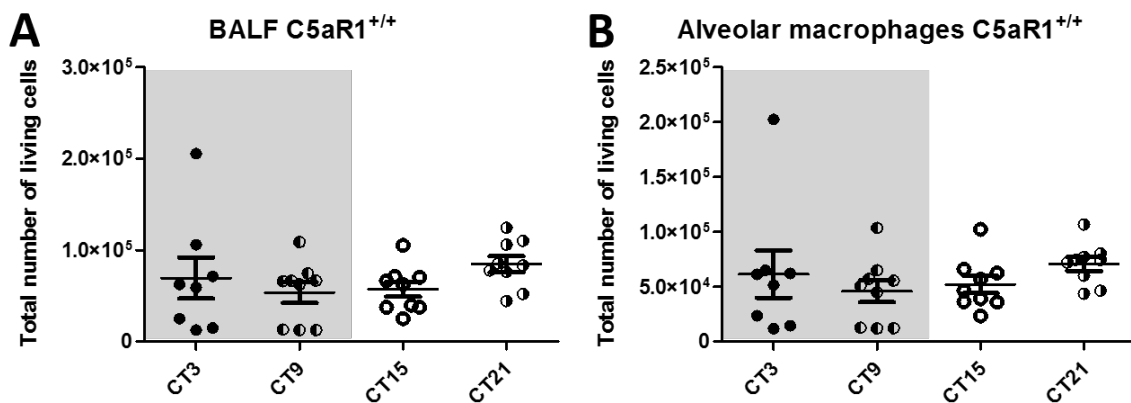


Figure 4-2: Alveolar macrophages do not fluctuate in a circadian manner.

Mice were kept in strict DD condition 48h before sacrificing to ensure the exclusion of any outer Zeitgeber. After sacrificing every 6h (CT3, CT9, CT15, CT21), BALF cells were obtained and processed as described. After staining with fluorescently labelled antibodies, cell suspensions were analyzed by flow cytometry and cell populations defined using the BALF gating strategy. A) Total number of BALF cells, and B) number of alveolar macrophages. Each dot represents the cell number of one individual mouse lung. n=8-9; three independent experiments. Data are expressed as mean \pm SD and were analyzed by one-way ANOVA with Tukey's multiple comparison test. Gray background = resting phase, white background = activity phase.

The overall number of pulmonary immune cells stayed stable over 24h (data not shown). In BALB/c WT mice, I observed an opposing oscillation of pulmonary macrophages and cDC2s (Figure 4-3 A and B). Pulmonary macrophages showed a significant ($p < 0.05$) peak at CT15, the early activity phase, compared to CT9, the late resting phase. In contrast, the

4 Results

number of CD11b⁺ cDC2s was significantly lower during the activity phase, i.e. at CT15 and CT21, as compared to CT3 ($p < 0.05$), during the early resting phase. There were no significant fluctuations in eosinophils or CD103⁺ cDC1s over time (Figure 4-3C and D).

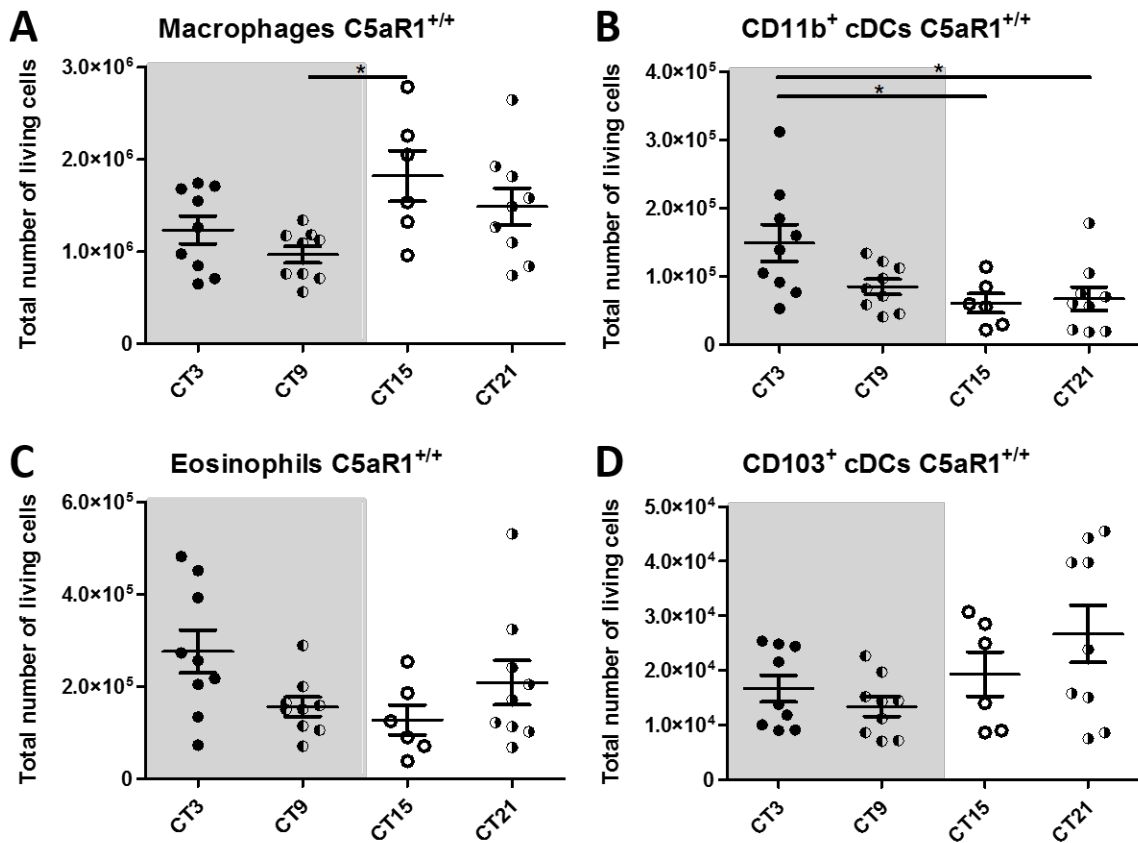


Figure 4-3: Pulmonary macrophages and cDC2 cells fluctuate over 24h in C5aR1^{+/+} WT mice.

Mice were kept in strict DD condition 48h before sacrificing to ensure the exclusion of any outer Zeitgeber. At CT3, CT9, CT15 and CT21, lungs were removed and pulmonary cells isolated and processed as described. After staining with fluorescently labelled antibodies, cell suspensions were analyzed by flow cytometry and cell populations defined using the DC gating strategy. Cell numbers of A) pulmonary macrophages, B) CD11b⁺ cDCs (cDC2), C) eosinophils, and D) CD103⁺ cDCs (cDC1) are depicted. Each dot represents the cell number of one individual mouse lung. $n = 6-9$; three independent experiments. Data are expressed as mean \pm SD and were analyzed by one-way ANOVA with Tukey's multiple comparison test. Gray background = resting phase, white background = activity phase. * $p < 0.05$

4.1.2 Impact of C5aR1-deficiency on circadian activity

Analogous to circadian analysis of C5aR1^{+/+} mice (Figure 4-1), an infrared scan analysis was also performed in C5aR1-deficient mice.

4 Results

Similar to the findings with WT mice, C5aR1^{-/-} mice showed significantly higher activity levels when the light was turned off (Figure 4-4).

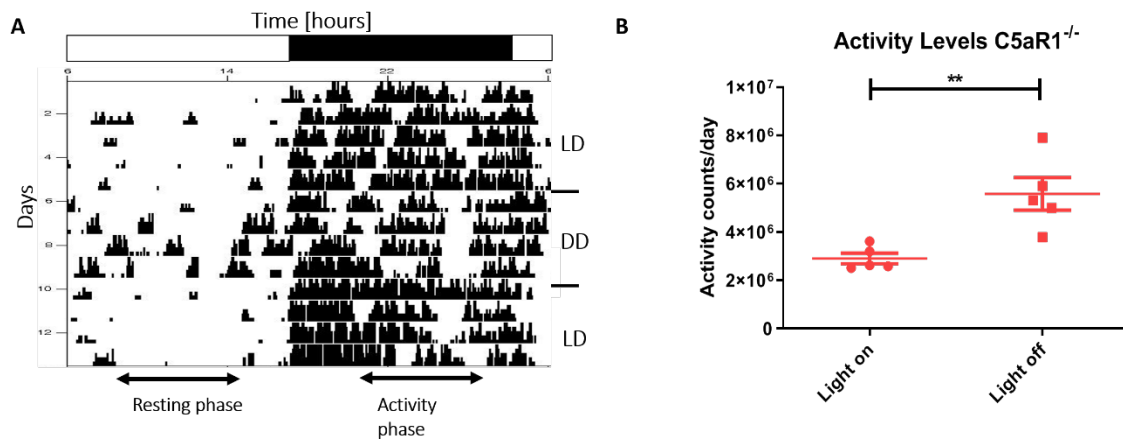


Figure 4-4: Activity levels in C5aR1^{-/-} mice

The actograms were analyzed as described above and a statistical analysis of the activity levels was performed. A) Actogram of a C5aR1-deficient mouse, depicting six days in 12:12h LD condition, followed by four days of total darkness (DD). Depicted are the registered activity counts over time. Each horizontal bar describes 24h, i.e. one day. The white and the black bars at the top of the actogram depict lights on and lights off. B) Quantification of the activity levels of C5aR1^{-/-} mice during the resting (light on) and the activity (light off) phases. Each dot represents the activity level of one individual mouse. n=5; data are expressed as mean \pm SD, approximately normally distributed (Shapiro-Wilk-Test $p > 0.05$) and were analyzed by t-test; red circles = light on, red squares = light off. ** $p < 0.01$

Furthermore, the individual activity counts were compared between both mouse strains (Figure 4-5). I found no significant difference between WT and C5aR1-deficient mice when comparing the activity levels during the activity or resting phase.

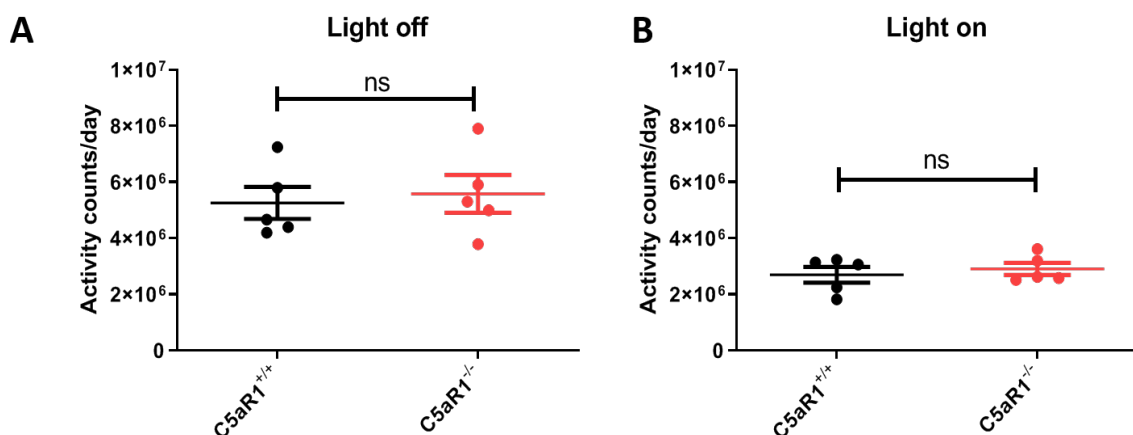


Figure 4-5: C5aR1^{+/+} and C5aR1^{-/-} mice exert a similar circadian activity

The actograms were analyzed as described above and a statistical analysis of the activity levels was performed. A) The number of activity counts is comparable in C5aR1^{+/+} and C5aR1^{-/-} mice when the light is turned off. B) The number of activity

4 Results

counts is similar in C5aR1^{+/+} mice and C5aR1^{-/-} mice when the light is turned on. Each dot represents the activity level of one individual mouse. n=5; data are expressed as mean \pm SD, approximately normally distributed (Shapiro-Wilk-Test $p > 0.05$) and were analyzed by t-test; black circles = C5aR1^{+/+} mice, red circles = C5aR1^{-/-} mice. ns non-significant

4.1.3 The C5a/C5aR1 axis drives the circadian oscillations of pulmonary APCs

Circadian fluctuations in the serum levels of the anaphylatoxins C3a and C5a were reported earlier¹³⁷. To determine the influence of the C5a/C5aR1 axis on the circadian fluctuations of pulmonary immune cells detected in WT mice (Figure 4-3), a C5ar1-deficient mouse strain was used and the experimental steady-state setup repeated.

Comparing BALF and pulmonary cells, C5ar1^{-/-} and WT mice showed no differences regarding the total number of immune cells (data not shown).

Assessing first alveolar macrophage number in C5ar1^{-/-} mice, there were no statistical differences over time (data not shown). Interestingly, while pulmonary macrophages in WT mice peaked at CT15, there were no significant changes in C5ar1^{-/-} mice over time (Figure 4-6A). Consequently, the cell number in C5ar1^{-/-} mice at CT15 ($p < 0.01$) and CT21 ($p < 0.05$) was significantly lower than in WT mice (Figure 4-7A). Regarding cDC2s, cell numbers at CT3 ($p < 0.05$) and CT9 ($p < 0.01$) were significantly higher than those at CT15 (Figure 4-6B). As shown in Figure 4-7B, the cDC2 numbers did not differ significantly between the WT and C5ar1^{-/-} strain at any time. Similar to the cDC2 numbers, the eosinophil numbers at CT3 ($p < 0.05$) and CT9 ($p < 0.01$) were higher than the numbers observed at CT15 (Figure 4-6C). Taken together, the eosinophil numbers in WT and C5ar1^{-/-} mice did not differ over time (Figure 4-7C). Finally, cDC1 numbers in C5ar1^{-/-} mice did not change during the 24 hour cycle (Figure 4-6D). However, I observed a significant difference of cDC1 numbers at CT21 ($p < 0.001$) between C5ar1^{-/-} and WT mice. The number of cDC1s was reduced in C5ar1^{-/-} mice when compared with WT mice (Figure 4-7D).

4 Results

In summary, the findings suggest that the C5a/C5aR1 axis regulates the circadian distribution of pulmonary macrophages and cDC1s.

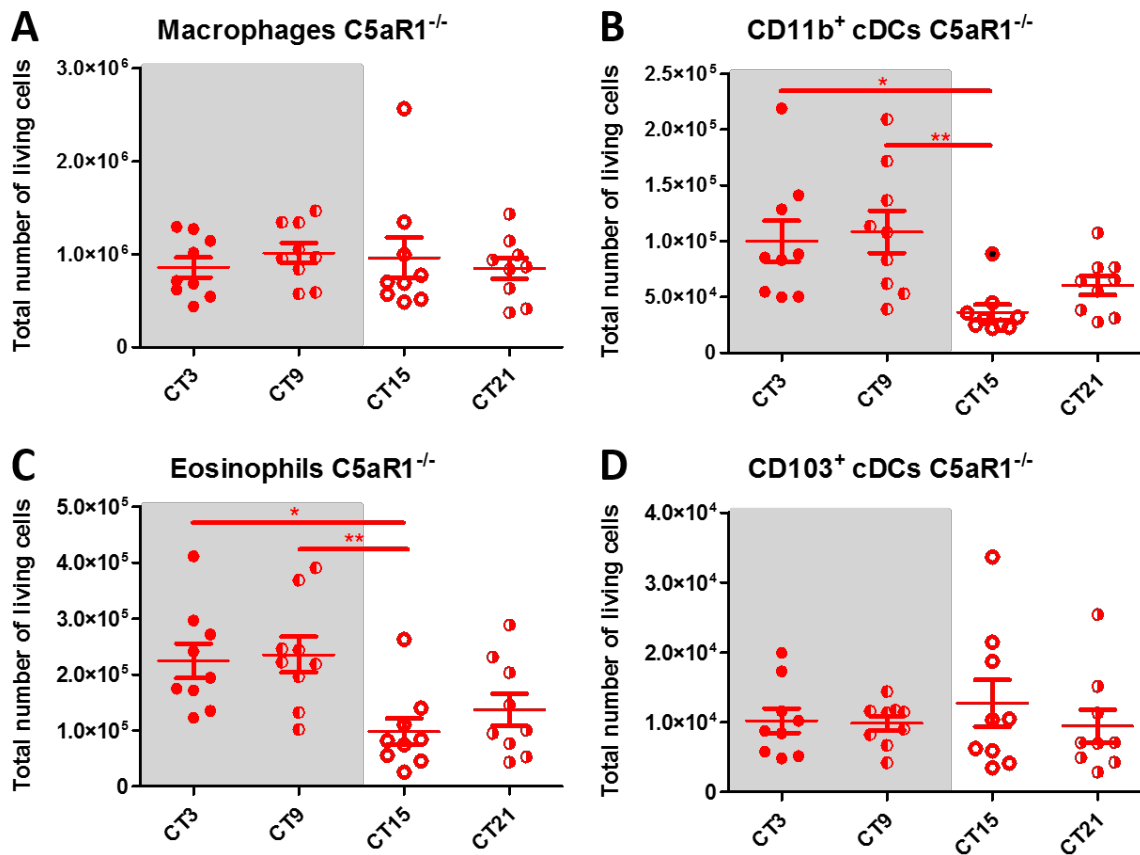


Figure 4-6: Pulmonary cDC2 cells and eosinophils fluctuate in $C5aR1^{-/-}$ mice over 24h.

Mice were kept in strict DD condition 48h before sacrificing to ensure the exclusion of any outer Zeitgeber. After sacrificing every 6h (CT3, CT9, CT15, CT21), lungs were removed and pulmonary cells isolated and processed as described. After staining with fluorescently labelled antibodies, cell suspensions were analyzed by flow cytometry and cell populations defined using the DC gating strategy. Cell numbers of A) pulmonary macrophages, B) $CD11b^{+}$ cDCs (cDC2), C) eosinophils, and D) $CD103^{+}$ cDCs (cDC1) are shown. Each dot represents the cell number of one individual mouse lung. $n=9$; three independent experiments. Data are expressed as mean \pm SD and were analyzed by one-way ANOVA with Tukey's multiple comparison test. Gray background = resting phase, white background = activity phase. * $p < 0.05$, ** $p < 0.01$

4 Results

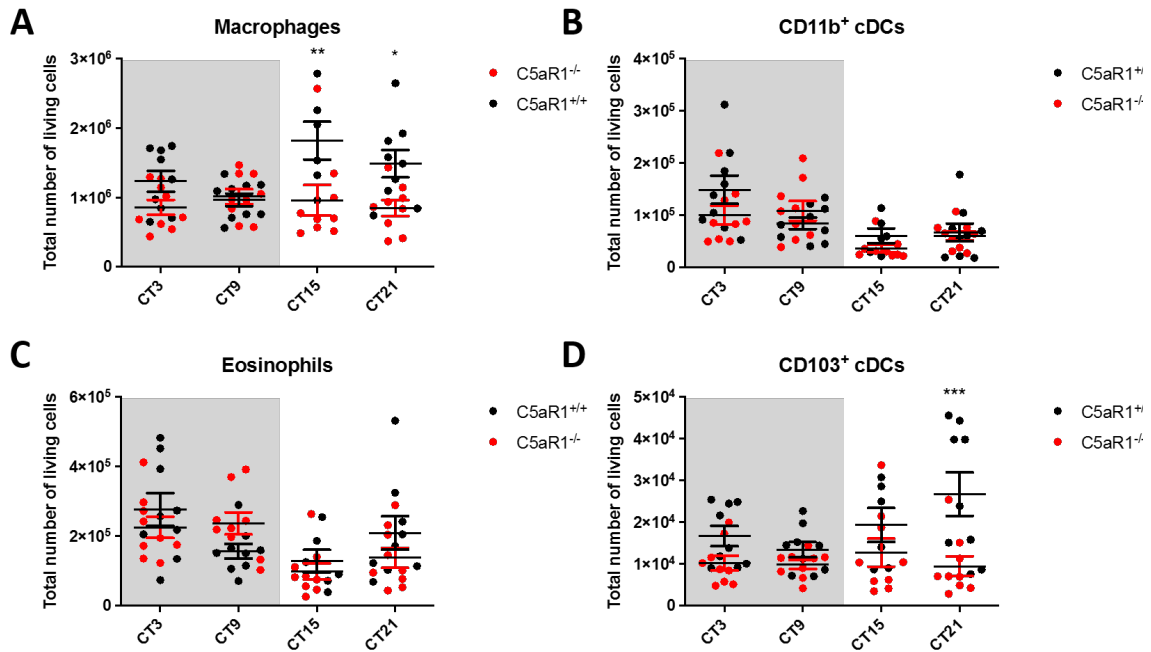


Figure 4-7: Macrophage and cDC1 numbers differ between $C5aR1^{+/+}$ and $C5aR1^{-/-}$ mice.

Mice were kept in strict DD condition 48h before sacrificing to ensure the exclusion of any outer Zeitgeber. After sacrificing every 6h (CT3, CT9, CT15, CT21), lungs were removed and pulmonary cells isolated and processed as described. After staining with fluorescently labelled antibodies, cell suspensions were analyzed by flow cytometry and cell populations defined using the DC gating strategy. Here, the cell numbers of pulmonary APCs in $C5aR1^{+/+}$ and $C5aR1^{-/-}$ mice are compared with each other over time. Depicted are A) pulmonary macrophages, B) CD11b⁺ cDCs (cDC2), C) eosinophils, and D) CD103⁺ cDCs (cDC1). Each dot represents the cell number of one individual mouse lung. $n=6-9$ per strain; three independent experiments each. Data are expressed as mean \pm SEM and were analyzed by two-way ANOVA with Tukey's multiple comparisons test. Gray background = resting phase, white background = activity phase. * $p < 0.05$, *** $p < 0.001$

4.2 The time of allergen sensitization impacts on the immune cell recruitment into the airways and the lung

As circadian fluctuations were observed in APCs in steady state, we hypothesized that the time of allergen contact may impact on the innate immune response after the first allergen contact. To test this hypothesis, mice entrained to 12:12h LD cycle were treated with HDM or PBS at ZT3 or ZT15 (ZT0 is the time when the lights turn on). The choice of immunization time was based on the base-line experiment, at which I

observed the most striking differences in APC numbers when comparing CT3 and CT15.

4.2.1 Allergen sensitization at ZT15 results in a strong recruitment of neutrophils into the airways

When BALB/c WT mice were immunized with HDM at ZT15, a strong neutrophil influx occurred into the airways. The number of neutrophils increased significantly in HDM-treated mice as compared to PBS-treated control mice at ZT15 ($p < 0.05$, Figure 4-8C). There was also a trend towards higher numbers of neutrophils after HDM immunization at ZT3 when compared to the PBS treatment, however, the differences did not reach the level of statistical significance. Interestingly, the number of alveolar macrophages was significantly higher upon HDM stimulation at ZT3 as compared to ZT15 ($p < 0.05$, Figure 4-8A). Also, there was a clear trend towards higher numbers of macrophages in the group that received PBS at ZT3 as compared with one at ZT15. There was a slight increase in eosinophil and T cell numbers upon HDM treatment at ZT3 and ZT15, however, this increase was not significant (Figure 4-8B/D).

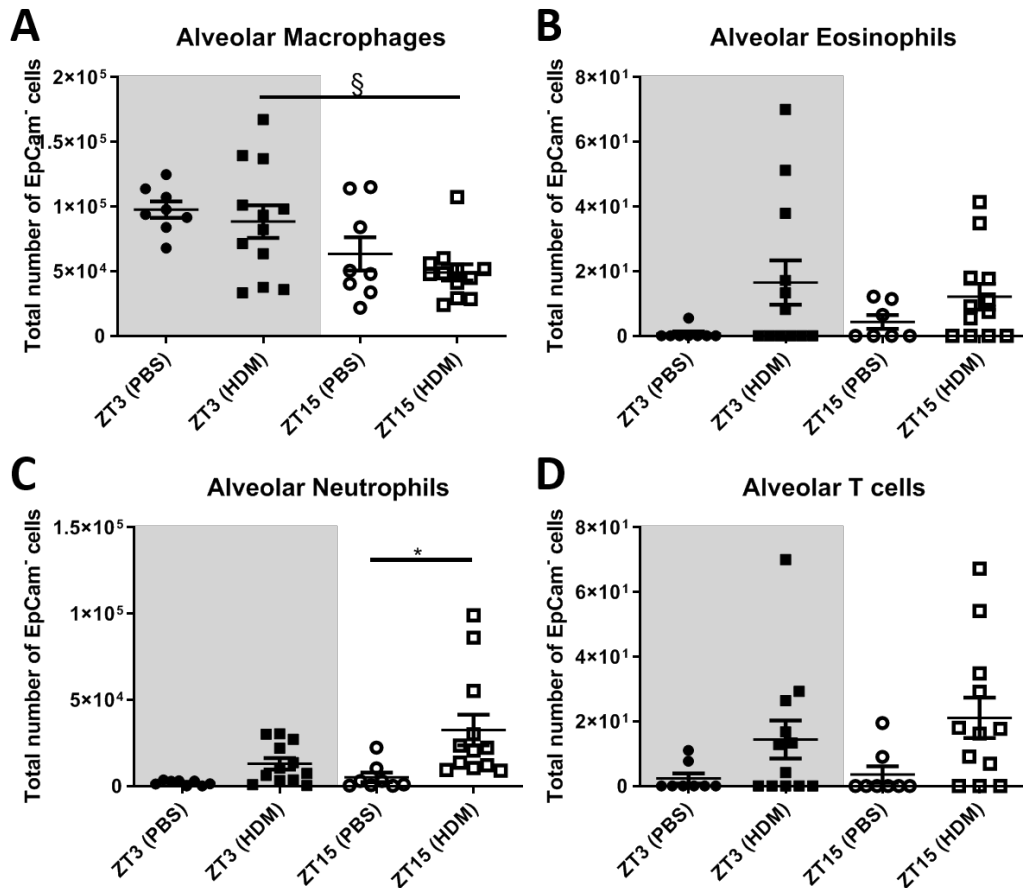


Figure 4-8: Strong increase in neutrophil numbers after HDM immunization during the activity phase at ZT15

Mice were entrained to 12:12h LD environment for at least 3 days, followed by a one-step HDM immunization. After sacrifice, BALF cells were isolated and processed as described. After staining with fluorescently labelled antibodies, cell suspensions were analyzed by flow cytometry and cell populations defined using the BALF gating strategy. Depicted are the cell numbers of alveolar A) macrophages, B) eosinophils, C) neutrophils and D) T cells upon one-step HDM immunization. Each dot represents the BALF cell number of one individual mouse. n=8-12; three independent experiments. Data are expressed as mean \pm SEM and were analyzed by one-way ANOVA with Tukey's multiple comparison test. Gray background = resting phase, white background = activity phase. Circles = PBS control, squares = HDM sensitized. *, § p<0.05

4.2.2 Impact of allergen sensitization during the resting or activity phase on the production of cytokines in the airways

In addition to the cellular components in the airways and the lung, a detailed analysis of cytokines was performed (Figure 4-9). I found an increase in several cytokines in response to HDM treatment at ZT3 and

4 Results

ZT15. The VEGF levels upon HDM immunization at ZT3 and ZT15 were much higher than that of PBS-treated individuals ($p < 0.05$, Figure 4-9A). Similarly, the TNF- α -production increased significantly in HDM-immunized mice at ZT3 ($p < 0.01$) and ZT15 ($p < 0.05$, Figure 4-9E) compared to PBS-treated mice. Interestingly, CXCL1 ($p < 0.01$) and IL-5 ($p < 0.05$) levels were only significantly increased upon HDM treatment during the resting phase, while there was a trend of increased cytokine levels at ZT15 (Figure 4-9B and C). IL-6 levels were low and did not differ upon HDM or PBS treatment at ZT3 or ZT15 (Figure 4-9D). The levels of GM-CSF, IL-1 β , IL-2, IL-4, IL-10, IL12p70, IL-13 and IFN- γ were below the detection limit (data not shown).

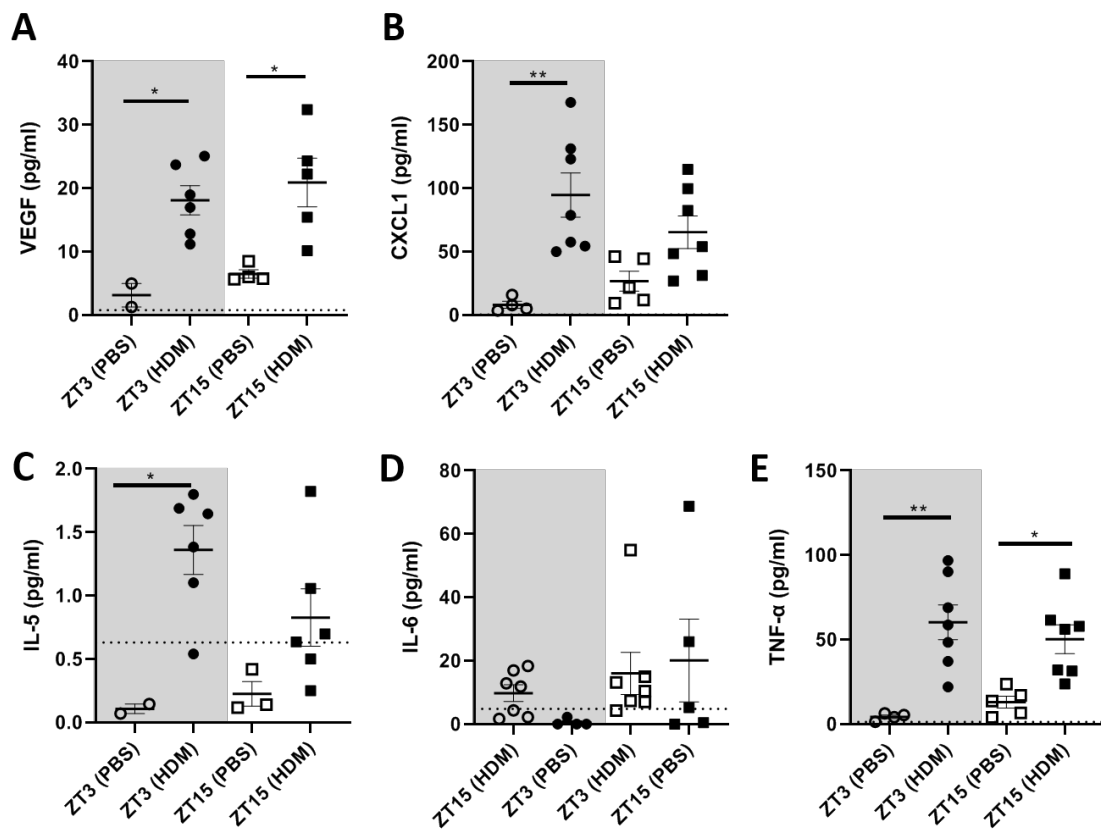


Figure 4-9: HDM stimulation during the activity or resting phase results in increased levels of proinflammatory cytokines in the airways

Mice were entrained to 12:12h LD environment for at least 3 days, followed by one-step HDM immunization as described above. After sacrifice, BALF was obtained and processed for multiplex analysis. Depicted are the cytokine levels of A) VEGF, B) CXCL1, C) IL-5, D) IL-6 and E) TNF- α from mice treated with PBS or HDM at the indicated time points. Two replicates of each mouse were analyzed. $n = 2-7$; data are expressed as mean \pm SEM and were analyzed by one-way ANOVA with Tukey's

4 Results

multiple comparisons test; empty signs = PBS, filled signs = HDM, circles = ZT3, squares = ZT15; dotted line = resp. detection limit; * <0.05, ** p<0.01

4.2.3 Impact of one-time HDM immunization at ZT3 or ZT15 on pulmonary immune cells

After one-step HDM immunization, pulmonary macrophage numbers did not change in response to PBS- or HDM treatment at ZT3 or ZT15 (Figure 4-10A). Concerning cDC2s, HDM treatment induced a significant increase in cell numbers at ZT15 compared to PBS-treated mice ($p<0.01$; Figure 4-10D). The increase in cDC2 numbers at ZT3 in response to HDM treatment did not reach the level of statistical significance (Figure 4-3A, p. 75).

The number of cDC1s did not change over time, neither after HDM nor after PBS treatment (Figure 4-10E). The numbers of pulmonary moDCs in HDM-treated mice were significantly higher when compared to PBS-treated controls at ZT15 ($p<0.001$). In contrast, there was no significant difference between both treatments at ZT3 (Figure 4-10F).

In the lungs, there was a significant increase in neutrophil numbers after HDM treatment at ZT3 as well as at ZT15 ($p<0.05$; Figure 4-10C).

After one-step immunization, there is no statistical difference among the numbers of eosinophils in the lungs between PBS and HDM treatment (Figure 4-10B). Interestingly, the cell number was significantly decreased in PBS-treated mice at ZT15 compared to PBS-treated mice at ZT3 ($p<0.05$) as well as in HDM-treated mice at ZT15 compared to CT3 ($p<0.05$). This reduction was already observed in the steady-state experiments, however, it did not reach significance (Figure 4-3C).

4.2.4 Naïve and memory T cell migration into the lungs increases after HDM administration at ZT3

After allergen administration, an inflammatory reaction occurs and T cells get attracted to the lungs where they drive the inflammatory response.

4 Results

To get at detailed picture of this process, the different T cell subsets (naïve T cells, effector and memory T cells) were analyzed after PBS/HDM administration during resting and activity phase.

In none of the three investigated T cell subsets a significant difference in cell number was observed regarding PBS versus HDM treatment (Figure 4-10G-I). However, naïve and memory T cell numbers were significantly higher after HDM administration at ZT3 compared to ZT15 ($p < 0.05$, Figure 4-10G and I). This effect was also apparent in effector T cells, but did not reach statistical significance (Figure 4-10H).

Additionally, I determined the T cell numbers in the mediastinal lymph nodes upon one-step HDM immunization. There were no significant differences in the number of naïve, effector or memory T cells in response to PBS or HDM treatment at ZT3 or ZT15 (data not shown).

4 Results

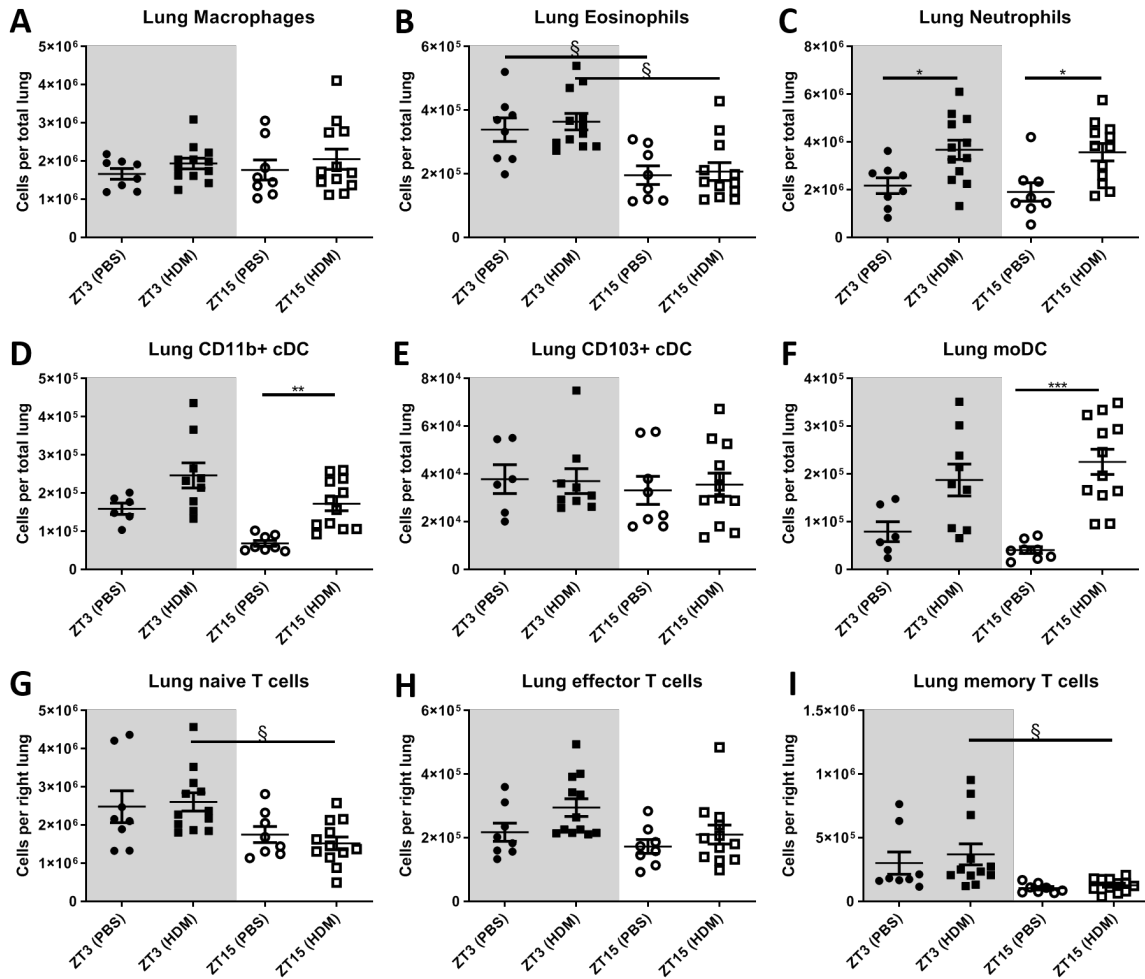


Figure 4-10: Pulmonary cell distribution in response to HDM immunization during the activity or the resting phase

Mice were entrained to 12:12h LD environment for at least 3 days, followed by one-step HDM immunization. After sacrifice, the lungs were removed, pulmonary cells were isolated and processed. After staining with fluorescently labelled antibodies, cell suspensions were analyzed by flow cytometry and cell populations defined using the neutrophil, DC and T cell gating strategies. Shown are the cell numbers of pulmonary A) macrophages, B) eosinophils, C) neutrophils, D) CD11b⁺ cDCs (cDC2), E) CD103⁺ cDCs (cDC1), F) moDCs, G) naive T cells, H) effector T cells, and I) memory T cells. Each dot represents the cell number of one individual mouse lung. n=8-12; three independent experiments. Data are expressed as mean ± SEM and were analyzed by one-way ANOVA with Tukey's multiple comparison test. Gray background = resting phase, white background = activity phase. Circles = PBS control, squares = HDM sensitized. *, § p<0.05, ** p<0.01, *** p<0.001

4.3 The impact of repeated HDM immunization during the resting or activity phase on the development of the allergic phenotype

The one-time HDM immunization during the activity or the resting phase resulted in clear differences in the recruitment of different immune cells to the airways and the lung as well as the induction of a pro-inflammatory environment in the airways. Based on these findings, I hypothesized that such differences will impact on the development of the allergic phenotype after repeated HDM immunization. To test this hypothesis, female WT mice were kept in strict 12:12h LD conditions and immunized following the four-step HDM immunization protocol. During the experiment, the activity level of mice were recorded by infrared scanning. 72h after the final immunization, the AHR was determined and organs taken to assess immune cell numbers by flow cytometry. Furthermore, lung cells were restimulated and supernatants examined for cytokine production. Finally, effector T cell differentiation was assessed by intracellular cytokine staining.

4.3.1 Repeated HDM administration at ZT15 enhances the activity level and reduces it when given at ZT3

Over the full four-week experimental period, a group of two PBS-treated mice per time point, four HDM-treated mice at ZT3 and three HDM-treated mice at ZT15 were observed by infrared scan. As shown in the exemplary actograms, immunization was associated with an immediate reduction of the amplitudes (see the orange arrows in Figure 4-11A and B). Also, we observed an increased number of activity counts during the resting phase. In the course of the four weeks, the increasing density and number of amplitudes was remarkable when the light was turned on in mice treated with HDM at ZT3 (Figure 4-11A) suggesting that the resting period was distracted. Regarding the mice treated with HDM at ZT15, the

4 Results

data suggest that the resting period was also altered, resulting in earlier wake up after repeated HDM treatment (Figure 4-11B).

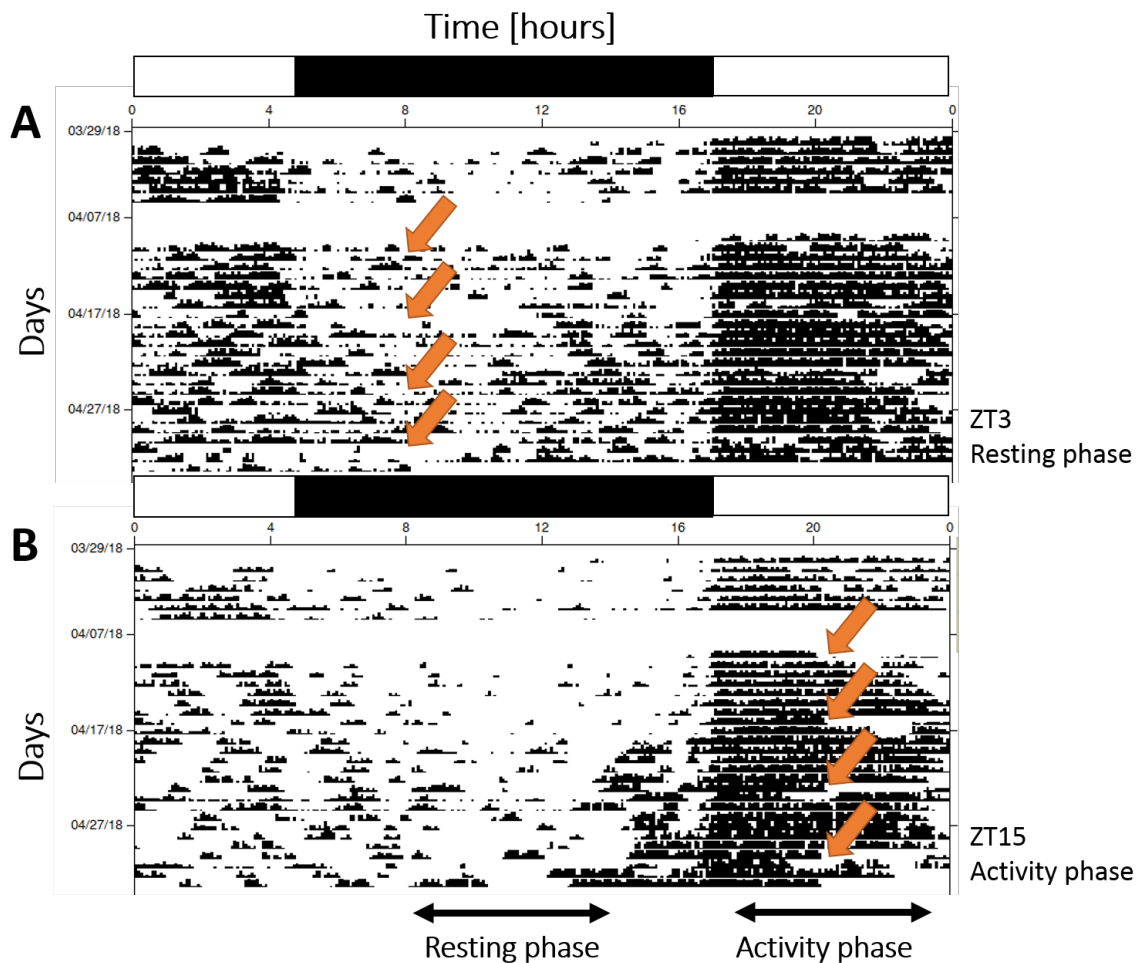


Figure 4-11: Repeated HDM administration alters the sleep-wake cycle

Mice were entrained to 12:12h LD environment for one week followed by the four-step HDM immunization protocol. Parallel, five to six individuals were monitored by infrared scan analysis at each time point. Two exemplary actograms after HDM administration at A) ZT3, the resting phase, and B) ZT15, the activity phase are depicted. The orange arrows highlight the time of anesthesia and immunization. Each horizontal bar describes 24h, resp. one day. The white and the black bar at top of the actogram depicts light and darkness.

Next, we quantified the overall activity levels of the mice in response to the PBS-/HDM-treatment and the immunization time over the four-week period (Figure 4-12). Analyzing the average activity levels over 24 hours, mice treated with PBS at ZT3 had significantly increased activity levels after the first immunization ($p < 0.05$). A significant reduction followed from week two to three ($p < 0.05$). Similarly, the activity level in mice treated with HDM at ZT3 dropped significantly after four weeks of

4 Results

treatment as compared with week one ($p < 0.05$) and week two ($p < 0.05$). In sharp contrast, mice treated with HDM at ZT15 showed significantly increased activity levels after two weeks of treatment when compared to their baseline activity ($p < 0.05$, Figure 4-12A). Also, the activity levels remained high during weeks 3 and 4. Focusing on resting phase after immunization with PBS or HDM, we observed more activity as compared with baseline activity (Figure 4-12B). Mice treated with PBS at ZT3 or ZT15 showed significantly increased activity after the first treatment ($p < 0.05$). In contrast, HDM-treatment at ZT3 led to a significant decrease in the activity level from week three to week four ($p < 0.01$).

In the next step, a detailed 24-hours activity profile was created for each experimental week (Figure 4-12C-L). First, a one-week observation was run before the experiment started. Here, HDM- and PBS-treated mice behaved in the same manner; we observed no significant differences in the activity levels between both groups at each time (Figure 4-12 C and D). Interestingly, both groups of mice treated at ZT3 showed an activity profile with an early peak in their activity level at ZT12, followed by a decline the next 5 hours and a second peak around ZT20/21. Mice treated at ZT15 showed a more continuous reduction in their activity level after the initial peak at ZT12 until the beginning of resting phase at ZT0.

After the first immunization at ZT3, mice treated with PBS showed a peak in their activity level at ZT12 (0.25 ± 0.017). During the next 7 hours, the activity level steadily declined to reach a minimum at 0.04 ± 0.001 , after which it increased again during the next 5 hours and reached a maximum of 0.12 ± 0.017 at ZT22. In contrast, HDM-treated mice showed a significantly reduced activity patterns during their activity phase as compared to PBS-treated mice ($p < 0.001$ at ZT12 and $p < 0.01$ at ZT23, Figure 4-12E). First, the peak activity at ZT12 was significantly lower in HDM-treated mice (0.14 ± 0.001). During the following decline phase, a minimum in activity level was reached at ZT19 (0.04 ± 0.011).

4 Results

After the second immunization at ZT3, the overall appearance of the activity profile was similar to the previous week (Figure 4-12G). PBS-treated mice showed a peak in activity level at ZT12 (0.23 ± 0.018) with a delayed decline until ZT20 (0.02 ± 0.012). HDM-treated mice reached a significantly reduced peak in their activity level at ZT12 ($p < 0.01$) and ZT23 ($p < 0.05$) as compared to PBS-treated mice.

After the third immunization at ZT3, the activity profiles of HDM- and PBS-treated mice differed more obvious from each other (Figure 4-12I). While PBS-treated mice keep a high level of activity at ZT12 (0.20 ± 0.021) with a following decline to a minimum at ZT20 (0.03 ± 0.011), they increased their activity level again with a second peak at ZT23 (0.13 ± 0.024). In contrast, HDM-treated mice showed a significantly reduced peak in their activity level at ZT12 (0.12 ± 0.012 , $p < 0.05$) with a continuously decline until reaching their resting phase. Activity levels were significantly reduced at ZT23 ($p < 0.05$) and ZT0 ($p < 0.001$) compared to PBS-treated mice.

After the complete four-step immunization, the activity patterns of PBS- and HDM-treated mice at ZT3 did no longer differ significantly (Figure 4-12K). The activity level of mice treated with PBS peaked at ZT12 (0.15 ± 0.041). Also, HDM-treated mice reached their maximum of activity at this time point (0.10 ± 0.018). The following hours, PBS-treated mice kept a high constant activity level for 3 hours before it declined. Mice treated with HDM showed a plateau in activity level for about 6 hours, only interrupted by a little decline at ZT14 (0.06 ± 0.014), before eventually declining.

Concerning the two groups of mice immunized at ZT15, the activity profile after the first immunization did not differ much from the pre-analysis (Figure 4-12F). PBS-treated mice peaked in their activity level at ZT12 (0.16 ± 0.012), while mice treated with HDM showed a first maximum of their activity level at ZT13 (0.16 ± 0.013), followed by a continuous decline until ZT0.

4 Results

After the second immunization, HDM-treated mice showed a significant increased activity level compared to PBS-treated mice from ZT13 until ZT16 ($p < 0.01$ at ZT14, $p < 0.001$ at ZT15 and ZT16, Figure 4-12H). Mice treated with HDM reached a peak in their activity level at ZT13 (0.22 ± 0.013) that declined strongly afterwards. PBS-treated mice reached their activity maximum at ZT12 (0.16 ± 0.012) followed by a flat decline.

This difference became even more striking after the third immunization (Figure 4-12J). Here, mice treated with HDM at ZT15 showed a significantly increased activity from ZT12 to ZT17 compared to PBS-treated mice ($p < 0.001$ at ZT12, ZT13, ZT14, and $p < 0.01$ at ZT15, ZT16, ZT17). Their maximum reached a level of 0.23 ± 0.016 at ZT12, compared to a much lower peak in PBS-treated mice at the same time point (0.13 ± 0.016). Furthermore, the activity level of PBS-treated mice was more constant during their active phase (around 0.08 ± 0.018) when compared to HDM-treated mice, whose activity level decreased strongly from ZT17 (0.18 ± 0.021) to ZT21 (0.05 ± 0.012).

After the full four-step immunization protocol, the group of HDM-treated mice kept a significantly increased activity level in the early activity phase from ZT12 to ZT14 compared to PBS-treated mice ($p < 0.05$ at ZT12, $p < 0.001$ at ZT13, $p < 0.01$ at ZT14, Figure 4-12L). Their activity maximum reached a level of 0.25 ± 0.018 , while the activity level of PBS-treated mice was only 0.14 ± 0.022 . Activity curves of both groups of mice showed a more irregular rhythmicity with interrupted resting phases and increased variations between the individual mice in each group (compare error bars per time point).

4 Results

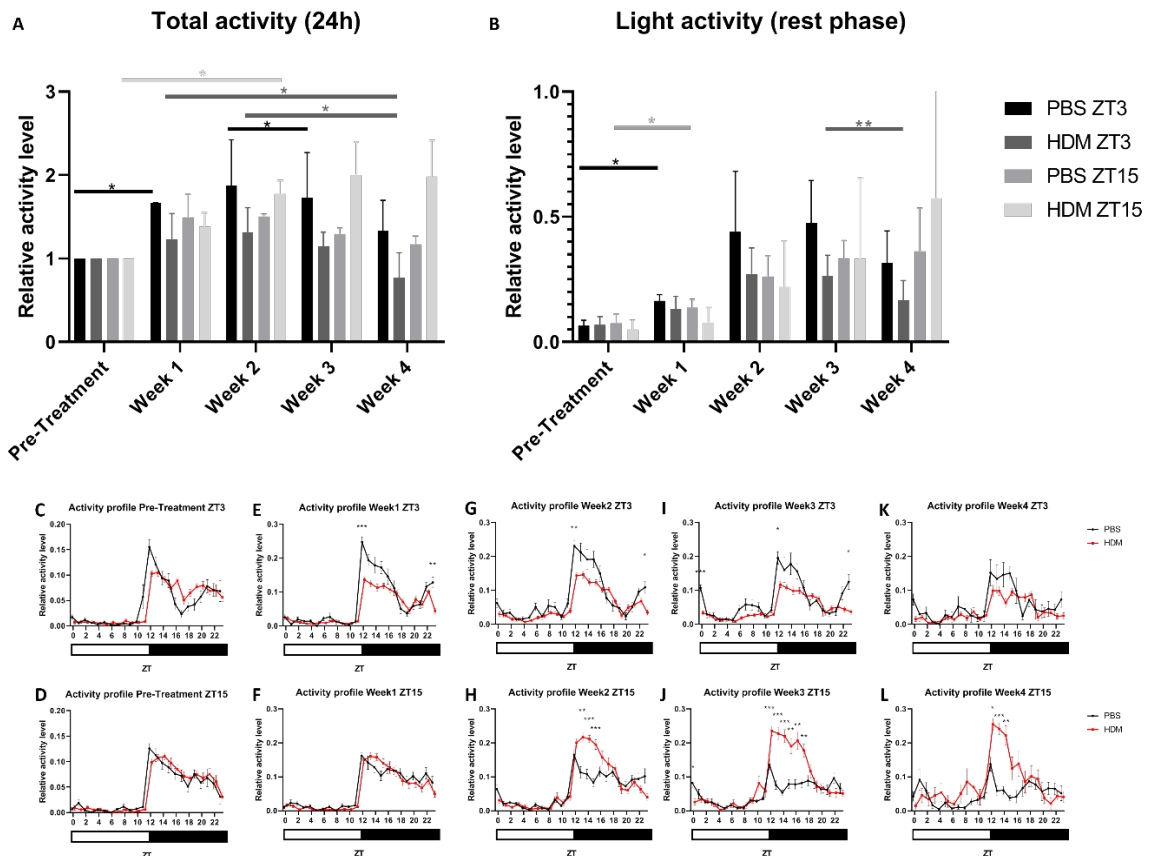


Figure 4-12: Oposing effects of HDM-treatment during the activity or resting phase on the overall activity level

Mice were entrained to 12:12h LD environment for one week followed by the four-step HDM immunization protocol. In parallel, two to four individuals were monitored by infrared scan analysis per treatment group. Activity levels of PBS- and HDM-treated mice were analyzed at the different time points of immunization. The total activity counts were corrected by the baseline activity. The resulting relative activity levels for the four groups over the four-week experimental period are displayed. Depicted are A) the average total activity per week; B) the average light phase activity per week; and the activity profiles per week in PBS- and HDM-treated mice at C) ZT3 pre-treatment, D) ZT15 pre-treatment, E) ZT3 week 1, F) ZT15 week 1, G) ZT3 week 2, H) ZT15 week 2, I) ZT3 week 3, J) ZT15 week 3, K) ZT3 week 4 and L) ZT15 week 4. See legend for detailed information. White bar below activity profiles = light on, black bar below activity profiles = light off. $n=2-4$; data are expressed as mean \pm SEM. Data were analyzed by mixed ANOVA with A and B) Tukey's multiple comparisons test, and C - L) Bonferroni posttest; * $p < 0.05$, ** $p < 0.01$, *** $p < 0.001$

Next, we compared the total activity counts in the activity period in response to HDM treatment at either ZT3 or ZT15 side-by-side (Figure 4-13). As expected from the data shown in Figure 4-12, we found that mice treated with HDM during their resting phase (ZT3) were less active than the mice treated with HDM during their active phase (ZT15). The mice treated with HDM at ZT3 showed only a minor increase in their

4 Results

activity level after the first and second HDM immunization and a return to the baseline level after the fourth immunization round. In contrast, mice treated with HDM at ZT15 steadily increased their activity level after the first to the third immunization round and remained at a high activity level after the fourth immunization. Total activity levels in mice treated with HDM at ZT15 were significantly higher than those observed in mice treated with HDM at ZT3 in weeks 2, 3 and 4 (week two: $p < 0.05$, week three: $p < 0.001$, week four: $p < 0.01$, Figure 4-13).

Additionally, we found an increase in the total activity during the resting phase in the course of the four-week experimental period in the HDM-treated group. However, the differences between PBS- and HDM-treated mice did not reach the level of statistical significance.

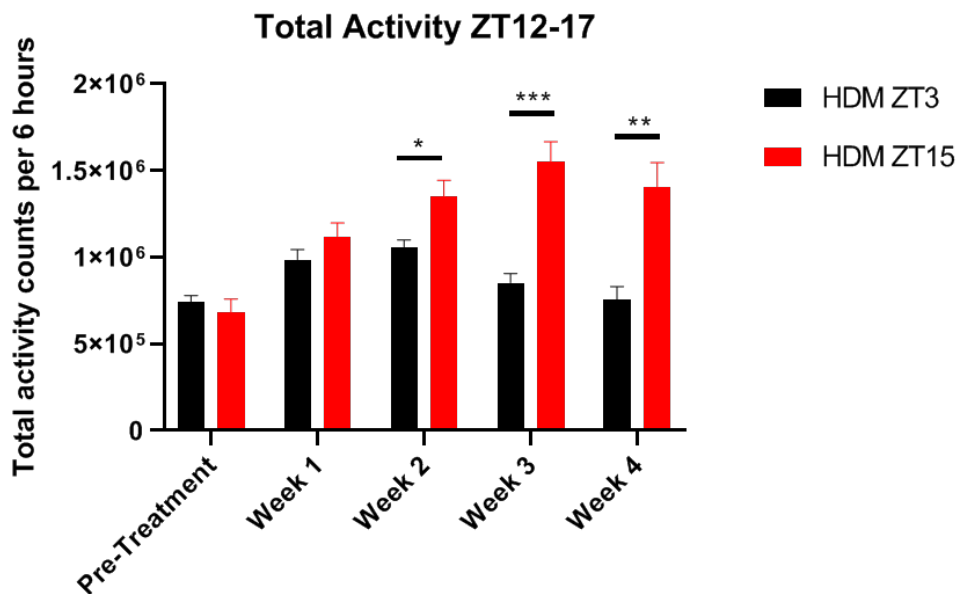


Figure 4-13: Higher total activity during the activity phase in mice treated with HDM at ZT15 compared with ZT3

Mice were entrained to 12:12h LD environment for one week followed by the four-step HDM immunization protocol. In parallel, two to four individuals were monitored by infrared scan analysis per treatment group. Activity levels of HDM-treated mice were determined with regard to the time of immunization. Here, the total activity counts between ZT12 and ZT17 over the four-week experimental period are displayed. Black bars = HDM ZT3, red bars = HDM ZT15. $n=3-4$; data are expressed as mean \pm SEM. Data were analyzed by mixed ANOVA with Bonferroni posttest; * $p < 0.05$, ** $p < 0.01$, *** $p < 0.001$

4.3.2 The airway resistance increases after immunization at ZT3 and ZT15

The airway hyperresponsiveness (AHR) was measured to illustrate the development of an allergic phenotype after four-step immunization. Furthermore, the influence of the immunization time on the strength of the developed airway resistance was determined.

Overall, HDM-challenged mice developed a higher airway resistance compared to the PBS control mice. Mice immunized with HDM during their resting phase showed a significant increase in the airway resistance at 10 ($p < 0.05$), 25 ($p < 0.05$) and 50 ($p < 0.05$) mg/mL methacholine compared to the respective PBS treatment (Figure 4-14A). Mice treated with HDM during their activity phase or resting phase showed an increase in AHR compared to PBS-treated controls. However, due to the relatively high AHR in response to PBS the increase did not reach the level of statistical significance whereas the AHR significantly increased in the ZT3 group in response to 10, 25 and 50 mg/mL methacholine. In a second step, the relative resistance was determined by (i) calculating the mean PBS values of ZT3 resp. ZT15-immunized mice in response to the individual methacholine concentrations, and (ii) divide each HDM value by its corresponding PBS value (Figure 4-14B). This calculation showed a significantly higher relative AHR value of mice treated with 25 mg/mL methacholine at ZT3 as compared with ZT15 ($p < 0.05$, Figure 4-14B).

4 Results

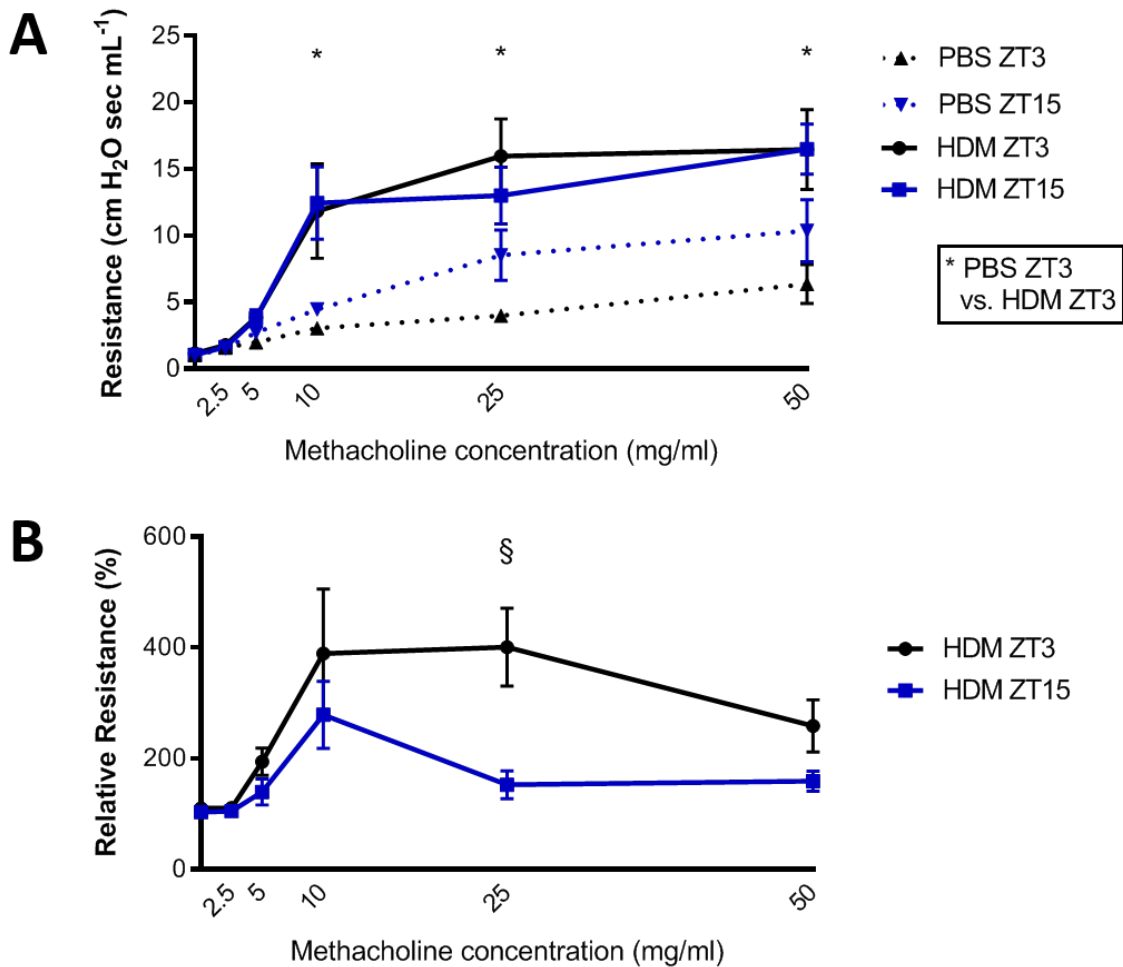


Figure 4-14: The relative increase in airway resistance is higher after immunization at ZT3 than at ZT15

Mice were entrained to 12:12h LD environment for at least 3 days followed by the four-step HDM immunization protocol. After anesthetizing, a lung function measurement was performed and the A) absolute and the B) relative resistances were calculated. $n=7-10$; continuous line = HDM-treated mice, dotted line = PBS-treated mice, black = resting phase (ZT3), blue = activity phase (ZT15); data are expressed as mean \pm SEM and were analyzed by ANOVA with A) Tukey's multiple comparisons test and B) Bonferroni posttest; depicted are only between group differences; */ \S $p < 0.05$

4.3.3 Strong airway inflammation in response to repeated HDM immunization at ZT3 and ZT15

HDM-immunized mice developed a strong increase in immune cell number in the airways as compared to PBS-treated mice after four times immunization. Alveolar macrophages were significantly increased upon HDM-challenge at ZT3 ($p < 0.01$) and ZT15 ($p < 0.05$) compared to PBS-treated mice (Figure 4-15A). Alveolar eosinophils were increased at ZT3

4 Results

($p < 0.001$) and at ZT15 ($p < 0.01$) when comparing HDM- with PBS-treated mice (Figure 4-15B). Also, alveolar T cell levels were significantly increased at ZT3 ($p < 0.001$) and at ZT15 ($p < 0.01$) when comparing HDM- with PBS-treated animals (Figure 4-15C). The number of airway neutrophils increased significantly upon immunization at ZT3 ($p < 0.001$), whereas no significant increase occurred at ZT15 (Figure 4-15D).

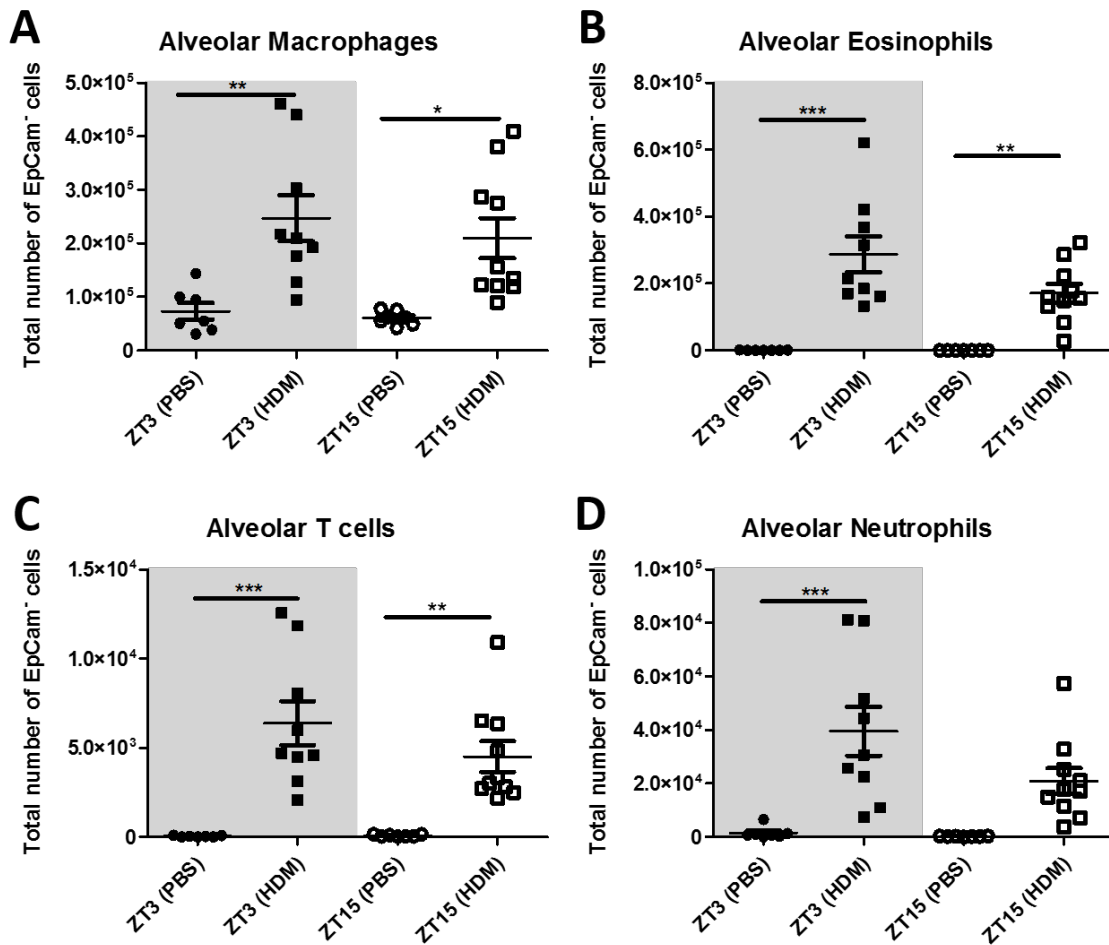


Figure 4-15: Airway immune cell distribution after repeated HDM immunization at ZT3 or ZT15

Mice were entrained to 12:12h LD environment for at least 3 days, followed by the four-step HDM immunization protocol. After AHR measurement, mice were sacrificed, BALF cells were processed as described. After staining with fluorescently labelled antibodies, cell suspensions were analyzed by flow cytometry and the different cell populations defined using the BAL gating strategy. Shown are cell numbers of airway A) macrophages, B) eosinophils, C) T cells, and D) neutrophils. Each dot represents the cell number in the airways of one individual mouse. $n = 7-10$; data are expressed as mean \pm SD and were analyzed by one-way ANOVA with Tukey's multiple comparison test; grey background = resting phase, white background = activity phase; circles = PBS control, squares = HDM sensitized; * $p < 0.05$, ** $p < 0.01$, *** $p < 0.001$

4.3.4 Repeated HDM immunization at ZT3 results in higher numbers of pulmonary macrophages and neutrophils as compared to immunization at ZT15

Parallel to the airway response, there was a substantial increase in immune cell number in the lungs. Furthermore, a new cell population, so-called inflammatory eosinophils (iEOS¹⁹⁴), appeared in HDM-immunized mice (compare Figure 4-16 A and B).

Looking at the different immune cell subsets, I found that the number of pulmonary macrophages was significantly increased in HDM-treated mice compared to PBS-controls at ZT3 ($p < 0.001$, Figure 4-16C). Moreover, mice treated with PBS at ZT15 had significantly higher numbers of pulmonary macrophages than the ones treated at ZT3 ($p < 0.05$). There were no significant differences among pulmonary eosinophil numbers (Figure 4-16D). Interestingly, iEOS numbers were significantly increased at ZT3 ($p < 0.01$) and ZT15 ($p < 0.001$, Figure 4-16E) when comparing HDM- with PBS-treated mice. In contrast, the numbers of eosinophils did not differ between ZT3 and ZT15 (Figure 4-16D). Pulmonary neutrophil numbers were significantly higher in response to HDM- as compared with PBS-treatment at ZT3 ($p < 0.05$, Figure 4-16F); in contrast, neutrophil numbers were similar at ZT15. All investigated DC subsets (cDC1s, cDC2s, moDCs) increased significantly after repeated HDM immunization when compared to PBS-treatment, both at ZT3 and ZT15 ($p < 0.01$, Figure 4-16 G-I).

4.3.5 Similar pulmonary migration of T cells at ZT3 and ZT15

Analyzing the pulmonary T cell subset migrations, I observed a strong influx of naïve, effector and memory T cells to the lungs after HDM treatment at ZT3 and ZT15 as compared to PBS controls (compare Figure 4-17 A and B). A significant rise in pulmonary naïve T cells in HDM-treated mice occurred when compared to PBS controls at ZT3 ($p < 0.05$; Figure

4-18A), while cell numbers between HDM- and PBS-treated groups did not differ at ZT15. Pulmonary effector T cells increased significantly at ZT3 ($p < 0.001$) and ZT15 ($p < 0.01$) when comparing HDM- with PBS-treated mice (Figure 4-18B). Finally, pulmonary memory T cells were significantly increased in HDM-immunized mice at ZT3 ($p < 0.01$) as well as at ZT15 ($p < 0.05$; Figure 4-18C) as compared with PBS controls.

4.3.6 Increased number of T cells in the draining lymph nodes after repeated HDM immunization at ZT3

In the next step, the inflammatory T cell response was analyzed in the mediastinal lymph nodes of PBS- and HDM-treated mice after immunization at either ZT3 or ZT15. There were remarkable increases in the number of naïve, central memory and effector T cells after HDM immunization compared to PBS treatment (compare Figure 4-17 C and D). Concerning naïve T cells, their numbers were significantly increased in HDM-treated mice compared to PBS controls at ZT3 ($p < 0.05$, Figure 4-18D). Also, naïve T cell numbers at ZT3 were significantly higher in response to HDM immunization at ZT3 than at ZT15 ($p < 0.01$). Effector T cells were significantly increased in HDM-challenged mice at ZT3 compared to PBS controls ($p < 0.05$) and compared to HDM-treated mice at ZT15 ($p < 0.05$, Figure 4-18E). Finally, the number of memory T cells was significantly increased in HDM-treated mice at ZT3 compared to the PBS controls ($p < 0.05$, Figure 4-18F).

4 Results

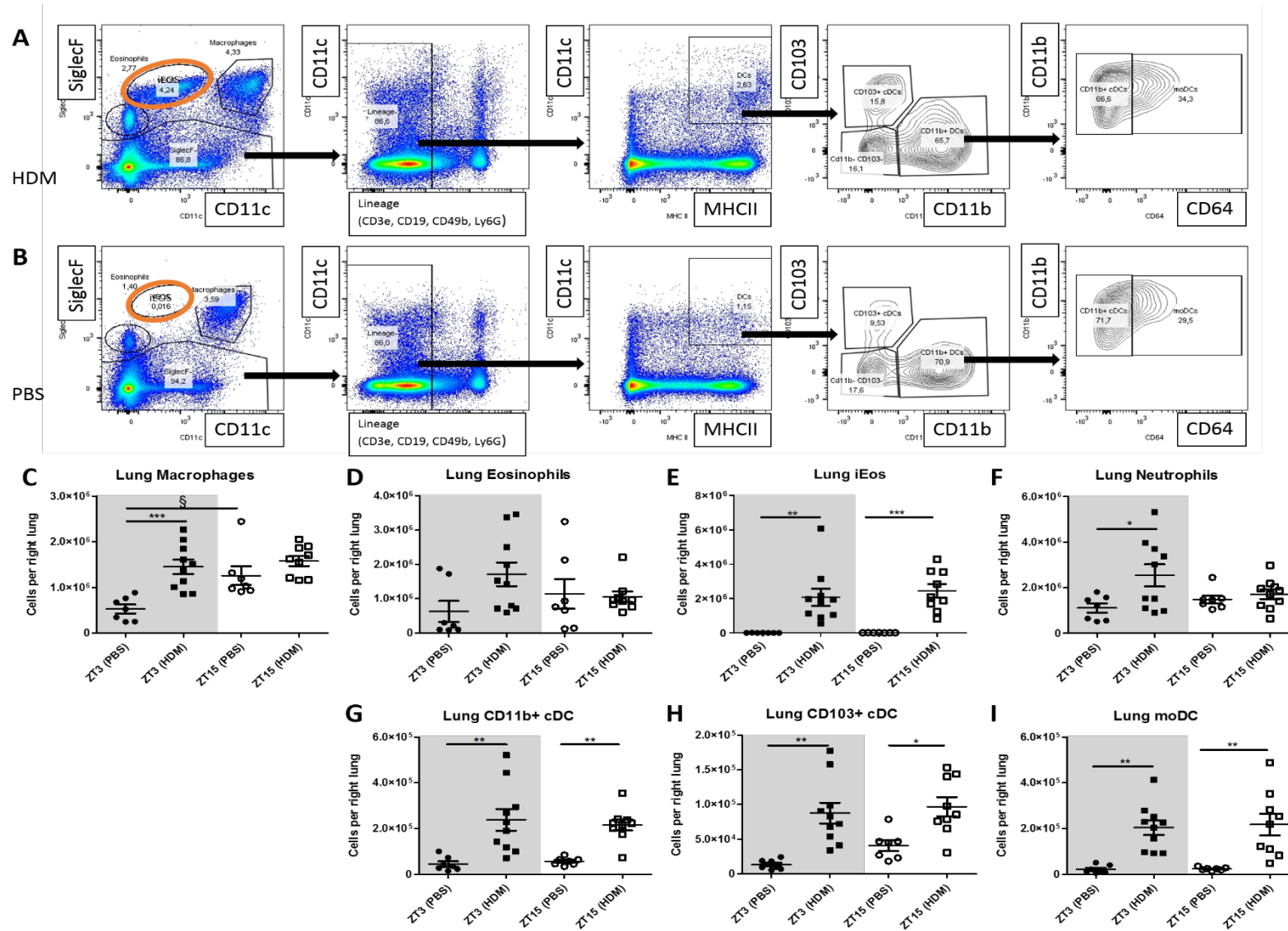


Figure 4-16: Recruitment of myeloid effector cells to the lung at ZT3 and ZT15

4 Results

Mice were entrained to 12:12h LD environment for at least 3 days, followed by the four-step HDM immunization protocol. After AHR measurement, mice were sacrificed, BALF was obtained and the right lung harvested. Pulmonary cells were isolated and processed as described. After staining with fluorescently labelled antibodies, cell suspensions were analyzed by flow cytometry and cell populations defined using the DC gating strategy. Shown is the gating strategy to define the different myeloid effector cells after A) HDM-immunization, and B) PBS-treatment; the new population of inflammatory eosinophils (iEOS) is marked by an orange circle. Cell numbers of pulmonary C) macrophages, D) eosinophils, E) iEOS, F) neutrophils, G) CD11b⁺ cDCs (cDC2), H) CD103⁺ cDCs (cDC1), and I) moDCs are shown. The exemplary graphs are representative for the performed flow analyses. Each dot represents the cell numbers counted in one individual right mouse lung. n=7-10; data are expressed as mean \pm SD and were analyzed by one-way ANOVA with Tukey's multiple comparison test; grey background = resting phase, white background = activity phase; circles = PBS control, squares = HDM immunized; */§ p<0.05, ** p<0.01, *** p<0.001

4 Results

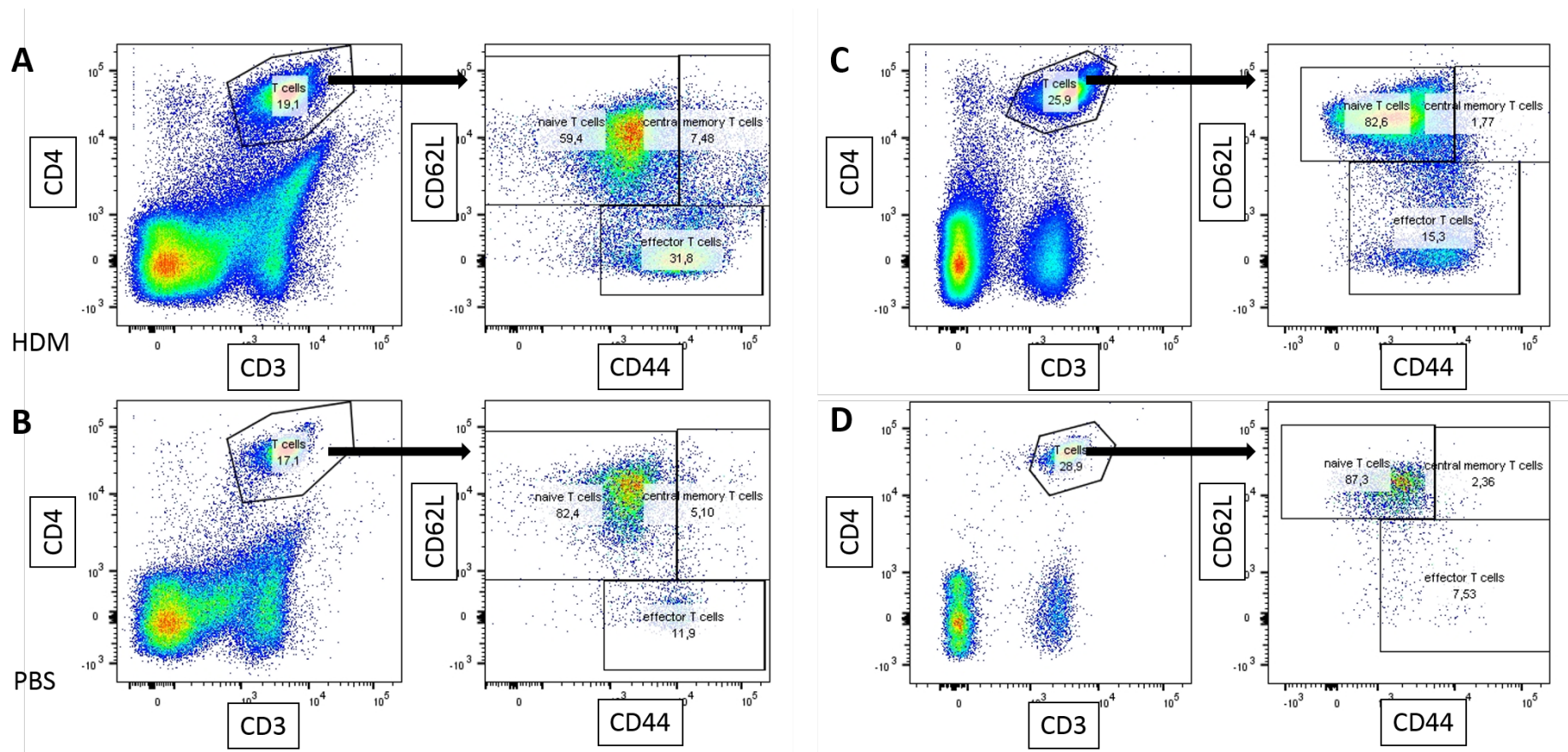


Figure 4-17: Gating strategy to define the different T cell subsets recruited to the lung and the draining lymph nodes at ZT3 and ZT15

Mice were entrained to 12:12h LD environment for at least 3 days, followed by the four-step HDM immunization protocol. After AHR measurement, mice were sacrificed, BALF was obtained, and the right lung as well as the mediastinal lymph nodes were harvested. Pulmonary and lymphoid cells were isolated and processed as described. After staining with fluorescently labelled antibodies, cell suspensions were analyzed by flow cytometry and cell populations defined using the T cell gating strategy. Shown is the gating strategy to define the different T cell subsets in the lung in response to A) HDM-immunization, and B) PBS treatment and in the draining lymph nodes in response to C) HDM-immunization, and D) PBS treatment. The exemplary graphs are representative for the performed flow analyses.

4 Results

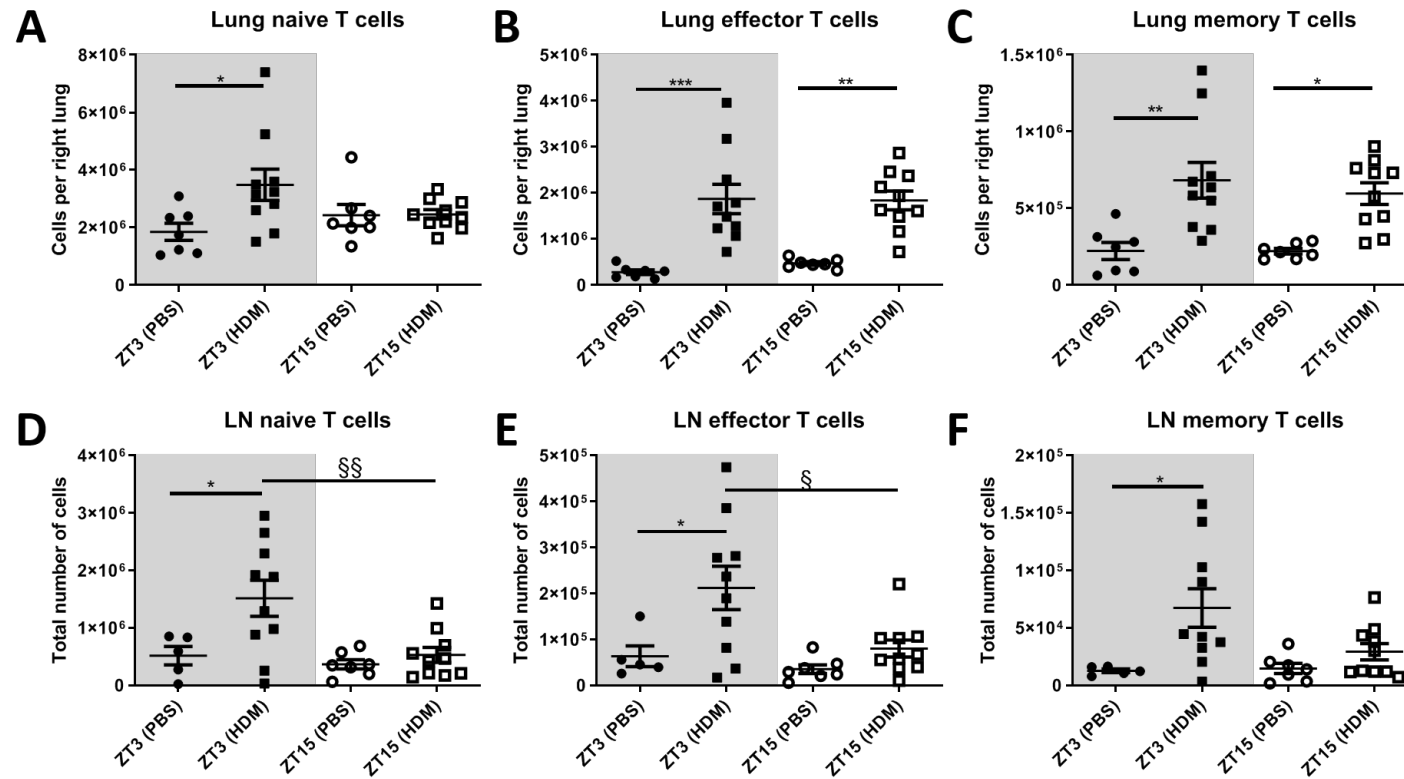


Figure 4-18: Quantification of the different T cell subsets in the lungs and the draining lymph nodes after HDM immunization at ZT3 and ZT15

Cell numbers of pulmonary A) naïve T cells, B) effector T cells, C) memory T cells, as well as D) naïve T cells, E) effector T cells, and F) memory T cells in the draining lymph nodes are depicted. Each dot represents the cell number counted in the right lung or all collected mediastinal lymph nodes per mouse. $n=7-10$; data are expressed as mean \pm SD and were analyzed by one-way ANOVA with Tukey's multiple comparison test; grey background = resting phase, white background = activity phase; circles = PBS control, squares = HDM sensitized; */§ $p < 0.05$, **/§§ $p < 0.01$, *** $p < 0.001$

4.3.7 Increased frequencies of Th2, Th17 and Treg cells upon HDM immunization at ZT3 and/or ZT15

T cell function was further analyzed by intracellular staining for subset-specific cytokines and transcription factors.

After defining effector T cells as a CD3⁺CD4⁺CD44^{int} population, the cytokine-expressing subpopulations were discriminated from their not-expressing counterparts by matching the dot plots with the respective FMO controls (Figure 4-19). Due to experimental limitations, the experiment was run with only a small number of samples and statistical evaluation has been omitted.

First, we did not see any significant differences among effector T cell numbers regarding the time point and the type of treatment (data not shown). Then, we analyzed the cytokine-expressing T cell subsets. We found a trend towards higher frequencies of Th2 cells (IL-13⁺, IL-4⁺ or IL-10⁺) after HDM treatment at either ZT3 or ZT15 (Figure 4-19A-F). In contrast, the frequency of Th1 cells (IFN- γ ⁺) did not seem to change after HDM immunization at ZT3 or ZT15 (Figure 4-19I, J). The frequency of FoxP3⁺ T_{reg} cells seemed to be higher at ZT3 in response to HDM treatment as compared with PBS treatment, whereas I found no change in the frequency of Foxp3⁺ T_{reg} cells at ZT15 (Figure 4-19K, L). Further, I found a trend towards a higher frequency of IL-17A⁺ effector T cells in mice treated with HDM at ZT3 as compared to ZT15 (Figure 4-19 G, H).

4 Results

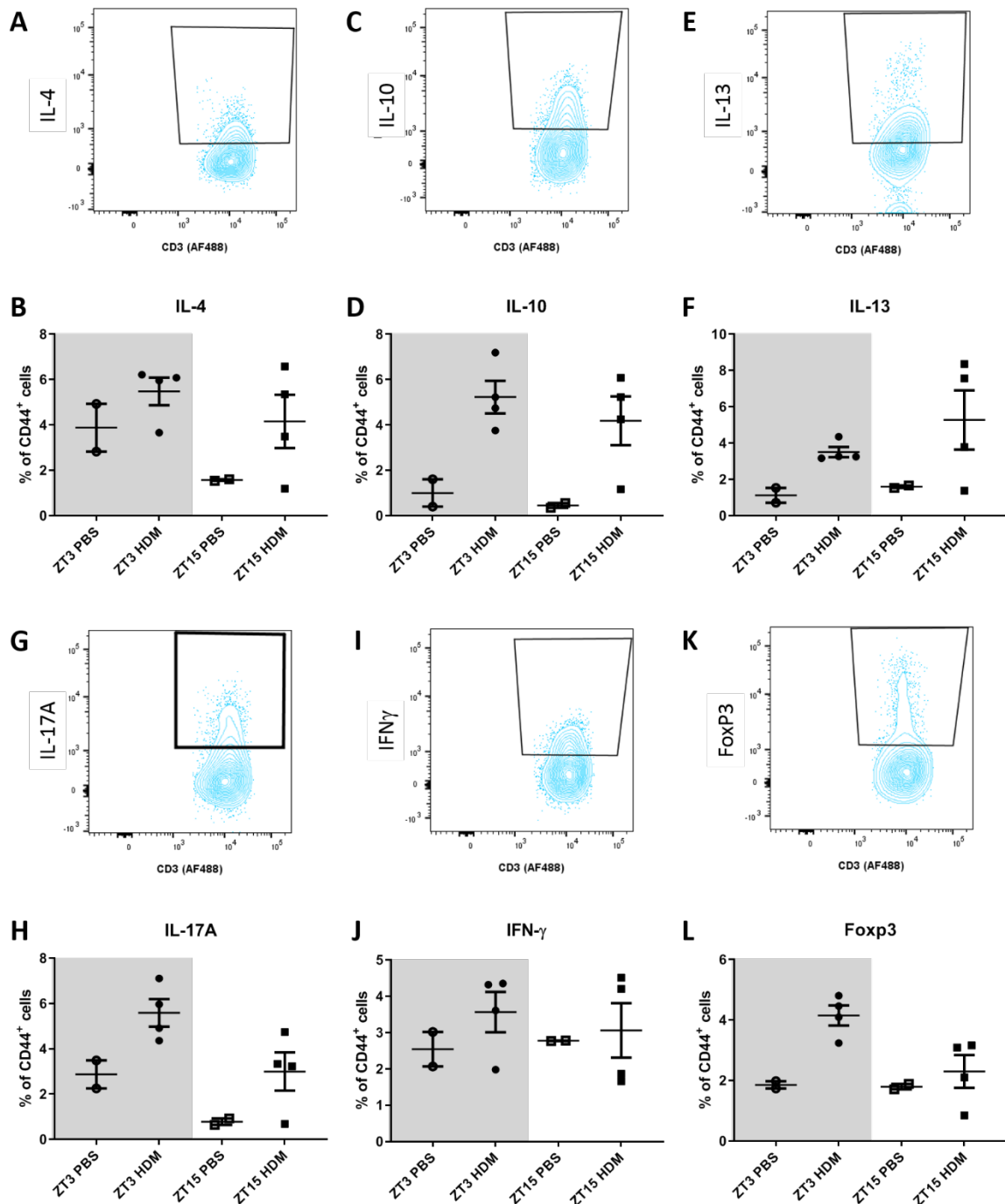


Figure 4-19: Increased frequency of pulmonary Th2, Th17 and Treg cells in response to HDM treatment at ZT3 and/or ZT15

Mice were entrained to 12:12h LD environment for at least 3 days, followed by the four-step HDM immunization protocol. After AHR measurement, mice were sacrificed, BALF was obtained, and the right lung harvested. Pulmonary cells were isolated and processed for intracellular staining as described. Stained cells were analyzed by flow cytometry and cell populations defined by the extended T cell gating strategy. Depicted are contour plots and the corresponding graphs showing the frequencies of T cells expressing A and B) IL-4; C and D) IL-10; E and F) IL-13; G and H) IL-17A; I and J) IFN- γ ; and K and L) FoxP3 at ZT3 and ZT15. n=2-4; data are expressed as mean \pm SEM; grey background = resting phase, white background = activity phase; circles = ZT3, squares = ZT15, white signs = PBS-treated, black signs = HDM-treated

4.3.8 Increased pulmonary IL-13, IL-17 and IFN- γ production in response to HDM treatment at ZT3

As I observed differences in the frequencies of Th2, Th17 and T_{reg} cells in response to HDM-immunization at ZT3 and/or ZT15, I determined the cytokine production from pulmonary cell cultures after HDM treatment at ZT3 or ZT15. I performed *in-vitro* restimulation of full lung cell suspensions of PBS- and HDM-treated mice and assessed the concentrations of the Th2 cytokines IL-4, IL-5, IL-13, the Th17 cytokine IL-17 and the Th1 cytokine IFN- γ in the culture supernatants by ELISA.

IL-4 and IL-5 levels were below the detection limit. In contrast, I found a significant increase in the IL-13-levels after HDM-immunization at ZT3 when compared to HDM-immunization at ZT15 ($p < 0.001$, Figure 4-20A). Also, IL-17 levels were significantly higher after HDM-immunization at ZT3 when compared with ZT15 ($p < 0.01$, Figure 4-20B). Finally, also IFN- γ levels were significantly higher at ZT3 compared with ZT15 ($p < 0.05$, Figure 4-20C).

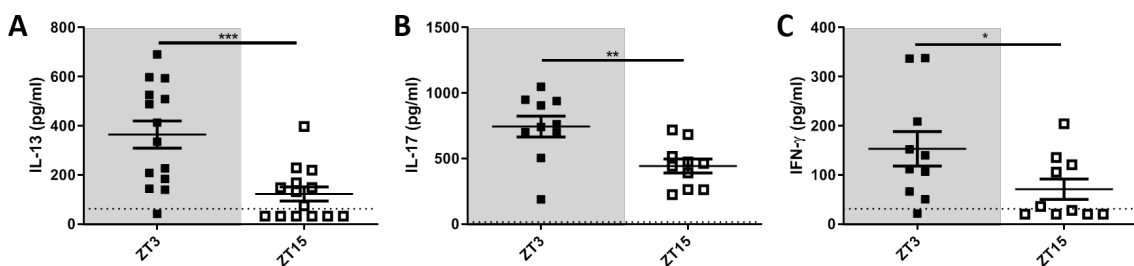


Figure 4-20: HDM treatment at ZT3 results in higher IL-13, IL-17 and IFN- γ production from pulmonary immune cells than HDM treatment at ZT15

Mice were entrained to 12:12h LD environment for at least 3 days, followed by the four-step HDM immunization protocol. After AHR measurement, mice were sacrificed, BALF was obtained, and the right lung harvested. Pulmonary cells were isolated and processed for ELISA as described. Depicted are the cytokine levels of IL-13, IL-17A and IFN- γ from HDM-treated mice. $n = 10-14$; data are expressed as mean \pm SD, according to Shapiro-Wilk-test: A and C were analyzed by U-test, B by t-test; black squares = ZT3, white squares = ZT15; dotted line = resp. detection limit; * < 0.05 , ** $p < 0.01$, *** $p < 0.001$

4.3.9 Minor production of Th2 cytokines in the airways after HDM treatment at ZT3 and ZT15

Finally, I determined the cytokine production in the airways after HDM treatment at ZT3 and ZT15 by multiplex assay.

I found strong production of CXCL1 after HDM treatment at ZT3 ($p < 0.001$) and ZT15 ($p < 0.01$, Figure 4-21B). In contrast, there was only a minor production of the Th2 cytokines IL-5 ($p < 0.01$ at ZT3 and $p < 0.05$ at ZT15, Figure 4-21C) and IL-10 ($p < 0.01$ at ZT3 and $p < 0.05$ at ZT15, Figure 4-21D) upon HDM immunization. Similarly, the concentrations of TNF- α and the growth factor VEGF were low (Figure 4-21A and E). The concentrations of GM-CSF, IFN- γ , IL-1 β , IL-4, IL-6, IL12P70 and IL-13 were below the detection limit (data not shown).

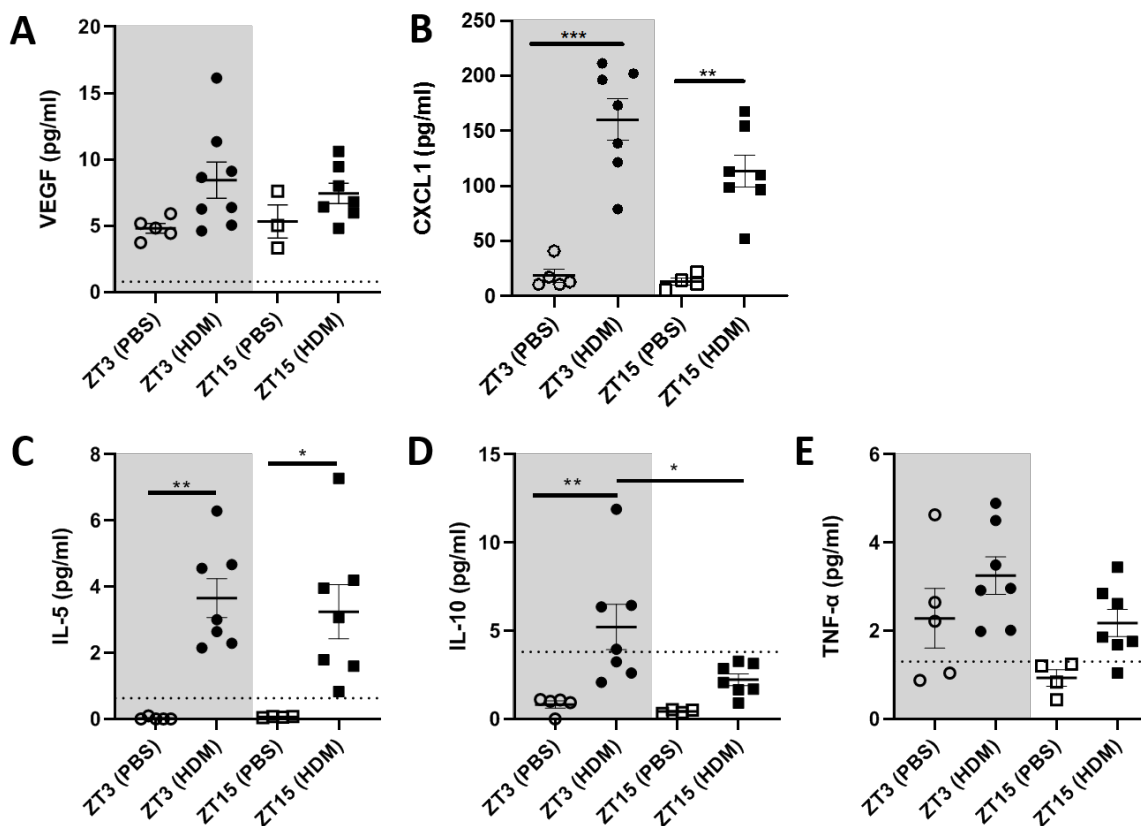


Figure 4-21: Proinflammatory mediators in the airways after HDM treatment at ZT3 and ZT15

Mice were entrained to 12:12h LD environment for at least 3 days, followed by the four-step HDM immunization protocol. After AHR measurement, mice were sacrificed and BALF was obtained. The BALF was processed for multiplex assay as described. Depicted are the cytokine levels of A) VEGF, B) CXCL1, C) IL-5, D) IL-10 and E) TNF- α of mice treated with PBS or HDM at either ZT3 or ZT15. Two replicates were analyzed

4 Results

for each mouse. n=3-7; data are expressed as mean \pm SEM and were analyzed by one-way ANOVA with Tukey's multiple comparisons test; white/grey signs = PBS, black signs = HDM, circles = ZT3, squares = ZT15; dotted line = resp. detection limit; * <0.05, ** p<0.01, *** p<0.001

4.3.10 Increased mucus production in response to HDM treatment at ZT3

The histological analysis of the left lung lobes was performed to visualize the mucus production in the effector phase of experimental allergic asthma. Prepared lung slides were stained with PAS to make the mucus area optically visible.

First, the number of PAS⁺ airways was calculated as seen in the exemplary histological slides (Figure 4-22A). There was no significant difference in the percentage of PAS⁺ airways at ZT3 compared to ZT15 (Figure 4-22B). However, when I calculated the area covered with mucus, I found that the frequency of the area filled with mucus was higher at ZT3 than at ZT15 (p<0.05, Figure 4-22D).

4 Results

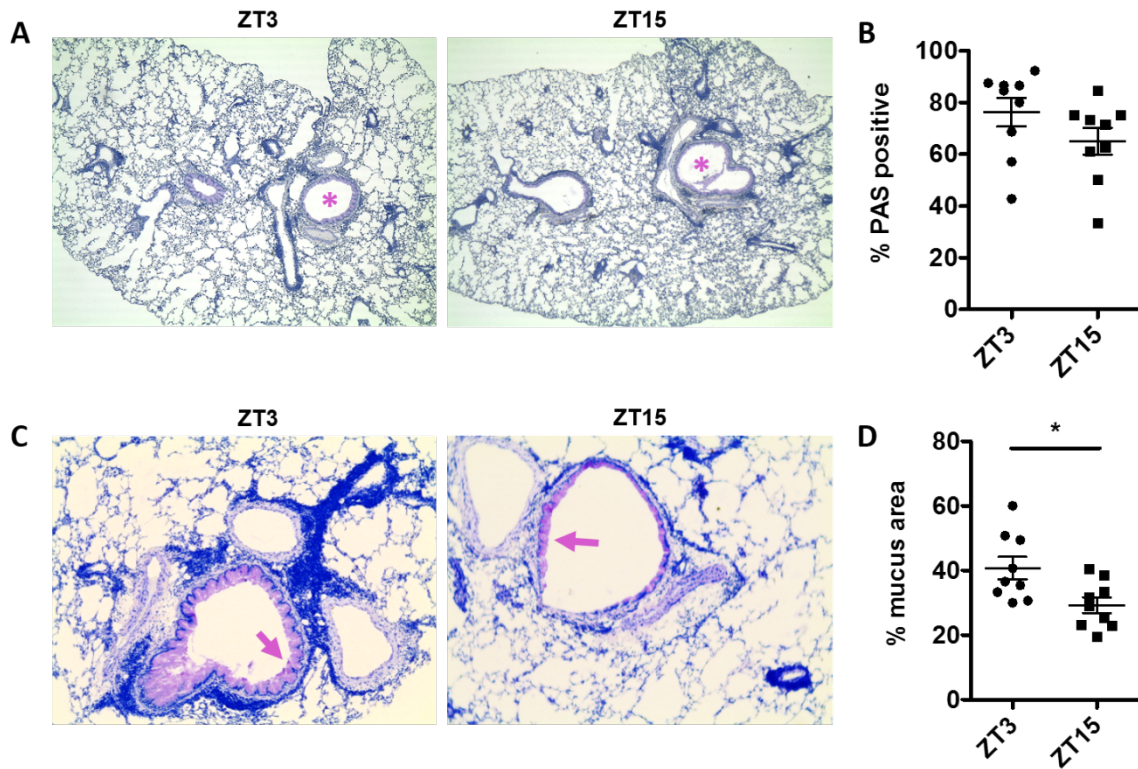


Figure 4-22: Increased frequency of mucus positive areas in the alveoli at ZT3

Mice were entrained to 12:12h LD environment for at least 3 days, followed by the four-step HDM immunization protocol. After AHR measurement, mice were sacrificed, and the left lung lobe prepared for histological examination. A) Histological examination of mucus production of HDM-treated mice at ZT3 and ZT15. Sections were stained with PAS for mucus production (original magnification $\times 200$, violet star marks PAS⁺ airway). B) Frequency of PAS-positive bronchi of HDM-treated mice at ZT3 and ZT15. Mucus producing airways are plotted relative to all airways that have been analyzed. C) Histological examination of mucus production of HDM-treated mice at ZT3 and ZT15. Sections were stained with PAS for mucus production (original magnification $\times 200$, violet arrow marks mucus layer). D) Frequency of mucus-containing area in the airways of HDM-treated mice at ZT3 vs. ZT15. The mucus area was calculated by computing the ratio of the mucus positive and the total area. $n=7-10$; data are expressed as mean \pm SD, approximately normally distributed (Shapiro-Wilk-Test $p>0.05$) and were analyzed by t-test; circles = resting phase (ZT3), squares = activity phase (ZT15); * $p<0.05$

5 Discussion

The awareness of circadian rhythms has risen over the last decades enormously. This might be even stressed by the recent assigned Nobel Prize in Medicine and Physiology that was awarded to Jeffrey C. Hall, Michael Rosbash and Michael W. Young, who discovered the molecular mechanisms controlling the circadian rhythm already back in the 1980's¹⁹⁵. Since their demonstration of a molecular clock driving the physiology and behavior in all organisms, the knowledge about the detailed mechanisms is rising. In this work, I have assessed the influence of the day-night-cycle on the development of allergic asthma. The initial focus was on circadian rhythmicity in immune cell migration under steady state conditions. Then, I investigated the impact of the circadian rhythm on allergen sensitization and the effector phase of allergic asthma. My findings point towards a marked influence of circadian mechanisms on the development of experimental allergic asthma (Figure 5-1).

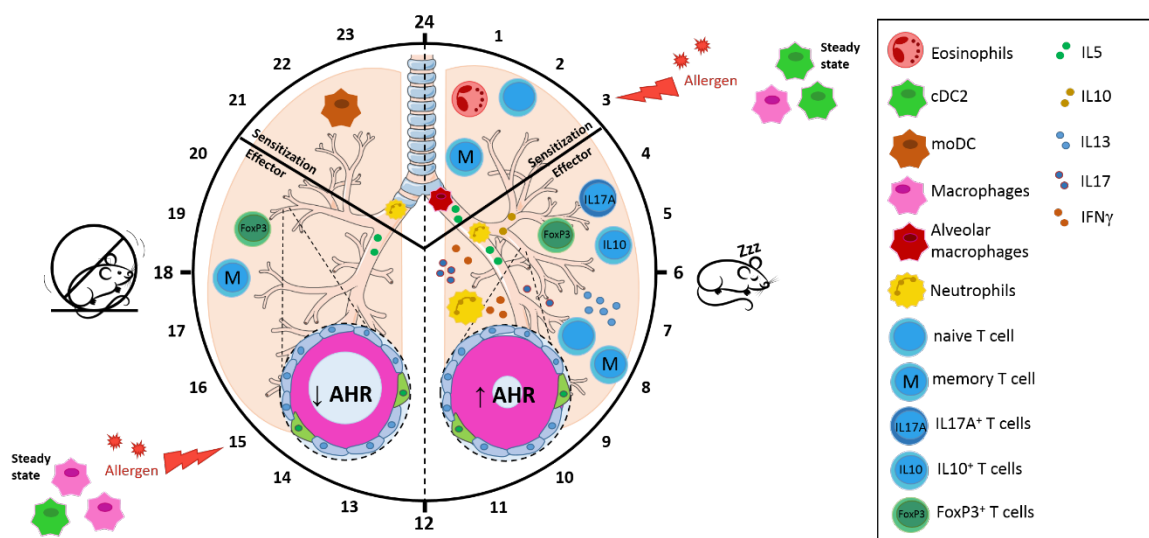


Figure 5-1: Impact of the circadian rhythm on airway and pulmonary inflammation in steady state and after allergen exposure

This graphical conclusion summarizes the results of the performed experiments. Outside of the clock, the cellular environment under steady-state conditions is depicted. Red arrows mark the allergen contact on the dial. The clock itself is divided into the sensitization phase (upper third) and the effector phase (lower two-thirds) for allergen contact at ZT15 (left side) resp. at ZT3 (right side). Inside the airways, results from BAL experiments are depicted, while outside the airways, data obtained by analyzing the lung tissue are summarized. Very important, only significant

differences between ZT3 and ZT15 were considered in the graph and general increases at both times were not included.

5.1 The circadian rhythm regulates immune cell distribution in the lungs at steady state

When discussing the cellular composition of the lung at steady state, this has to be seen as the balance of multiple regulating factors: recruitment of cells, their survival, proliferation and differentiation of cell progenitors as well as survival and apoptosis of the mature immune cells¹⁹⁶. All these components influence the final immune cell number as determined by flow cytometry experiments. I found that these cell numbers are fluctuating during the day and night cycle, suggesting that circadian rhythms regulate the cellular pulmonary composition.

In particular, I could show that pulmonary antigen-presenting cells fluctuate rhythmically during the day and night cycle when the outer Zeitgeber light was excluded. Of particular interest, pulmonary macrophages and cDC2s oscillated inversely, which may have an impact on their major roles as antigen taking cell population. I observed, that cDC2s peak during the early resting phase, while pulmonary macrophages peak during the early activity phase. Comparing the absolute numbers of IMs (approximately 1 200 000) and cDC2s (approximately 150 000) at CT3, results in an 8:1 ratio of IMs to cDC2s in the early resting phase. Regarding CT15, the ratio of IMs (1 900 000) to cDC2s (60 000) is about 32:1 in the early activity phase. In other words, the IM:cDC2 ratio almost quadrupled at daytime with regard to IMs. Interestingly, alveolar macrophage levels stayed stable over time and did not show any circadian fluctuations.

Dendritic cells play a pivotal role at night

This difference in IM:cDC2 ratio might be of particular importance to understand the underlying mechanisms for the varying sensitivity towards airborne allergens at day and night. cDC2s are not only efficient

5 Discussion

in allergen recognition and uptake, they are also the main migratory APC subset in the lungs and specialized in priming T cells towards Th2 cell differentiation^{90,92}. Druzd et al. found a circadian migration of lymphocytes with trafficking towards lymph nodes at night and back to the tissue during the day in steady state and in an experimental autoimmune encephalomyelitis model¹⁹⁷. The group observed the same rhythmicity in MHCII⁺CD11c⁺ DCs peaking during nighttime in the lymphatic tissues leading to an efficient onset of the adaptive immune response. Interestingly, I observed a peak of the DC subset cDC2s in the lung tissue at the same time. Whether these findings refer to an overall increase in migrating dendritic cells at night remains elusive. On the one hand, Druzd et al. performed their investigations in LD conditions, while I used constant darkness and light could therefore be an important outer Zeitgeber in DC migration. Unfortunately, I was not able to characterize the basal levels of DC subsets in the diminutive steady-state mediastinal lymph nodes. Therefore, a direct comparison between my data and those published by Druzd et al. is not possible.

According to the recent knowledge, the steady-state migration of cDCs trafficking to the lymph nodes to present endogenous and exogenous antigens requires a continuous replenishment of the pulmonary cDC pool. Here, an important role for CCR2 and CX3CR1 was pointed out in directing the migration of DC precursors toward the lungs in steady state¹⁹⁶. Whether these receptors are regulated by the molecular clock still remains elusive. In a mouse model of acute liver failure, it was shown that the central clock molecule Per1 binds to the peroxisome proliferator-activated receptor gamma (PPAR- γ) thereby downregulating CCR2 expression¹⁹⁸. A rhythmic release of CCL2 by myeloid cells was also seen in a model of atherosclerosis, where myeloid cells were recruited to the blood vessel in a circadian manner¹⁹⁹. It is possible that the same mechanism is driving DC trafficking to and from the lungs seen in our setting. Concerning CX3CR1 expression, the circadian regulator REV-ERB represses CX3CR1 expression in macrophages and might control

macrophage polarization towards proinflammatory M1 or anti-inflammatory M2 macrophages^{200,201}. However, this mechanism has not been investigated in DCs yet and further conclusions have to be drawn carefully.

Pulmonary macrophages defend the lungs at daytime

Regarding the literature, it is difficult to find information about pulmonary macrophage (also termed interstitial macrophages (IM)) as compared to alveolar macrophages (AM), which have been more frequently studied in the course of allergic asthma in the past years. However, it was recently reported that IMs produce high amounts of IL-10, a DC-suppressing cytokine, when challenged with LPS¹⁰⁶. At daytime, when the organism is exposed to high amounts of airborne allergens, IMs might reduce the DC numbers directly by producing high amounts of IL-10 as seen in the antagonistic migration behavior of macrophages and dendritic cells at steady state.

Circadian rhythms are important to appropriately deal with daily changes in the environment. Concerning immunity, it is of great interest to be prepared right at the time when pathogens meet the organism. Consequently, energy can be saved and an undesired immune response avoided, which may lead to autoimmune reactions²⁰². Regarding the findings from our steady-state experiments, the dominance of pulmonary macrophages at daytime might reflect this circadian adaption to the environment. Most airborne allergens are inhaled during the day, as mice have a higher infection risk at the time of increased activity²⁰³. It is obvious that the organism tries to prepare for inhaling antigens by increasing the number of available pulmonary macrophages in the lungs, which are critical in first-line defense, at daytime. Thus, the probability of infection is reduced. At nighttime, when the number of Th2-favouring cDC2s is relatively increased, the genetic susceptible organism is more vulnerable towards allergens⁹⁰. As the steady-state experiment was

performed in total darkness, this regulation is not controlled by light input rather by intern circadian-driven mechanisms.

Cell trafficking underlies overall clock gene expression

Previous research focused on the expression of self-sustained circadian clocks in immune cell subsets. Especially macrophages were in the focus of interest, as they contain a very robust molecular clock *in-vitro* and *in-vivo* ^{164,204}. Circadian variation in innate immune response in isolated splenic macrophages has been described, which oscillate in TNF- α and IL-6 production due to LPS stimulation with a peak during the day ¹⁶⁴. Focusing on the lung, the circadian expression of several clock genes (e.g. Bmal1, Rev-Erb α , Per2, analyzed by RT-PCR) in the pulmonary tissue of DD-entrained Balb/c mice were described ²⁰⁵. Going one step further, it could be proven that this peripheral pulmonary clock was self-sustained and tissue-specific ¹⁴³. Importantly, the whole lung was analyzed without separation into epithelial or immune cells. That was later optimized by using immunohistochemical techniques in murine lung slides, verifying the strict expression of core clock proteins in bronchiolar cells ¹⁵⁵. Gibbs et al. demonstrated that contrary to the described independent rhythms in splenic macrophages, bronchial epithelial cells might be highly responsive to glucocorticoids, as the glucocorticoids receptor (GR) is coexpressed with clock proteins. Ince et al. could later add that the GR is important, but not pivotal for sufficient circadian control of neutrophil inflammation. There might be more undetected mechanisms in the myeloid cell lineage driving the circadian variations in immune responses ¹⁵⁶. How far cell-intrinsic circadian mechanisms or rather epithelial rhythms regulate APC trafficking at steady state remains elusive and further investigations on pulmonary immune cell subsets are needed.

The circadian rhythm may drive monocyte-derived macrophages

Regarding the origin of pulmonary macrophages, the current understanding is the following: alveolar macrophages derive from fetal

liver-derived monocytes that seed the lungs during the embryonic period²⁰⁶. These monocytes mature to AMs as soon as they arrive in the lungs. Parallel, a small number of macrophages mature in the yolk sac and invade the tissues in the early embryonic stage. Both macrophage types are self-sustaining through local self-renewal²⁰⁷. In addition, a monocyte-derived macrophage type has been described, that has a minimal role in the macrophage pool in the lungs at steady-state, but might be the origin of pulmonary IMs^{208,209}. The reported stable number of AMs in the bronchoalveolar fluid over 24h observed in our study might be due to a constant number of fetal-liver derived progenitors that renew themselves continuously without circadian regulation. In contrast, IMs that are assumed to origin from monocytes, may migrate by a circadian-regulated mechanism. However, there is no molecular mechanism known that drives macrophage trafficking in steady state. It was reported, that the CCL2 expression on macrophages is clock-controlled and drives migration upon inflammation, but whether there exists a related mechanisms at steady state is still elusive^{159,210}.

5.1.1 The C5a/C5aR1 axis contributes to circadian-driven pulmonary sensitivity

As the underlying mechanism that drives the cellular distribution in steady state remains elusive, I aimed to assess the potential contribution of the C5a/C5aR1 axis to this process.

Interestingly, the absence of C5aR1 in a C5ar1^{-/-} mouse strain showed that this receptor has several effects on immune cells of the myeloid lineage. First, the circadian oscillations in macrophages were diminished, while cDC2s had a delayed peak at CT9 instead of CT3. Furthermore, eosinophils oscillated significantly in contrast to the findings in WT mice, where no significant changes in cell number were detectable over time. Comparing cell numbers of macrophage and cDC1 from WT and KO mice, I found marked differences. C5ar1^{-/-} mice had less macrophages in the

lungs at CT15 than the WT population; cDC1 numbers were markedly reduced at CT21 in KO mice.

Recently, expression of C5aR1 on airway and tissue alveolar macrophages, pulmonary eosinophils, neutrophils, cDC2s and moDCs, but not on cDC1s, has been demonstrated ^{128,211}. However, C5aR1 expression is not immune cell specific, as the receptor is also widely expressed on bronchial epithelial cells ¹²⁷. Intense research points towards an important role of C5aR1 in the development of allergic asthma, however, there is not much known about its function at steady-state ^{117,131}.

The analysis of the immune cell distribution in C5ar1^{-/-} mice at steady state might hint to its importance in cell migration. Tissue alveolar macrophages, eosinophils, and cDC2s show modulated rhythmicity in C5ar1^{-/-} mice. Interestingly, the circadian oscillation in macrophages is completely abrogated, while eosinophils oscillate only in C5aR1 KO mice. Concerning the macrophages, it is well-appreciated that the C5a receptor has a major importance in cellular distribution at steady state ¹³⁰. This importance might be even higher according to my findings, as the C5a levels might be the major force driving macrophage migration. As C5a is an important chemoattractant and proinflammatory molecule, its direct influence on the main phagocytic cell type might be consistent.

Eosinophils also express C5aR1 as mentioned already; however, C5a works in the opposite direction here. In WT mice, C5aR1 stabilizes the eosinophil numbers, which fluctuate in the absence of C5aR1 with a peak at the resting phase and a trough during the activity phase. It was earlier reported, that C5a is a main activator of eosinophil adhesion and transmigration in and through the venal endothelium ²¹². In the lungs, the fluctuating C5a levels may keep the constant eosinophil number in steady state, which might be beneficial in immune cleanup work. However, our findings have to be interpreted with caution: due to experimental limitations, there we different numbers of analyzed

5 Discussion

individuals in WT and KO mice – in fact, there were only six mice investigated at CT15 in WT mice. This might be one reason for the reduced significance, as fluctuating cell numbers were also observable in WT mice.

Concerning the modulation of circadian oscillation in cDC2s, this findings point towards a relevant, but not exclusive influence of the C5aR1 expression. The circadian changes in cell number are comparable in WT and C5ar1^{-/-} mice, where the C5aR1 expression stabilize rhythmicity to a symmetric 12h-lasting in- and decrease. The cDC2 distribution might depend on other regulatory mechanisms driving its circulation, too. Conceivable is e.g. a higher affinity of C5a to the C5aR2 in C5ar1^{-/-} mice whose expression has been shown in tdTomato-C5aR2 mouse ²¹³, leading to a continuous oscillation in the presence of C5a. Otherwise, C3a may exert a critical role in cDC2 numbers, as C3aR is also expressed on the cell surface in this subset at steady state ^{178,214,215}. Eventually, the influence of macrophage-produced IL-10 might be another driver in modulating cDC2 fluctuation as a stabilized number in the pulmonary tissue might lead to a more robust IL-10 production and thereby influence DC migration.

Interestingly, cDC1s, which do not express C5aR1 showed a significant drop in cell numbers during the activity period compared to the cell numbers in WT mice ^{128,211}. As a direct effect of C5a on cDC1s is excluded, there might be an indirect mechanism diminishing their number at this time. As the C5aR1 is also expressed on bronchial epithelial cells, they may have the modulating role ¹²⁷. The airway epithelium is known to produce a range of cyto- and chemokines, many of which were proven to be clock-controlled. There is currently no data available concerning a probable C5aR2 expression that might otherwise be a potent regulator of cDC1 cell number over time ²¹⁶. In contrast to the strongly migrating cDC2s it was shown that cDC1s are neighboring the airway epithelium and penetrating the epithelial layer by their dendrites ^{23,87}. This tight

connection between this DC subset and the epithelium might also support stable cell numbers over time.

Taken all findings together, I could prove that the C5a/C5aR1 axis has a particular influence on the immune cell distribution in the lung. It might be of interest to undertake more studies to elucidate the precise involvement of the C5a/C5aR1 axis in circadian cell migration, e.g. by using myeloid-cell specific deletion of C5aR1, which are already available in the Köhl lab ¹²⁸ or by deletion of C5aR1 in epithelial cells.

5.1.2 The time of allergen sensitization impacts on the development of airway and pulmonary inflammation

The differences in cellular distribution in steady-state conditions suggest that immunization at different times might result in different immune responses in response to allergen sensitization. The data obtained after one-step immunization with HDM support this view. The BALF analysis showed a strong increase in neutrophilic airway inflammation when immunization was performed during the activity period, but not during the resting phase.

The neutrophil response is time-dependent

Neutrophils play an important role in initiating the innate and modulating the adaptive immune response by expressing a range of key inflammatory mediators, e.g. complement components, chemokines and cytokines, as well as anti-inflammatory molecules ^{217,218}. Production of CXCL8 by epithelial cells, fibroblasts or alveolar macrophages attracts neutrophils to the site of inflammation and drives the generation of reactive oxygen species (ROS). Interestingly, the HDM allergen contains two components that support neutrophil attraction. Derp1 induces CXCL8 production in bronchial epithelial cells initiating neutrophil recruitment ²¹⁹. Derp2 resembles the myeloid differentiation protein 2 (MD2), thereby

enhancing TLR-4 expression on epithelial cells and triggering DC activation³⁰. Thus, HDM mobilizes peripheral neutrophils to migrate to the lungs where they start ROS generation and promote allergic inflammation^{220,221}. The neutrophil recruitment is regulated by CXCL8 expression of bronchial epithelial cells, which depends on MD2-expression on their outer surface. Our findings could point toward a circadian expression of the respective receptors, MD2 and CXCL8, as the amount of HDM antigen was equal at both times, while the neutrophil attraction markedly differed. In contrast, alveolar macrophages were residing in the airways and started upregulating the production of monocyte attracting proteins (MCP) after allergen challenge, thereby increasing the number of macrophages²²². Parallel findings were obtained in an experiment, in which circadian-entrained mice were stimulated with LPS, and the BALF was analyzed afterwards. In this setting, neutrophil, but not macrophage numbers, differed between the immunization times¹⁵⁴. The findings demonstrated a greater importance of the epithelial clock instead of cell-intrinsic clocks in regulating the inflammatory response. Here, the chemokine CXCL5 was found to serve as a clock-controlled regulator of neutrophil homeostasis.

Proinflammatory cytokine milieu upon nighttime stimulation

In addition to the neutrophil analysis, a detailed analysis of the chemokine and cytokine environment in the BAL was performed. CXCL1 and IL-5 were increased during the resting phase when compared to the activity phase. The chemokine CXCL1, also known as KC/GRO, is produced by resident macrophages and bronchial epithelial cells, and is critical for neutrophil recruitment via the CXCL1/CXCR2 axis in the course of chronic airway diseases²²³⁻²²⁵. Interestingly, circadian regulation of both, CXCL1 and CXCR2, have been described recently. First, Park et al. found that tissue inhibitor of metalloproteinase 3 (TIMP3) is being CLOCK-controlled and which results in rhythmic expression of

5 Discussion

inflammatory cytokines such as CXCL1 in human keratinocytes ²²⁶. Upon ultraviolet light type B (UVB) input, CLOCK and TIMP3 expression was downregulated and cytokine production enhanced. In our study, CXCL1 production increased upon HDM exposure during the resting phase, when the light was turned on. This could point to a similar regulation of neutrophil recruitment in murine airway epithelium. Interestingly, the authors found the same regulatory process for TNF- α production, whereas we found no impact of the immunization time. Second, Adrover et al. could described Bmal1-regulated production of CXCL2 inducing CXCR2 expression ²²⁷. Thereby, circadian-regulated CXCR2 induced neutrophil aging that determined the migration from blood vessels towards peripheral tissues. To sum up, there is increasing evidence for highly regulated circadian trafficking of neutrophils throughout the body.

IL-5, important for eosinophil differentiation and trafficking, is mainly produced by Th2 cells, ILC2 and mast cells ^{228,229}. Our findings of increased IL-5 levels in the BALF after HDM exposure during the resting phase suggest that ILC2 and/or mast cells are more sensitive to HDM-triggered IL-5 production during rest. It has been demonstrated that constant IL-5 production occurs in intestinal ILC2, however, vasoactive intestinal peptide (VIP) adds a circadian component when adjusting the immune response to metabolism ⁶³. This was not confirmed regarding pulmonary IL-5 production. In human BAL samples of asthmatic individuals a correlation of lung function and increased CD4⁺ T cell numbers has been shown ¹⁵². The authors explained the IL-5 increase with the enhanced IL-5 production by the increased number of T cells. At least, our findings point towards an increased number of naïve T cells in the pulmonary tissue, however, T cell numbers in the BAL reached similar levels after immunization at night- or daytime. A more detailed analysis of the alveolar immune cell subsets and the crosstalk with the epithelium might help to define the mechanisms underlying the increased IL-5 levels after HDM during the resting phase.

The allergic potential merges during the resting phase

The airway inflammation was associated with a strong pulmonary increase in inflammatory cells. More specifically, neutrophils increased after one-time allergen contact independent of time, which is in contrast to the airway neutrophils. Taking a closer look, the total neutrophil number was much higher in the pulmonary tissue than in the airways pointing towards a neutrophil migration from the lungs towards the alveolar space. This observation points toward another underlying mechanism regulating the airway neutrophil number which depends in both cases on the MD2 and CXCL8 expression ²³⁰. Focusing on the epithelial barrier, circadian changes in the tight junction integrity were proven in the corneal epithelium ²³¹. This might also occur in the bronchial epithelial layer leading towards increased epithelial vulnerability during the activity phase.

cDC2 and moDC numbers increased strongly after allergen contact in the activity phase. Inflammatory moDCs enter the lung quickly when the immune system reacts to microbes or complex airway allergens. They were not detectable in steady-state conditions, but can support antigen-uptake once mobilized from the circulation into the lung. The low steady-state cell number of cDC2s increased markedly after one-step HDM immunization, resulting in equal cDC2 levels during resting and activity phase upon immunization. The moDC recruitment was shown to depend on the CCL2/CCR2 axis as mentioned earlier. As CCL2 and CCR2 were proven to be regulated by the circadian rhythm, they likely influence the time-dependent moDC trafficking ²³. However, this axis plays no role in cDC2 migration. Upon one-time HDM stimulation, both DC subsets reached equal levels at day and night, but the overall increase surpassed the numbers of PBS controls exposed during the activity phase. Cytokine profiling may help to better understand time-related changes in their functions, as absolute cell numbers were similar.

5 Discussion

Eosinophil numbers, in contrast to the main APCs macrophages and DCs, were massively increased upon immunization during the resting phase when compared to the activity phase. This finding is in line with the increased IL-5 levels in the BAL. Among others, IL-5 is one of the main cytokines that mobilize eosinophils upon inflammation ²²⁸. As IL-5 levels were increased during the resting phase, increased eosinophil numbers in the lungs could be the consequence. Furthermore, circadian cycles have been shown for blood eosinophils, leading to a circadian expression of eosinophil-derived protein production ¹⁶¹. However, the analyzed proteins were all part of the granules and regulate eosinophil effector function that might also differ over time. Unfortunately, there were no chemoattractant proteins analyzed. Therefore, it remains elusive whether these receptors are regulated by the circadian clock, too.

Similar to eosinophil fluctuations, naïve and memory T cells migrated much more efficient during the resting phase than during the activity phase towards the lungs. These findings are in line with earlier reports, as the antigen-specific immune response as well as T cell proliferation is clock-gene controlled ¹⁶⁷. The authors demonstrated different T cell responses upon immunization with OVA-peptide-loaded DCs and found a stronger response during the resting phase. Our data support these findings, as T cell numbers were increased in response to HDM in a similar way. These data points towards an overall circadian regulation of molecules critical for proliferation, defense as well as migration. However, we found no influence of the immunization time on T cell trafficking towards the lymph nodes as seen previously in EAE models ¹⁹⁷. However, we immunized the mice twice with a gap of twelve hours between HDM treatments. Even though there were differences in T cell numbers in the pulmonary tissue at these times, migration towards the lymph nodes might be shifted and therefore time-related differences might be difficult to see.

Taken together, we found a strong impact of the immunization time (activity vs. resting phase) on the initial phase of allergen sensitization in a model of HDM-driven experimental allergic asthma.

5.1.3 The allergic phenotype in response to repeated allergen exposure during the sleeping phase is stronger as compared with exposure during the activity phase

Summarizing the findings of the four-step immunization experiment, allergen contact during the activity phase dampens, while allergen contact during the resting phase enhances the development of the allergic phenotype (Figure 5-1, p. 108). Similar to this observation the timing of sepsis induction had direct influence on the dying probability of septic patients ^{146,232}.

The overall influence of the immunization time is clearly visible regarding the AHR and mucus production. Concerning the AHR, mice immunized during their sleeping time, showed a significantly higher AHR when compared to mice immunized during the activity phase associated with increased mucus production. These results in a mouse model of allergic asthma match some of the well-known fluctuations in symptom severity in asthmatic patients ²³³. Analyses in asthmatic patients showed an aggravation of symptoms at night upon allergen contact in genetic susceptible individuals which were correlated to infections. The experimental setting used in our experiments allowed the direct comparison of allergen exposure at a defined time point during the night or the day cycle. With this setting the mouse models adds to the understanding of the specific mechanism underlying the development of allergic asthma related to circadian changes in the pulmonary environment. Increased AHR and mucus overproduction during the resting phase point towards an increased Th2 immune response with the

production of the characteristic proinflammatory cytokines IL-4, IL-5 and IL-13.

Increased recruitment of inflammatory cells upon immunization during the resting phase

Analyzing the cellular immune response associated with high AHR and mucus production in response to allergen exposure during the resting phase, we found several differences when compared to allergen exposure during the activity phase. There was a strong influx of inflammatory cells (alveolar macrophages, eosinophils, T cells) to the airways at both times; however, neutrophils increased only during the resting phase. This is in contrast to the findings in the sensitization phase, where the neutrophil number raised only during the activity phase. Our findings suggested an influence of the circadian driven production of neutrophil-attracting chemokines by the broncho-epithelial cells. However, upon four-time allergen exposure, a parallel and strong increase in macrophage numbers was characteristic for the ongoing inflammation. Macrophages, as well as neutrophils, produce high amounts of CXCL8 thereby driving or amplifying neutrophil attraction ²³⁴. As the number of macrophages was strongly increased during the resting phase, the massive production of this chemokine may account for the neutrophil increase.

Concerning the pulmonary inflammation, APC subsets and eosinophils increased similarly upon allergen contact, independent of the time of allergen exposure. Similar to the airways, neutrophil numbers in the lung increased only upon allergen contact during the resting phase, probably due to CXCL8 production.

With regard to the T cell response, we found that T cell numbers differed between the two immunization times in the lungs and the lymph nodes. While naïve T cells were dominant during the resting phase in the lungs, all T cell subset levels (naïve, effector, and memory T cells) were increased in the lymph nodes at that time. Our findings are in line with a report, in which T cell activation upon antigen presentation via

ovalbumin-loaded DCs was analyzed. Mice immunized during their resting phase had a higher splenic immune response than mice immunized during their activity period ¹⁶⁷. The authors excluded the influence of an APC intrinsic molecular clock, and showed an important role of an intrinsic T cell clock as well as systemic influences, like immunomodulatory hormones from the adrenal gland ^{235,236}. Interestingly, blood analyses in humans showed that naïve T cells were peaking at nighttime, while effector T cells increased at daytime ²³⁷. They explained these findings by the high cortisol sensitivity of naïve T cells due to a pronounced CXCR4 expression and catecholamine sensitivity of effector T cells because of strong CX3CR1 expression. We did not find any differences in effector T cell numbers in the murine lung in response to allergen exposure during the resting or activity period. In contrast, naïve, effector and memory T cells peaked upon immunization in the resting phase. These differences may originate from the dominant cell-intrinsic clock expressed in T lymphocytes. Several groups described the expression of clock proteins in T cells as well as a prominent role of these genes in regulating T cell trafficking and function ²³⁸.

T cell differentiation and cytokine production is increased during the resting phase

Next, we performed a detailed analysis of the pulmonary effector T cells, as they differentiate into effector cells upon allergen contact due to the produced cytokines by surrounding immune and epithelial cells. Intracellular staining revealed that IL-17A producing T cells, resp. Th17 cells, as well as IL-10 producing T cells, Th2 and iT_{reg} cells dominated after allergen exposure during the resting phase, whereas the change in IFN- γ ⁺ Th1 cells was minor. However, these findings have to be interpreted with caution, as the number of individuals evaluated was very low (n=2-4) due to experimental limitations. At best, they can be seen as a hint for T cell differentiation in the pulmonal tissue.

5 Discussion

In addition to intracellular cytokine measurements in T cells, we determined the cytokines in the supernatants of pulmonary cells. High IL-13, IL-17 and IFN- γ levels were significantly higher during the resting as compared with the activity phase. The strong IL-17 production during rest matches the increased frequency of Th17 cells observed in mice exposed to HDM during the resting phase. Mechanistically, a direct link between the transcription factor E4BP4 and the lineage-specific promotor ROR γ t²³⁹ has been described. The latter is directly related to the transcription factor Rev-Erb α that is a member of the circadian transcriptional-translational feedback loop driving the molecular clock (see introduction). However, there was no direct influence of BMAL1 deficiency in a T cell-specific BMAL1-knock out mouse on Th17 cell differentiation²⁴⁰, suggesting other mechanism that account for the differences that we have observed.

Interestingly, Th2-cell-produced IL-13 was also high after resting phase exposure, which was also associated with an increase in IL-13⁺ Th2 cells. However, the low IL-13 production that we found in pulmonary cells from mice exposed to HDM during the activity phase did not match the relatively high frequency of IL13⁺ Th2 cells. In line with the discrete increase in the frequency of IL-13⁺ T cells, we found an increase in the frequency of IL-4⁺ T cells in mice exposed to HDM during the resting and the activity phase. Both, IL-4 and IL-13, are mainly produced by Th2 cells and lead the asthma-defining symptoms of IgE synthesis, eosinophil activation, mucus overproduction as well as airway remodeling. Interestingly, both cytokines bind and activate related cytokine receptors sharing the same IL-4R α chain. Namely, there are two distinct IL-4 receptors (IL-4R) distinguished: type I IL-4R is composed of IL-4R α / γ C heterodimers and binds only IL-4, while type II IL-4R is composed of IL-4R α and IL-13R α 1 binding IL-4 as well as IL-13²⁴¹. By that, IL-4 and IL-13 are able to activate the same JAK/STAT signal cascade to modulate allergic diseases. This mechanism has recently come in the focus of intense research, as blocking the IL-4 and IL-13 signal cascade by

5 Discussion

monoclonal antibodies, e.g. dupilumab, is promising in treating allergic diseases²⁴². Referring to our results, a circadian up- and downregulation of the two decent IL-4Rs with an increase of type II IL-4R during the activity phase could be an explanation for the lower IL-13 level at the same time. Unfortunately, circadian regulation of the IL-4R has not been in the focus of research yet, however, similar fluctuations of IL-4 and IL-13 levels have been reported in a mouse model of allergic rhinitis²⁴³. There, a correlation of cytokine levels and the expression of the circadian clock gen Per2 was proven and an influencing role of Per2 in regulating symptom severity suggested.

IFN- γ , mainly produced by Th1 cells and primarily considered as the counterpart to Th2 cells, was also measurable in the supernatant of mice immunized during the resting phase, although the absolute amounts were lower than what was found for IL-13 or IL-17A. The significantly higher amount of IFN- γ in mice exposed to HDM during the resting phase was not matched by a difference between IFN- γ ⁺ Th1 cells between the two treatment groups. The high IL-10 concentrations in the airways found during the resting phase are in line with the high frequency of IL-10⁺ effector T cells in the lung tissue at the same time. In summary, the higher production of IL-17A and IL-13 in mice immunized with HDM during the resting phase support the view of a stronger allergic phenotype induced by allergen exposure during rest. More data are required to directly link the increased Th17 and Th2 cytokine production from pulmonary cells to a higher frequency of IL-17A⁺ Th17 and IL-13⁺ Th2 cells.

Recently, the expression of clock genes in T lymphocytes came into the focus of research. It was shown that T cells harbor a functional intrinsic clock driving IL-2, IL-4, IFN- γ and CD40L expression *in vitro* and *in vivo*²⁴⁴. The authors further identified a range of circadian-expressed transcription factors, namely NF- κ B, AP1, E4PB4, and ROR α . They detected a rhythmic expression of KLRC2, a gene indicating a time-dependent Th1 response as it encodes a natural killer cell-specific

transmembrane protein that is missing in Th2 cells. Our findings support the idea that not only Th1 cells but also Th2 or Th17 cells are regulated by an intrinsic molecular clock. As recently reported, the transcription factor E4BP4 regulates the transcription of IL-10 and IL-13 production in CD4⁺ T cells, including Th2 cells. Since E4BP4 is clock-controlled, it might also affect the Th2 specific cytokines ²²³. Bollinger et al. demonstrated that human CD4⁺ T cells produced IL-2, IFN- γ , TNF- α and IL-10 rhythmically *in-vitro* ²⁴⁶. They also found evidence for natural T_{reg} cells regulating these diurnal variations in cytokine production together with cortisol and prolactin levels. Supporting findings were obtained in a human study, in which T_{reg} cell numbers and their suppressive function oscillated over day and night in a circadian manner ²⁴⁷. During regular sleep-wake cycles, the T_{reg} numbers and serum IL-2 levels were highest during the resting phase and dropped to its trough in the early activity phase. The group further analyzed FoxP3 expression levels, which did not follow a circadian rhythmicity. This goes in line with our findings, as the percentage of FoxP3⁺ T cells did not change over time. However, we found fluctuating IL-10 levels which are produced by T_{reg} cells, but also by Th effector cells which may explain the detected variation there.

Considering our findings, T cells seem to be part of a wide-ranging circadian system, with self-sustained circadian rhythms in the T cells. Further, centrally regulated hormones and neuropeptides influence peripheral clocks in epithelial cells and professional immune cells.

In-vitro studies with sorted immune cell subsets from naïve mice could help to gain more insights in the mechanisms controlling the circadian fluctuations that we have observed. A molecular analysis of activated APCs, neutrophils and T cells for clock-controlled cytokine expression by qPCR could point out the mechanism behind our findings. Furthermore, the examination of circulating hormones such as glucocorticoid and neuropeptide levels during the entire experimental period might prove useful.

5.2 Allergic asthma interrupts the regular sleep-wake cycle

The infrared scan analysis of mice that underwent the four-step immunization protocol points toward an important influence of the developing asthmatic phenotype on the sleep-wake cycle. The HDM-immunized mice developed a disrupted sleep-wake rhythm and did not follow the light entrainment that was consequently running in a 12:12h LD cycle. Our findings can be summarized as follows: i) HDM-treatment during the activity phase led to higher activity levels compared to PBS-controls; ii) HDM-treatment during the resting phase resulted in reduced activity levels compared to PBS-controls; iii) anesthesia resulted in more restlessness during resting phase in mice, predominately upon HDM-treatment.

Following HDM-treated mice over the whole experimental period, mice treated during the resting phase became less active during the day, probably by exhaustion due to excessive breathing work. Another aspect might be the sleep interruption by performing the experimental procedure during their rest time. Mice immunized during their activity phase were significantly more active during their activity phase and showed a more disrupted sleeping pattern during the resting phase. However, also the control mice were affected, in particular through anesthesia, which was associated with changes in their wake-sleep-patterns.

Thus, it will be important to investigate the influence of the anesthesia on the sleep-wake cycle together with the PBS- or HDM-treatment. We used the established method of injecting xylazine (Rompun) and ketamine (Ketavet) intraperitoneally ²⁴⁸. Ketamine is an N-methyl-D-aspartate (NMDA) receptor antagonist and xylazine an α_2 -adrenergic agonist leading to analgesia, hypnosis and muscular relaxation for about 20 minutes when given in combination ²⁴⁹. Mihara and colleagues investigated how the timing of ketamine anesthesia disrupts the sleep-

5 Discussion

wake cycle in rats ²⁵⁰. Rats were treated either with ketamine or pentobarbital during their resp. resting or activity phase. The circadian rhythmicity was checked by analyzing the pineal melatonin secretion, a nocturnal sleep-regulating hormone, and the locomotor activity the days after anesthesia ²⁵¹. Here, the effect of ketamine administration was found to depend on the timing. When ketamine was injected during the resting phase of the rats, the peak for melatonin secretion and locomotor activity was accelerated. When ketamine was injected during the activity phase, the authors observed an opposing effect and the acrophase for melatonin secretion and locomotor activity were delayed. This phase shift occurred on the first day, 2.5 – 4 hours after the procedure. Furthermore, ketamine administration during the activity phase led to a melatonin reduction, while there was no effect during the resting phase. These points towards the influence of anesthetics on the circadian activity. Concerning our results, the administration of anesthesia during the activity phase resulted in overall increased activity levels, which could be explained by the described melatonin reduction. Having this in mind, the strong differences between the activity profile of mice treated with HDM during their active or resting phase might origin not only from the severity of the asthmatic phenotype, but also from the time of anesthesia and its impact on the interruption of physiological sleep-wake cycles.

Additionally, the repeated use of anesthesia might interfere with the behavior of the mice, as we recognized changes in activity patterns also in PBS-treated control mice, which did not develop an asthmatic phenotype. Hohlbaum et al. reported the influence of repeated anesthesia on the wellbeing of mice and found short-term effects on anxiety ²⁵². However, the mice seemed to adopt to the repeating stress episodes and no accumulating effect was observed. However, even though the mice did not develop severe distress, the effect of four times intervention (i.e. *i.t.* injection) should not be underestimated and may contribute to the increased restlessness in PBS-control mice.

5 Discussion

Our findings in experimental asthma are corroborated by clinical studies. A study conducted with American children found that poor asthma control and certain genetic backgrounds, as African American and Latino children, were main drivers of severe sleep problems ²⁵³. An older study from 1998 analyzed the sleep behavior of children by polysomnography together with cognitive testing ²⁵⁴. Polysomnography works similar to our infrared analysis and is a tool to analyze human physical activity by recording an electroencephalogram (EEG), submental electromyogram (EMG) and electro-oculogram (EOG). The group discovered that children awoke more frequently at night when suffering from allergic asthma and had severe concentration problems at daytime.

As sleep is known to be very important in maintaining mental and physical health, sleep disruption and deprivation leads to a reduced immune function and prolonged recovery times due to illnesses and injuries ²⁵⁵. A poor sleep quality in asthmatic patients points towards a poor disease control ⁵. The patient is not only suffering from a bad night, the effect on his daytime functioning and life quality is not to underestimate ²⁵⁶. The different influences on disease severity are summarized in Figure 5-2, p. 130. Our experiments demonstrate that circadian fluctuations in inflammatory cells and cytokines are worsening the asthma symptoms after HDM exposure during the resting cycle. Interestingly, it was shown that histamine, which is released during allergic inflammation and mediates the allergic phenotype via its histamine H4 receptor ²⁵⁷, is also able to regulate the sleep-wake-cycle by controlling the cortical arousal in the brain by the histamine H3 receptor ^{258,259}. However, this is only one important mediator in allergic asthma, and further research has to be performed to get a better understanding of the influence of allergic asthma on the sleep-wake cycle and the other way round. By understanding the mechanisms in detail, treatment strategies might be optimized and hopefully morbidity and mortality rates in allergic asthma patients reduced in the future.

5 Discussion

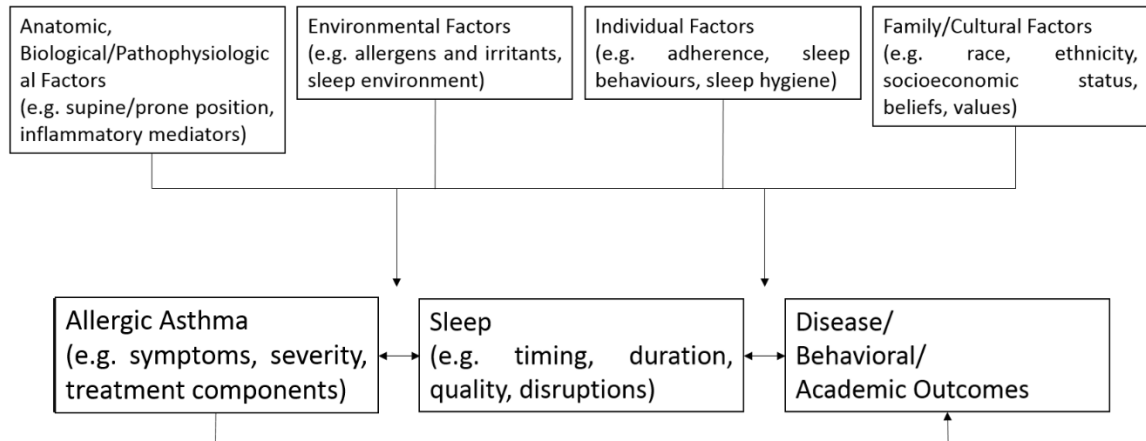


Figure 5-2: Conceptual model of the relation between allergic asthma and sleep

The model depicts the association of allergic disease, sleep and disease outcome in relation to biological, environmental, individual and family factors. Modified according to 'Sleep and allergic disease: A summary of the literature and future directions for research' ²⁶⁰.

6 References

1. Kassiopeia. Michael Ende | Offizielle Webseite. Published July 9, 2018. Accessed July 27, 2021. <http://michaelende.de/figur/kassiopeia>
2. Svoboda M. Zitate von Michael Ende (62 Zitate) | Zitate berühmter Personen. Beruhmte-zitate.de. Accessed July 27, 2021. <http://beruhmte-zitate.de/autoren/michael-ende/>
3. Selroos O, Kupczyk M, Kuna P, et al. National and regional asthma programmes in Europe. *Eur Respir Rev.* 2015;24(137):474-483. doi:10.1183/16000617.00008114
4. Langen U, Schmitz R, Steppuhn H. Prevalence of Allergic Diseases in Germany: Results of the German Health Interview and Examination Survey for Adults (DEGS1). *Bundesgesundheitsblatt Gesundheitsforschung Gesundheitsschutz.* Published online May 2013. doi:10.1007/s00103-012-1652-7
5. Bundesärztekammer (BÄK), Kassenärztliche Bundesvereinigung (KBV), Arbeitsgemeinschaft der Wissenschaftlichen Medizinischen Fachgesellschaften (AWMF). Nationale VersorgungsLeitlinie Asthma - Langfassung. 2018;3. Auflage (Version 1). doi:10.6101/AZQ/000400.
6. Sutherland E. Nocturnal asthma. *J Allergy Clin Immunol.* 2005;116(6):1179-1186. doi:10.1016/j.jaci.2005.09.028
7. Gervais P, Reinberg A, Gervais C, Smolensky M, DeFrance O. Twenty-four-hour rhythm in the bronchial hyperreactivity to house dust in asthmatics. *J Allergy Clin Immunol.* 1977;59(3):207-213. doi:10.1016/0091-6749(77)90151-8
8. Nakao A, Nakamura Y, Shibata S. The circadian clock functions as a potent regulator of allergic reaction. *Allergy.* 2015;70(5):467-473. doi:10.1111/all.12596
9. Rink L, Kruse A, Haase H. Kapitel 9: Autoimmunität. In: Rink L, Kruse A, Haase H, eds. *Immunologie Für Einsteiger.* 14th ed. Spektrum Akademischer Verlag; 2012:169-184.
10. Rink L, Kruse A, Haase H. Kapitel 10: Allergie. In: Rink L, Kruse A, Haase H, eds. *Immunologie Für Einsteiger.* 14th ed. Spektrum Akademischer Verlag; 2012:185-200.
11. Rackemann FM. A working classification of asthma. *Am J Med.* 1947;3(5):601-606. doi:10.1016/0002-9343(47)90204-0

6 References

12. Wenzel SE. Asthma phenotypes: the evolution from clinical to molecular approaches. *Nat Med.* 2012;18(5):716-725. doi:10.1038/nm.2678
13. Humbert M, Durham SR, Ying S, et al. IL-4 and IL-5 mRNA and protein in bronchial biopsies from patients with atopic and nonatopic asthma: evidence against "intrinsic" asthma being a distinct immunopathologic entity. *Am J Respir Crit Care Med.* 1996;154(5):1497-1504. doi:10.1164/ajrccm.154.5.8912771
14. Lötvall J, Akdis CA, Bacharier LB, et al. Asthma endotypes: a new approach to classification of disease entities within the asthma syndrome. *J Allergy Clin Immunol.* 2011;127(2):355-360. doi:10.1016/j.jaci.2010.11.037
15. Holt PG, Sly PD. Interaction between adaptive and innate immune pathways in the pathogenesis of atopic asthma: operation of a lung/bone marrow axis. *Chest.* 2011;139(5):1165-1171. doi:10.1378/chest.10-2397
16. Thomson NC, Chaudhuri R. Asthma in smokers: challenges and opportunities. *Curr Opin Pulm Med.* 2009;15(1):39-45. doi:10.1097/MCP.0b013e32831da894
17. van den Berge M, Heijink HI, van Oosterhout AJM, Postma DS. The role of female sex hormones in the development and severity of allergic and non-allergic asthma. *Clin Exp Allergy J Br Soc Allergy Clin Immunol.* 2009;39(10):1477-1481. doi:10.1111/j.1365-2222.2009.03354.x
18. Jatzlauk G, Bartel S, Heine H, Schloter M, Krauss-Etschmann S. Influences of environmental bacteria and their metabolites on allergies, asthma, and host microbiota. *Allergy.* 2017;72(12):1859-1867. doi:10.1111/all.13220
19. Chau-Etchepare F, Hoerger JL, Kuhn BT, et al. Viruses and non-allergen environmental triggers in asthma. *J Investig Med Off Publ Am Fed Clin Res.* 2019;67(7):1029-1041. doi:10.1136/jim-2019-001000
20. Maestrelli P, Boschetto P, Fabbri LM, Mapp CE. Mechanisms of occupational asthma. *J Allergy Clin Immunol.* 2009;123(3):531-542; 543-544. doi:10.1016/j.jaci.2009.01.057
21. Lambrecht BN, Hammad H. The immunology of asthma. *Nat Immunol.* 2015;16(1):45-56. doi:10.1038/ni.3049
22. Farlex. Farlex Partner Medical Dictionary. Atopy. Published 2012. Accessed September 28, 2017. <http://medical-dictionary.thefreedictionary.com/atopy>

6 References

23. Hoffmann F, Ender F, Schmutte I, et al. Origin, Localization, and Immunoregulatory Properties of Pulmonary Phagocytes in Allergic Asthma. *Front Immunol.* 2016;7:107. doi:10.3389/fimmu.2016.00107
24. Xiao C, Puddicombe S, Field S, et al. Defective epithelial barrier function in asthma. *J Allergy Clin Immunol.* 2011;128(3):549-556. doi:10.1016/j.jaci.2011.05.038
25. Gangl K, Waltl EE, Vetr H, et al. Infection with Rhinovirus Facilitates Allergen Penetration Across a Respiratory Epithelial Cell Layer. *Int Arch Allergy Immunol.* 2015;166(4):291-296. doi:10.1159/000430441
26. Tatsuta M, Kan-O K, Ishii Y, et al. Effects of cigarette smoke on barrier function and tight junction proteins in the bronchial epithelium: protective role of cathelicidin LL-37. *Respir Res.* 2019;20(1):251. doi:10.1186/s12931-019-1226-4
27. Gon Y, Hashimoto S. Role of airway epithelial barrier dysfunction in pathogenesis of asthma. *Allergol Int Off J Jpn Soc Allergol.* 2018;67(1):12-17. doi:10.1016/j.alit.2017.08.011
28. Jeong SK, Kim HJ, Youm J-K, et al. Mite and Cockroach Allergens Activate Protease-Activated Receptor 2 and Delay Epidermal Permeability Barrier Recovery. *J Invest Dermatol.* 2008;128(8):1930-1939. doi:10.1038/jid.2008.13
29. Tan AM, Chen H-C, Pochard P, Eisenbarth SC, Herrick CA, Bottomly HK. TLR4 signaling in stromal cells is critical for the initiation of allergic Th2 responses to inhaled antigen. *J Immunol Baltim Md 1950.* 2010;184(7):3535-3544. doi:10.4049/jimmunol.0900340
30. Hammad H, Chieppa M, Perros F, Willart M, Germain R, Lambrecht BN. House dust mite allergen induces asthma via TLR4 triggering of airway structural cells. *Nat Med.* 2009;15(4):410-416. doi:10.1038/nm.1946
31. Lambrecht BN, Hammad H. Allergens and the airway epithelium response: Gateway to allergic sensitization. *J Allergy Clin Immunol.* 2014;134(3):499-507. doi:10.1016/j.jaci.2014.06.036
32. Halim TYF, Rana BMJ, Walker JA, et al. Tissue-Restricted Adaptive Type 2 Immunity Is Orchestrated by Expression of the Costimulatory Molecule OX40L on Group 2 Innate Lymphoid Cells. *Immunity.* 2018;48(6):1195-1207.e6. doi:10.1016/j.immuni.2018.05.003
33. Tamachi T, Maezawa Y, Ikeda K, et al. IL-25 enhances allergic airway inflammation by amplifying a TH2 cell-dependent pathway in

6 References

- mice. *J Allergy Clin Immunol.* 2006;118(3):606-614. doi:10.1016/j.jaci.2006.04.051
34. Drake LY, Kita H. IL-33: biological properties, functions, and roles in airway disease. *Immunol Rev.* 2017;278(1):173-184. doi:10.1111/imr.12552
35. Lambrecht BN, Hammad H. Biology of Lung Dendritic Cells at the Origin of Asthma. *Immunity.* 2009;31(3):412-424. doi:10.1016/j.immuni.2009.08.008
36. Krabbendam L, Bal SM, Spits H, Golebski K. New insights into the function, development, and plasticity of type 2 innate lymphoid cells. *Immunol Rev.* 2018;286(1):74-85. doi:10.1111/imr.12708
37. Pelaia G, Vatrella A, Maselli R. The potential of biologics for the treatment of asthma. *Nat Rev Drug Discov.* 2012;(11.12):958-972.
38. Holgate ST. Innate and adaptive immune responses in asthma. *Nat Med.* 2012;18(5):673-683. doi:10.1038/nm.2731
39. Kaplan MH, Schindler U, Smiley ST, Grusby MJ. Stat6 is required for mediating responses to IL-4 and for development of Th2 cells. *Immunity.* 1996;4(3):313-319. doi:10.1016/s1074-7613(00)80439-2
40. Takeda K, Tanaka T, Shi W, et al. Essential role of Stat6 in IL-4 signalling. *Nature.* 1996;380(6575):627-630. doi:10.1038/380627a0
41. Zhu J. T helper 2 (Th2) cell differentiation, type 2 innate lymphoid cell (ILC2) development and regulation of interleukin-4 (IL-4) and IL-13 production. *Cytokine.* 2015;75(1):14-24. doi:10.1016/j.cyto.2015.05.010
42. Zhang Y, Zhang Y, Gu W, Sun B. Th1/Th2 Cell Differentiation and Molecular Signals. *T Help Cell Differ Their Funct.* Published online 2014:15-44. doi:10.1007/978-94-017-9487-9_2
43. Seder RA, Gazzinelli R, Sher A, Paul WE. Interleukin 12 acts directly on CD4+ T cells to enhance priming for interferon gamma production and diminishes interleukin 4 inhibition of such priming. *Proc Natl Acad Sci.* 1993;90(21):10188-10192. doi:10.1073/pnas.90.21.10188
44. Manetti R, Parronchi P, Giudizi MG, et al. Natural killer cell stimulatory factor (interleukin 12 [IL-12]) induces T helper type 1 (Th1)-specific immune responses and inhibits the development of IL-4-producing Th cells. *J Exp Med.* 1993;177(4):1199-1204. doi:10.1084/jem.177.4.1199

6 References

45. van Panhuys N, Prout M, Forbes E, Min B, Paul WE, Le Gros G. Basophils are the major producers of IL-4 during primary helminth infection. *J Immunol Baltim Md 1950*. 2011;186(5):2719-2728. doi:10.4049/jimmunol.1000940
46. Hammad H, Plantinga M, Deswarte K, et al. Inflammatory dendritic cells--not basophils--are necessary and sufficient for induction of Th2 immunity to inhaled house dust mite allergen. *J Exp Med*. 2010;207(10):2097-2111. doi:10.1084/jem.20101563
47. Korn T, Bettelli E, Oukka M, Kuchroo VK. IL-17 and Th17 Cells. *Annu Rev Immunol*. 2009;27:485-517. doi:10.1146/annurev.immunol.021908.132710
48. Veldhoen M, Hocking RJ, Atkins CJ, Locksley RM, Stockinger B. TGFbeta in the context of an inflammatory cytokine milieu supports de novo differentiation of IL-17-producing T cells. *Immunity*. 2006;24(2):179-189. doi:10.1016/j.immuni.2006.01.001
49. Steel N, Faniyi AA, Rahman S, et al. TGFβ-activation by dendritic cells drives Th17 induction and intestinal contractility and augments the expulsion of the parasite *Trichinella spiralis* in mice. *PLoS Pathog*. 2019;15(4):e1007657. doi:10.1371/journal.ppat.1007657
50. Yang XO, Panopoulos AD, Nurieva R, et al. STAT3 regulates cytokine-mediated generation of inflammatory helper T cells. *J Biol Chem*. 2007;282(13):9358-9363. doi:10.1074/jbc.C600321200
51. Zhu J, Yamane H, Paul WE. Differentiation of Effector CD4 T Cell Populations. *Annu Rev Immunol*. 2010;28:445-489. doi:10.1146/annurev-immunol-030409-101212
52. Duhon T, Geiger R, Jarrossay D, Lanzavecchia A, Sallusto F. Production of interleukin 22 but not interleukin 17 by a subset of human skin-homing memory T cells. *Nat Immunol*. 2009;10(8):857-863. doi:10.1038/ni.1767
53. Eyerich S, Eyerich K, Pennino D, et al. Th22 cells represent a distinct human T cell subset involved in epidermal immunity and remodeling. *J Clin Invest*. 2009;119(12):3573-3585. doi:10.1172/JCI40202
54. Tumes DJ, Papadopoulos M, Endo Y, Onodera A, Hirahara K, Nakayama T. Epigenetic regulation of T-helper cell differentiation, memory, and plasticity in allergic asthma. *Immunol Rev*. 2017;278(1):8-19. doi:10.1111/imr.12560
55. Koch S, Sopel N, Finotto S. Th9 and other IL-9-producing cells in allergic asthma. *Semin Immunopathol*. 2017;39(1):55-68. doi:10.1007/s00281-016-0601-1

6 References

56. Chang H-C, Sehra S, Goswami R, et al. The transcription factor PU.1 is required for the development of IL-9-producing T cells and allergic inflammation. *Nat Immunol.* 2010;11(6):527-534. doi:10.1038/ni.1867
57. Chang H-C, Han L, Jabeen R, Carotta S, Nutt SL, Kaplan MH. PU.1 regulates TCR expression by modulating GATA-3 activity. *J Immunol Baltim Md* 1950. 2009;183(8):4887-4894. doi:10.4049/jimmunol.0900363
58. Chang H-C, Zhang S, Thieu VT, et al. PU.1 expression delineates heterogeneity in primary Th2 cells. *Immunity.* 2005;22(6):693-703. doi:10.1016/j.immuni.2005.03.016
59. Perros F, Hoogsteden HC, Coyle AJ, Lambrecht BN, Hammad H. Blockade of CCR4 in a humanized model of asthma reveals a critical role for DC-derived CCL17 and CCL22 in attracting Th2 cells and inducing airway inflammation. *Allergy.* 2009;64(7):995-1002. doi:10.1111/j.1398-9995.2009.02095.x
60. Wills-Karp M, Luyimbazi J, Xu X, et al. Interleukin-13: Central Mediator of Allergic Asthma. *Science.* 1998;282(5397):2258-2261. doi:10.1126/science.282.5397.2258
61. Gour N, Wills-Karp M. IL-4 and IL-13 Signaling in Allergic Airway Disease. *Cytokine.* 2015;75(1):68-78. doi:10.1016/j.cyto.2015.05.014
62. Yanagibashi T, Satoh M, Nagai Y, Koike M, Takatsu K. Allergic diseases: From bench to clinic - Contribution of the discovery of interleukin-5. *Cytokine.* 2017;98:59-70. doi:10.1016/j.cyto.2016.11.011
63. Nussbaum JC, Dyken SJV, Moltke J von, et al. Type 2 innate lymphoid cells control eosinophil homeostasis. *Nature.* 2013;502(7470):245. doi:10.1038/nature12526
64. Newcomb DC, Peebles RS. Th17-mediated inflammation in asthma. *Curr Opin Immunol.* 2013;25(6):755-760. doi:10.1016/j.coi.2013.08.002
65. Nakajima M, Kawaguchi M, Ota K, et al. IL-17F induces IL-6 via TAK1-NF κ B pathway in airway smooth muscle cells. *Immun Inflamm Dis.* 2017;5(2):124-131. doi:10.1002/iid3.149
66. Evasovic JM, Singer CA. Regulation of IL-17A and implications for TGF- β 1 comodulation of airway smooth muscle remodeling in severe asthma. *Am J Physiol - Lung Cell Mol Physiol.* 2019;316(5):L843-L868. doi:10.1152/ajplung.00416.2018

6 References

67. Fang P, Zhou L, Zhou Y, Kolls JK, Zheng T, Zhu Z. Immune Modulatory Effects of IL-22 on Allergen-Induced Pulmonary Inflammation. *PLoS ONE*. 2014;9(9). doi:10.1371/journal.pone.0107454
68. Berker M, Frank LJ, Geßner AL, et al. Allergies - A T cells perspective in the era beyond the TH1/TH2 paradigm. *Clin Immunol Orlando Fla*. 2017;174:73-83. doi:10.1016/j.clim.2016.11.001
69. Schoenborn JR, Wilson CB. Regulation of interferon-gamma during innate and adaptive immune responses. *Adv Immunol*. 2007;96:41-101. doi:10.1016/S0065-2776(07)96002-2
70. Yu M, Eckart MR, Morgan AA, et al. Identification of an IFN- γ /mast cell axis in a mouse model of chronic asthma. *J Clin Invest*. 2011;121(8):3133-3143. doi:10.1172/JCI43598
71. Sallmann E, Reininger B, Brandt S, et al. High-affinity IgE receptors on dendritic cells exacerbate Th2-dependent inflammation. *J Immunol Baltim Md 1950*. 2011;187(1):164-171. doi:10.4049/jimmunol.1003392
72. Galli SJ, Tsai M, Piliponsky AM. The development of allergic inflammation. *Nature*. 2008;454(7203):445. doi:10.1038/nature07204
73. Sallusto F, Lenig D, Förster R, Lipp M, Lanzavecchia A. Two subsets of memory T lymphocytes with distinct homing potentials and effector functions. *Nature*. 1999;401(6754):708-712. doi:10.1038/44385
74. Mueller SN, Gebhardt T, Carbone FR, Heath WR. Memory T cell subsets, migration patterns, and tissue residence. *Annu Rev Immunol*. 2013;31:137-161. doi:10.1146/annurev-immunol-032712-095954
75. Hondowicz BD, An D, Schenkel JM, et al. Interleukin-2-Dependent Allergen-Specific Tissue-Resident Memory Cells Drive Asthma. *Immunity*. 2016;44(1):155-166. doi:10.1016/j.immuni.2015.11.004
76. Rivas MN, Chatila TA. Regulatory T cells in Allergic Diseases. *J Allergy Clin Immunol*. 2016;138(3):639-652. doi:10.1016/j.jaci.2016.06.003
77. Fontenot JD, Gavin MA, Rudensky AY. Foxp3 programs the development and function of CD4⁺CD25⁺ regulatory T cells. *Nat Immunol*. 2003;4(4):330-336. doi:10.1038/ni904

6 References

78. Chen W, Jin W, Hardegen N, et al. Conversion of peripheral CD4+CD25- naive T cells to CD4+CD25+ regulatory T cells by TGF-beta induction of transcription factor Foxp3. *J Exp Med.* 2003;198(12):1875-1886. doi:10.1084/jem.20030152
79. Lim HW, Hillsamer P, Banham AH, Kim CH. Cutting edge: direct suppression of B cells by CD4+ CD25+ regulatory T cells. *J Immunol Baltim Md 1950.* 2005;175(7):4180-4183. doi:10.4049/jimmunol.175.7.4180
80. Lewkowich IP, Herman NS, Schleifer KW, et al. CD4+CD25+ T cells protect against experimentally induced asthma and alter pulmonary dendritic cell phenotype and function. *J Exp Med.* 2005;202(11):1549. doi:10.1084/jem.20051506
81. Mamessier E, Nieves A, Lorec A-M, et al. T-cell activation during exacerbations: a longitudinal study in refractory asthma. *Allergy.* 2008;63(9):1202-1210. doi:10.1111/j.1398-9995.2008.01687.x
82. Massoud AH, Charbonnier L-M, Lopez D, Pellegrini M, Phipatanakul W, Chatila TA. An asthma-associated IL4R variant exacerbates airway inflammation by promoting conversion of regulatory T cells to TH17-like cells. *Nat Med.* 2016;22(9):1013-1022. doi:10.1038/nm.4147
83. Sabat R, Grütz G, Warszawska K, et al. Biology of interleukin-10. *Cytokine Growth Factor Rev.* 2010;21(5):331-344. doi:10.1016/j.cytogfr.2010.09.002
84. Dolch A, Kunz S, Dorn B, et al. IL-10 signaling in dendritic cells is required for tolerance induction in a murine model of allergic airway inflammation. *Eur J Immunol.* 2019;49(2):302-312. doi:10.1002/eji.201847883
85. Rink L, Kruse A, Haase H. Kapitel 4: Antigenpräsentation. In: Rink L, Kruse A, Haase H, eds. *Immunologie Für Einsteiger*. 14th ed. Spektrum Akademischer Verlag; 2012:59-74.
86. Lambrecht BN, Hammad H. Lung Dendritic Cells in Respiratory Viral Infection and Asthma: From Protection to Immunopathology | Annual Review of Immunology. *Annu Rev Immunol.* 2012;31. doi:10.1016/j.immuni.2009.08.008
87. Sung S-SJ, Fu SM, Rose CE, Gaskin F, Ju S-T, Beaty SR. A Major Lung CD103 (αE)-β7 Integrin-Positive Epithelial Dendritic Cell Population Expressing Langerin and Tight Junction Proteins. *J Immunol.* 2006;176(4):2161-2172. doi:10.4049/jimmunol.176.4.2161

6 References

88. Thornton E, Looney M, Bose O, et al. Spatiotemporally separated antigen uptake by alveolar dendritic cells and airway presentation to T cells in the lung. *J Exp Med*. 2012;209(6):1184-1199. doi:10.1084/jem.20112667
89. Nakano H, Free M, Whitehead G, et al. Pulmonary CD103+ dendritic cells prime Th2 responses to inhaled allergens. *Mucosal Immunol*. 2012;5(1):53-65. doi:10.1038/mi.2011.47
90. Plantinga M, Guillems M, Vanheerswynghe M, et al. Conventional and Monocyte-Derived CD11b+ Dendritic Cells Initiate and Maintain T Helper 2 Cell-Mediated Immunity to House Dust Mite Allergen. *Immunity*. 2013;38(2):322-335. doi:10.1016/j.immuni.2012.10.016
91. Bernatchez E, Gold MJ, Langlois A, et al. Pulmonary CD103 expression regulates airway inflammation in asthma. *Am J Physiol - Lung Cell Mol Physiol*. 2015;308(8):L816-L826. doi:10.1152/ajplung.00319.2014
92. Furuhashi K, Suda T, Hasegawa H, et al. Mouse Lung CD103+ and CD11bhigh Dendritic Cells Preferentially Induce Distinct CD4+ T-Cell Responses. *Am J Respir Cell Mol Biol*. 2012;Vol. 46(No. 2). doi:10.1165/rcmb.2011-0070OC
93. Khare A, Krishnamoorthy N, Oriss TB, Fei M, Ray P, Ray A. Inhaled Antigen Upregulates Retinaldehyde Dehydrogenase In Lung CD103+ But Not Plasmacytoid Dendritic Cells To Induce Foxp3 De Novo in CD4+ T cells and Promote Airway Tolerance. *J Immunol Baltim Md 1950*. 2013;191(1):25. doi:10.4049/jimmunol.1300193
94. Norimoto A, Hirose K, Iwata A, et al. Dectin-2 Promotes House Dust Mite-Induced T Helper Type 2 and Type 17 Cell Differentiation and Allergic Airway Inflammation in Mice. *Am J Respir Cell Mol Biol*. 2014;51(2). doi:10.1165/rcmb.2013-0522OC
95. Ito T, Wang Y-H, Duramad O, et al. TSLP-activated dendritic cells induce an inflammatory T helper type 2 cell response through OX40 ligand. *J Exp Med*. 2005;202(9):1213-1223. doi:10.1084/jem.20051135
96. Smit JJ, Rudd BD, Lukacs NW. Plasmacytoid dendritic cells inhibit pulmonary immunopathology and promote clearance of respiratory syncytial virus. *J Exp Med*. 2006;203(5):1153. doi:10.1084/jem.20052359
97. Chen L, Arora M, Yarlagadda M, et al. Distinct responses of lung and spleen dendritic cells to the TLR9 agonist CpG oligodeoxynucleotide. *J Immunol Baltim Md 1950*. 2006;177(4):2373-2383. doi:10.4049/jimmunol.177.4.2373

6 References

98. de Heer H, Hammad H, Soullie T, et al. Essential role of lung plasmacytoid dendritic cells in preventing asthmatic reactions to harmless inhaled antigen. *J Exp Med*. 2004;200(1):89-98. doi:10.1084/jem.20040035
99. Lewkowich I, Lajoie S, Clark J, Herman N, Sproles A, Wills-Karp M. Allergen uptake, activation, and IL-23 production by pulmonary myeloid DCs drives airway hyperresponsiveness in asthma-susceptible mice. *PLoS ONE*. 2008;3(12). doi:10.1371/journal.pone.0003879
100. Kool M, Nimwegen M van, Willart MAM, et al. An Anti-Inflammatory Role for Plasmacytoid Dendritic Cells in Allergic Airway Inflammation. *J Immunol*. 2009;183(2):1074-1082. doi:10.4049/jimmunol.0900471
101. Pichavant M, Charbonnier A-S, Taront S, et al. Asthmatic bronchial epithelium activated by the proteolytic allergen Der p 1 increases selective dendritic cell recruitment. *J Allergy Clin Immunol*. 2005;115(4):771-778. doi:10.1016/j.jaci.2004.11.043
102. Rodero MP, Poupel L, Loyher P-L, et al. Immune surveillance of the lung by migrating tissue monocytes. *eLife*. 2015;4. doi:10.7554/eLife.07847
103. Kitamura H, Cambier S, Somanath S, et al. Mouse and human lung fibroblasts regulate dendritic cell trafficking, airway inflammation, and fibrosis through integrin $\alpha\beta 8$ -mediated activation of TGF- β . *J Clin Invest*. 2011;121(7):2863. doi:10.1172/JCI45589
104. McMillan SJ, Xanthou G, Lloyd CM. Manipulation of Allergen-Induced Airway Remodeling by Treatment with Anti-TGF- β Antibody: Effect on the Smad Signaling Pathway. *J Immunol*. 2005;174(9):5774-5780. doi:10.4049/jimmunol.174.9.5774
105. Garnier C von, Figueira L, Wikstrom M, et al. Anatomical Location Determines the Distribution and Function of Dendritic Cells and Other APCs in the Respiratory Tract. *J Immunol*. 2005;175(3):1609-1618. doi:10.4049/jimmunol.175.3.1609
106. Bedoret D, Wallemacq H, Marichal T, et al. Lung interstitial macrophages alter dendritic cell functions to prevent airway allergy in mice. *J Clin Invest*. 2009;119(12):3723-3738. doi:10.1172/JCI39717
107. Westphalen K, Gusarova GA, Islam MN, et al. Sessile alveolar macrophages modulate immunity through connexin 43-based epithelial communication. *Nature*. 2014;506(7489):503. doi:10.1038/nature12902

6 References

108. Draijer C, Peters-Golden M. Alveolar Macrophages in Allergic Asthma: the Forgotten Cell Awakes. *Curr Allergy Asthma Rep.* 2017;17(2):12. doi:10.1007/s11882-017-0681-6
109. Robbe P, Draijer C, Borg TR, et al. Distinct macrophage phenotypes in allergic and nonallergic lung inflammation. *Am J Physiol - Lung Cell Mol Physiol.* 2015;308(4):L358-L367. doi:10.1152/ajplung.00341.2014
110. Meyts I, Hellings PW, Hens G, et al. IL-12 contributes to allergen-induced airway inflammation in experimental asthma. *J Immunol Baltim Md 1950.* 2006;177(9):6460-6470. doi:10.4049/jimmunol.177.9.6460
111. Schyns J, Bureau F, Marichal T. Lung Interstitial Macrophages: Past, Present, and Future. *J Immunol Res.* 2018;2018:5160794. doi:10.1155/2018/5160794
112. Kolev M, Fric GL, Kemper C. Complement — tapping into new sites and effector systems. *Nat Rev Immunol.* 2014;14(12):811-820. doi:10.1038/nri3761
113. Rink L, Kruse A, Haase H. Kapitel 3: Das angeborene Immunsystem. In: Rink L, Kruse A, Haase H, eds. *Immunologie Für Einsteiger.* 14th ed. Spektrum Akademischer Verlag; 2012:39-58.
114. Ricklin D, Hajishengallis G, Yang K, Lambris JD. Complement - a key system for immune surveillance and homeostasis. *Nat Immunol.* 2010;11(9):785-797. doi:10.1038/ni.1923
115. Rink L, Kruse A, Haase H, eds. *Immunologie Für Einsteiger.* 14th ed. Spektrum Akademischer Verlag; 2012.
116. Müller-Eberhard HJ. The Killer Molecule of Complement. *J Invest Dermatol.* 1985;85(1, Supplement):S47-S52. doi:10.1111/1523-1747.ep12275445
117. Köhl J. The role of complement in danger sensing and transmission. *Immunol Res.* 2006;34(2):157-176. doi:10.1385/IR:34:2:157
118. Kohl J, Willskarp M. A dual role for complement in allergic asthma. *Curr Opin Pharmacol.* 2007;7(3):283-289. doi:10.1016/j.coph.2007.01.005
119. Kemper C, Köhl J. Novel roles for complement receptors in T cell regulation and beyond. *Mol Immunol.* 2013;56(3):181-190. doi:10.1016/j.molimm.2013.05.223
120. Krug N, Tschernig T, Erpenbeck VJ, Hohlfeld JM, Köhl J. Complement factors C3a and C5a are increased in bronchoalveolar

6 References

- lavage fluid after segmental allergen provocation in subjects with asthma. *Am J Respir Crit Care Med.* 2001;164(10 Pt 1):1841-1843. doi:10.1164/ajrccm.164.10.2010096
121. Maruo K, Akaike T, Ono T, Okamoto T, Maeda H. Generation of anaphylatoxins through proteolytic processing of C3 and C5 by house dust mite protease. *J Allergy Clin Immunol.* 1997;100(2):253-260. doi:10.1016/S0091-6749(97)70233-1
 122. Huber-Lang M, Younkin EM, Sarma JV, et al. Generation of C5a by phagocytic cells. *Am J Pathol.* 2002;161(5):1849-1859. doi:10.1016/S0002-9440(10)64461-6
 123. Guo R-F, Ward P. Role of C5a in Inflammatory Responses. *Annu Rev Immunol.* 2005;23:821-852. doi:10.1146/annurev.immunol.23.021704.115835
 124. Atkinson JJ, Senior RM. Matrix metalloproteinase-9 in lung remodeling. *Am J Respir Cell Mol Biol.* 2003;28(1):12-24. doi:10.1165/rcmb.2002-0166TR
 125. Hawlisch H, Wills-Karp M, Karp CL, Köhl J. The anaphylatoxins bridge innate and adaptive immune responses in allergic asthma. *Mol Immunol.* 2004;41(2-3):123-131. doi:10.1016/j.molimm.2004.03.019
 126. Monk PN, Scola A-M, Madala P, Fairlie DP. Function, structure and therapeutic potential of complement C5a receptors. *Br J Pharmacol.* 2007;152(4):429-448. doi:10.1038/sj.bjp.0707332
 127. Drouin SM, Kildsgaard J, Haviland J, et al. Expression of the Complement Anaphylatoxin C3a and C5a Receptors on Bronchial Epithelial and Smooth Muscle Cells in Models of Sepsis and Asthma. *J Immunol.* 2001;166(3):2025-2032. doi:10.4049/jimmunol.166.3.2025
 128. Karsten CM, Laumonier Y, Eurich B, et al. Monitoring and Cell-Specific Deletion of C5aR1 Using a Novel Floxed GFP-C5aR1 Reporter Knock-in Mouse. *J Immunol.* 2015;194(4):1841-1855. doi:10.4049/jimmunol.1401401
 129. Antoniou K, Ender F, Vollbrandt T, et al. Allergen-Induced C5a/C5aR1 Axis Activation in Pulmonary CD11b + cDCs Promotes Pulmonary Tolerance Through Downregulation of CD40. *Cells.* Published online January 26, 2020. doi:10.3390/cells9020300
 130. Wiese A, Ender F, Quell K, et al. The C5a/C5aR1 axis controls the development of experimental allergic asthma independent of LysM-expressing pulmonary immune cells. *PLOS ONE.* 2017;12:e0184956. doi:10.1371/journal.pone.0184956

6 References

131. Staab EB, Sanderson SD, Wells SM, Poole JA. Treatment with the C5a Receptor/CD88 Antagonist PMX205 Reduces Inflammation in a Murine Model of Allergic Asthma. *Int Immunopharmacol.* 2014;21(2):293. doi:10.1016/j.intimp.2014.05.008
132. Yang J, Ramirez Moral I, van 't Veer C, et al. Complement factor C5 inhibition reduces type 2 responses without affecting group 2 innate lymphoid cells in a house dust mite induced murine asthma model. *Respir Res.* 2019;20(1):165. doi:10.1186/s12931-019-1136-5
133. Gerard NP, Lu B, Liu P, et al. An anti-inflammatory function for the complement anaphylatoxin C5a-binding protein, C5L2. *J Biol Chem.* 2005;280(48):39677-39680. doi:10.1074/jbc.C500287200
134. Bamberg CE, Mackay CR, Lee H, et al. The C5a receptor (C5aR) C5L2 is a modulator of C5aR-mediated signal transduction. *J Biol Chem.* 2010;285(10):7633-7644. doi:10.1074/jbc.M109.092106
135. Zhang X, Schmutte I, Laumonnier Y, et al. A Critical Role for C5L2 in the Pathogenesis of Experimental Allergic Asthma. *J Immunol.* 2010;185(11):6741-6752. doi:10.4049/jimmunol.1000892
136. Li R, Coulthard LG, Wu MCL, Taylor SM, Woodruff TM. C5L2: a controversial receptor of complement anaphylatoxin, C5a. *FASEB J.* 2013;27(3):855-864. doi:10.1096/fj.12-220509
137. Reis ES, Lange T, Köhl G, et al. Sleep and circadian rhythm regulate circulating complement factors and immunoregulatory properties of C5a. *Brain Behav Immun.* 2011;25(7):1416-1426. doi:10.1016/j.bbi.2011.04.011
138. Bell-Pedersen D, Cassone VM, Earnest DJ, et al. Circadian Rhythms from Multiple Oscillators: Lessons from diverse Organisms. *Nat Rev Genet.* 2005;6(7):544. doi:10.1038/nrg1633
139. Berson DM, Dunn FA, Takao M. Phototransduction by Retinal Ganglion Cells That Set the Circadian Clock. *Science.* 2002;295(5557):1070-1073. doi:10.1126/science.1067262
140. Hirota T, Fukada Y. Resetting Mechanism of Central and Peripheral Circadian Clocks in Mammals. *BioOne.* 2004;21(4):359-368. doi:10.2108/zsj.21.359
141. Takahashi JS. Molecular components of the circadian clock in mammals. *Diabetes Obes Metab.* 2015;17(0 1):6. doi:10.1111/dom.12514
142. Dibner C, Schibler U, Albrecht U. The Mammalian Circadian Timing System: Organization and Coordination of Central and Peripheral

6 References

- Clocks | Annual Review of Physiology. *Annu Rewiew Physiol.* 2010;72:517-549. doi:10.1146/annurev-physiol-021909-135821
143. Yoo S-H, Yamazaki S, Lowrey PL, et al. PERIOD2::LUCIFERASE real-time reporting of circadian dynamics reveals persistent circadian oscillations in mouse peripheral tissues. *Proc Natl Acad Sci U S A.* 2004;101(15):5339. doi:10.1073/pnas.0308709101
 144. Mohawk JA, Green CB, Takahashi JS. Central and Peripheral Circadian Clocks in Mammals. *Annu Rev Neurosci.* 2012;35:445. doi:10.1146/annurev-neuro-060909-153128
 145. Curtis AM, Bellet M, Sassone-Corsi P, O'Neill LAJ. Circadian Clock Proteins and Immunity. *Immunity.* 2014;40(2):178-186. doi:10.1016/j.immuni.2014.02.002
 146. Arjona A, Silver AC, Walker WE, Fikrig E. Immunity's fourth dimension: approaching the circadian-immune connection. *Trends Immunol.* 2012;33(12):607. doi:10.1016/j.it.2012.08.007
 147. Narasimamurthy R, Hatori M, Nayak SK, Liu F, Panda S, Verma IM. Circadian clock protein cryptochrome regulates the expression of proinflammatory cytokines. *Proc Natl Acad Sci U S A.* 2012;109(31):12662. doi:10.1073/pnas.1209965109
 148. Kraft M, Martin RJ, Wilson S, Djukanovic R, Holgate S. Lymphocyte and Eosinophil Influx into Alveolar Tissue in Nocturnal Asthma. *Am J Respir Crit Care Med.* 1999;159(1). doi:10.1164/ajrccm.159.1.9804033
 149. Spengler CM, Shea SA. Endogenous circadian rhythm of pulmonary function in healthy humans. *Am J Respir Crit Care Med.* 2000;162(3 Pt 1):1038-1046. doi:10.1164/ajrccm.162.3.9911107
 150. Nosal C, Ehlers A, Haspel JA. Why Lungs Keep Time: Circadian Rhythms and Lung Immunity. *Annu Rev Physiol.* 2020;82:391-412. doi:10.1146/annurev-physiol-021119-034602
 151. Patke A, Young MW, Axelrod S. Molecular mechanisms and physiological importance of circadian rhythms. *Nat Rev Mol Cell Biol.* 2020;21(2):67-84. doi:10.1038/s41580-019-0179-2
 152. Kelly E a. B, Houtman JJ, Jarjour NN. Inflammatory changes associated with circadian variation in pulmonary function in subjects with mild asthma. *Clin Amp Exp Allergy.* 2004;34(2):227-233. doi:10.1111/j.1365-2222.2004.01866.x
 153. Panzer SE, Dodge AM, Kelly EAB, Jarjour NN. Circadian variation of sputum inflammatory cells in mild asthma. *J Allergy Clin Immunol.* 2003;111(2):308-312. doi:10.1067/mai.2003.65

6 References

154. Gibbs J, Ince L, Matthews L, et al. An epithelial circadian clock controls pulmonary inflammation and glucocorticoid action. *Nat Med*. 2014;20(8):919. doi:10.1038/nm.3599
155. Gibbs JE, Beesley S, Plumb J, et al. Circadian Timing in the Lung; A Specific Role for Bronchiolar Epithelial Cells. *Endocrinology*. 2009;150(1):268. doi:10.1210/en.2008-0638
156. Ince LM, Zhang Z, Beesley S, et al. Circadian variation in pulmonary inflammatory responses is independent of rhythmic glucocorticoid signaling in airway epithelial cells. *FASEB J Off Publ Fed Am Soc Exp Biol*. 2019;33(1):126-139. doi:10.1096/fj.201800026RR
157. Zastona Z, Case S, Early JO, et al. The circadian protein BMAL1 in myeloid cells is a negative regulator of allergic asthma. *Am J Physiol Lung Cell Mol Physiol*. 2017;312(6):L855-L860. doi:10.1152/ajplung.00072.2017
158. Pariollaud M, Gibbs JE, Hopwood TW, et al. Circadian clock component REV-ERBa controls homeostatic regulation of pulmonary inflammation. *J Clin Invest*. 2018;128(6):2281-2296. doi:10.1172/JCI93910
159. Sato S, Sakurai T, Ogasawara J, et al. A Circadian Clock Gene, Rev-erba, Modulates the Inflammatory Function of Macrophages through the Negative Regulation of Ccl2 Expression. *J Immunol*. 2014;192(1):407-417. doi:10.4049/jimmunol.1301982
160. He W, Holtkamp S, Hergenhan SM, et al. Circadian Expression of Migratory Factors Establishes Lineage-Specific Signatures that Guide the Homing of Leukocyte Subsets to Tissues. *Immunity*. 2018;49(6):1175-1190. doi:10.1016/j.immuni.2018.10.007
161. Baumann A, Gönnerwein S, Bischoff SC, et al. The circadian clock is functional in eosinophils and mast cells. *Immunology*. 2013;140(4):465-474. doi:10.1111/imm.12157
162. Baumann A, Feilhauer K, Bischoff SC, Froy O, Lorentz A. IgE-dependent activation of human mast cells and fMLP-mediated activation of human eosinophils is controlled by the circadian clock. *Mol Immunol*. 2015;64(1):76-81. doi:10.1016/j.molimm.2014.10.026
163. Boivin DB. Circadian clock genes oscillate in human peripheral blood mononuclear cells. *Blood*. 2003;102(12):4143-4145. doi:10.1182/blood-2003-03-0779
164. Keller M, Mazuch J, Abraham U, et al. A circadian clock in macrophages controls inflammatory immune responses. *Proc Natl*

6 References

- Acad Sci U S A.* 2009;106(50):21407.
doi:10.1073/pnas.0906361106
165. Nguyen KD, Fentress SJ, Qiu Y, Yun K, Cox JS, Chawla A. Circadian gene *Bmal1* regulates diurnal oscillations of Ly6Chi inflammatory monocytes. *Science.* 2013;341(6153). doi:10.1126/science.1240636
166. Silver AC, Arjona A, Hughes ME, Nitabach MN, Fikrig E. Circadian expression of clock genes in mouse macrophages, dendritic cells, and B cells. *Brain Behav Immun.* 2012;26(3):407. doi:10.1016/j.bbi.2011.10.001
167. Fortier EE, Rooney J, Dardente H, Hardy M-P, Labrecque N, Cermakian N. Circadian Variation of the Response of T Cells to Antigen. *J Immunol.* 2011;187(12):6291-6300. doi:10.4049/jimmunol.1004030
168. Langwinski W, Sobkowiak P, Narozna B, et al. Association of circadian clock TIMELESS variants and expression with asthma risk in children. *Clin Respir J.* Published online August 13, 2020. doi:10.1111/crj.13260
169. Kurien P, Hsu P-K, Leon J, et al. TIMELESS mutation alters phase responsiveness and causes advanced sleep phase. *Proc Natl Acad Sci U S A.* 2019;116(24):12045-12053. doi:10.1073/pnas.1819110116
170. Krakowiak K, Durrington HJ. The Role of the Body Clock in Asthma and COPD: Implication for Treatment. *Pulm Ther.* 2018;4(1):29-43. doi:10.1007/s41030-018-0058-6
171. Durrington HJ, Farrow SN, Loudon AS, Ray DW. The circadian clock and asthma. *Thorax.* 2014;69(1):90-92. doi:10.1136/thoraxjnl-2013-203482
172. Chinwalla A, Cook L, Delehaunty K. Initial sequencing and comparative analysis of the mouse genome. *Nature.* 2002;420(6915):520-562. doi:10.1038/nature01262
173. Houdebine L-M. Chapter 6: The Mouse as an Animal Model for Human Diseases. In: Hedrich H, Bullock G, eds. *The Laboratory Mouse.* Academic Press; 2004:97-110.
174. Hedrich H, Bullock G. *The Laboratory Mouse.* Academic Press; 2004.
175. Finkelman FD, Wills-Karp M. Usefulness and optimization of mouse models of allergic airway disease. *J Allergy Clin Immunol.* 2008;121(3). doi:10.1016/j.jaci.2008.01.008

6 References

176. Suarez CJ, Dintzis SM, Frevort CW. Respiratory. In: Treuting P, Dintzis S, eds. *Comparative Anatomy and Histology*. Elsevier; 2012:121-134. doi:10.1016/B978-0-12-381361-9.00009-3
177. Braun A, Ernst H, Hoymann H, Rittinghausen S. Chapter 14: Respiratory Tract. In: Hedrich H, Bullock G, eds. *The Laboratory Mouse*. Academic Press; 2004:225-244.
178. Zhang X, Lewkowich IP, Köhl G, Clark JR, Wills-Karp M, Köhl J. A Protective Role for C5a in the Development of Allergic Asthma Associated with Altered Levels of B7-H1 and B7-DC on Plasmacytoid Dendritic Cells. *J Immunol Baltim Md 1950*. 2009;182(8):5123. doi:10.4049/jimmunol.0804276
179. Klante G, Steinlecher S. A Short Red Light Pulse During Dark Phase of LD-cycle Perturbs the Hamster's Circadian Clock. *J Comp Physiol [A]*. Published online December 1995. doi:10.1007/BF00187636
180. Steinlechner S, Stieglitz A, Ruf T. Djungarian Hamsters: A Species with a Labile Circadian Pacemaker? Arrhythmicity under a Light-Dark Cycle Induced by Short Light Pulses. *J Biol Rhythms*. Published online June 29, 2016. doi:10.1177/074873040201700308
181. Jud C, Schmutz I, Hampp G, Oster H, Albrecht U. A guideline for analyzing circadian wheel-running behavior in rodents under different lighting conditions. *Biol Proced Online*. 2005;7:101. doi:10.1251/bpo109
182. Jilge B, Kunz E. Chapter 20: Circadian rhythms of the Mouse. In: Hedrich H, Bullock G, eds. *The Laboratory Mouse*. Academic Press; 2004:311-326.
183. Jung S, Aliberti J, Graemmel P, et al. Analysis of Fractalkine Receptor CX3CR1 Function by Targeted Deletion and Green Fluorescent Protein Reporter Gene Insertion. *Mol Cell Biol*. 2000;20(11):4106-4114. doi:0270-7306/00/\$04.00+0
184. Engelke C, Wiese AV, Schmudde I, et al. Distinct Roles of the Anaphylatoxins C3a and C5a in Dendritic Cell-Mediated Allergic Asthma. *J Immunol*. 2014;193(11):5387-5401. doi:10.4049/jimmunol.1400080
185. Höpken UE, Lu B, Gerard NP, Gerard C. The C5a chemoattractant receptor mediates mucosal defence to infection. *Nature*. 1996;383(6595):86-89. doi:10.1038/383086a0
186. Mousset CM, Hobo W, Woestenenk R, Preijers F, Dolstra H, Waart AB van der. Comprehensive Phenotyping of T Cells Using Flow Cytometry. *Cytometry A*. 2019;95(6):647-654. doi:10.1002/cyto.a.23724

6 References

187. James M, Inokuma M, McIntyre C, Mittar D. Detection of Intracellular Cytokines in T Lymphocytes using the BD FastImmune™ Assay on the BD FACSVerser™ System. *BD Biosci.* 2011;101:100.
188. Mesoscale D. High Performance Biomarker Assays and Services, Singleplex and Multiplex Assay List. Published 2020. <https://www.mesoscale.com/~media/files/handout/assaylist.pdf>
189. Meso-Scale-Discovery. U-PLEX Biomarker Group 1 (Mouse) Multiplex Assays. MESO SCALE DIAGNOSTICS, LLC. Published 2015. Accessed August 10, 2021. <https://www.mesoscale.com/en/products/u-plex-biomarker-group-1-mouse-assays-sector-1-pl-k15069/>
190. Grubbs FE. Procedures for detecting outlying observations in samples. *Technometrics.* 1969;11:1-21. doi:10.1080/00401706.1969.10490657
191. Abdi H. The Bonferonni and Šidák Corrections for Multiple Comparisons. In: Salkind N, ed. *Encyclopedia of Measurement and Statistics.* Thousand Oaks (CA): Sage.; 2007.
192. Shapiro S, Wilk MB. An Analysis of Variance Test for Normality (Complete Samples). *Biometrika.* 1965;Vol. 52(No. 3/4):591-611.
193. Blanca Mena MJ, Alarcón Postigo R, Arnau Gras J, Bono Cabré R, Bendayan R. Non-normal data: Is ANOVA still a valid option? Published online 2017. Accessed August 19, 2020. <http://diposit.ub.edu/dspace/handle/2445/122126>
194. Mesnil C, Raulier S, Paulissen G, et al. Lung-resident eosinophils represent a distinct regulatory eosinophil subset. *J Clin Invest.* 126(9):3279-3295. doi:10.1172/JCI85664
195. Nobelförsamlingen. The Nobel Prize in Physiology or Medicine 2017. Nobel Media A B 2014. Published 2017. Accessed October 6, 2017. https://www.nobelprize.org/nobel_prizes/medicine/laureates/2017/
196. Nakano H, Lyons-Cohen MR, Whitehead GS, Nakano K, Cook DN. Distinct functions of CXCR4, CCR2, and CX3CR1 direct dendritic cell precursors from the bone marrow to the lung. *J Leukoc Biol.* 2017;101(5):1143-1153. doi:10.1189/jlb.1A0616-285R
197. Druzd D, Matveeva O, Ince L, et al. Lymphocyte Circadian Clocks Control Lymph Node Trafficking and Adaptive Immune Responses. *Immunity.* 2017;46(1):120-132. doi:10.1016/j.immuni.2016.12.011

6 References

198. Wang T, Wang Z, Yang P, et al. PER1 prevents excessive innate immune response during endotoxin-induced liver injury through regulation of macrophage recruitment in mice. *Cell Death Dis.* 2016;7:e2176. doi:10.1038/cddis.2016.9
199. Winter C, Silvestre-Roig C, Ortega-Gomez A, et al. Chrono-pharmacological Targeting of the CCL2-CCR2 Axis Ameliorates Atherosclerosis. *Cell Metab.* 2018;28(1):175-182. doi:10.1016/j.cmet.2018.05.002
200. Lam MTY, Cho H, Lesch HP, et al. Rev-Erbs repress macrophage gene expression by inhibiting enhancer-directed transcription. *Nature.* 2013;498(7455):511-515. doi:10.1038/nature12209
201. Song C, Tan P, Zhang Z, et al. REV-ERB agonism suppresses osteoclastogenesis and prevents ovariectomy-induced bone loss partially via FABP4 upregulation. *FASEB J.* 2018;32(6):3215-3228. doi:10.1096/fj.201600825RRR
202. Labrecque N, Cermakian N. Circadian Clocks in the Immune System. *J Biol Rhythms.* 2015;20(10). doi:10.1177/0748730415577723
203. Halberg F, Johnson EA, Brown BW, Bittner JJ. Susceptibility Rhythm to E. coli Endotoxin and Bioassay. *Exp Biol Med.* 1960;103(1). doi:10.3181/00379727-103-25439
204. Gibbs JE, Blaikley J, Beesley S, et al. From the Cover: The nuclear receptor REV-ERB α mediates circadian regulation of innate immunity through selective regulation of inflammatory cytokines. *Proc Natl Acad Sci U S A.* 2012;109(2):582. doi:10.1073/pnas.1106750109
205. Yamamoto T, Nakahata Y, Soma H, Akashi M, Mamine T, Takumi T. Transcriptional oscillation of canonical clock genes in mouse peripheral tissues. *BMC Mol Biol.* 2004;5:18. doi:10.1186/1471-2199-5-18
206. Guillemins M, Kleer ID, Henri S, et al. Alveolar macrophages develop from fetal monocytes that differentiate into long-lived cells in the first week of life via GM-CSF. *J Exp Med.* 2013;210(10):1977. doi:10.1084/jem.20131199
207. Ginhoux F, Jung S. Monocytes and macrophages: developmental pathways and tissue homeostasis. *Nat Rev Immunol.* 2014;14(6):392-404. doi:10.1038/nri3671
208. Hashimoto D, Chow A, Noizat C, et al. Tissue resident macrophages self-maintain locally throughout adult life with minimal contribution

6 References

- from circulating monocytes. *Immunity*. 2013;38(4). doi:10.1016/j.immuni.2013.04.004
209. Kopf M, Schneider C, Nobs SP. The development and function of lung-resident macrophages and dendritic cells. *Nat Immunol*. 2014;16(1):36-44. doi:10.1038/ni.3052
210. Sukumaran S, Jusko WJ, DuBois DC, Almon RR. Light-dark oscillations in the lung transcriptome: implications for lung homeostasis, repair, metabolism, disease, and drug action. *J Appl Physiol*. 2011;110(6):1732. doi:10.1152/jappphysiol.00079.2011
211. Ender F, Wiese AV, Schmutte I, et al. Differential regulation of C5a receptor 1 in innate immune cells during the allergic asthma effector phase. *PLoS ONE*. 2017;12(2). doi:10.1371/journal.pone.0172446
212. DiScipio RG, Daffern PJ, Jagels MA, Broide DH, Sriramarao P. A Comparison of C3a and C5a-Mediated Stable Adhesion of Rolling Eosinophils in Postcapillary Venules and Transendothelial Migration In Vitro and In Vivo. *J Immunol*. 1999;162(2):1127-1136.
213. Karsten CM, Wiese AV, Mey F, et al. Monitoring C5aR2 Expression Using a Floxed tdTomato-C5aR2 Knock-In Mouse. *J Immunol Baltim Md* 1950. 2017;199(9):3234-3248. doi:10.4049/jimmunol.1700710
214. Kandasamy M, Ying PC, Ho AWS, et al. Complement Mediated Signaling on Pulmonary CD103+ Dendritic Cells Is Critical for Their Migratory Function in Response to Influenza Infection. *PLoS Pathog*. 2013;9(1). doi:10.1371/journal.ppat.1003115
215. Quell KM, Karsten CM, Kordowski A, et al. Monitoring C3aR Expression Using a Floxed tdTomato-C3aR Reporter Knock-in Mouse. *J Immunol*. 2017;199(2):688-706. doi:10.4049/jimmunol.1700318
216. Laumonier Y, Karsten CM, Köhl J. Novel insights into the expression pattern of anaphylatoxin receptors in mice and men. *Mol Immunol*. 2017;89:44-58. doi:10.1016/j.molimm.2017.05.019
217. Mantovani A, Cassatella M, Costantini C, Jaillon S. Neutrophils in the activation and regulation of innate and adaptive immunity. *Nat Rev Immunol*. 2011;11:519-531. doi:10.1038/nri3024
218. Mocsai A. Diverse novel functions of neutrophils in immunity, inflammation, and beyond. *J Exp Med*. 2013;210(7):1283-1299. doi:10.1084/jem.20122220
219. Bossios A, Gourgiotis D, Skevaki L, et al. Rhinovirus infection and house dust mite exposure synergize in inducing bronchial epithelial

6 References

- cell interleukin-8 release. *Clin Exp Allergy*. 2008;38(10):1615-1626. doi:10.1111/j.1365-2222.2008.03058.x
220. Hosoki K, Boldogh I, Sur S. Neutrophil recruitment by allergens contribute to allergic sensitization and allergic inflammation. *Curr Opin Allergy Clin Immunol*. 2016;16(1):45-50. doi:10.1097/ACI.0000000000000231
221. Sevin CM, Newcomb DC, Shinji T, et al. Deficiency of gp91phox Inhibits Allergic Airway Inflammation. *Am J Respir Cell Mol Biol*. 2013;49(3):396-402. doi:10.1165/rcmb.2012-0442OC
222. Lee YG, Jeong JJ, Nyehuis S, et al. Recruited Alveolar Macrophages, in Response to Airway Epithelial-Derived Monocyte Chemoattractant Protein 1/CCL2, Regulate Airway Inflammation and Remodeling in Allergic Asthma. *Am J Respir Cell Mol Biol*. 2015;52(6):772-784. doi:10.1165/rcmb.2014-0255OC
223. Inui T, Watanabe M, Nakamoto K, et al. Bronchial epithelial cells produce CXCL1 in response to LPS and TNF α : A potential role in the pathogenesis of COPD. *Exp Lung Res*. 2018;44(7):323-331. doi:10.1080/01902148.2018.1520936
224. Rutledge H, Aylor DL, Carpenter DE, et al. Genetic regulation of Zfp30, CXCL1, and neutrophilic inflammation in murine lung. *Genetics*. 2014;198(2):735-745. doi:10.1534/genetics.114.168138
225. Sawant KV, Xu R, Cox R, et al. Chemokine CXCL1-Mediated Neutrophil Trafficking in the Lung: Role of CXCR2 Activation. *J Innate Immun*. 2015;7(6):647-658. doi:10.1159/000430914
226. Park S, Kim K, Bae I-H, et al. TIMP3 is a CLOCK-dependent diurnal gene that inhibits the expression of UVB-induced inflammatory cytokines in human keratinocytes. *FASEB J Off Publ Fed Am Soc Exp Biol*. 2018;32(3):1510-1523. doi:10.1096/fj.201700693R
227. Adrover JM, Del Fresno C, Crainiciuc G, et al. A Neutrophil Timer Coordinates Immune Defense and Vascular Protection. *Immunity*. 2019;50(2):390-402. doi:10.1016/j.immuni.2019.01.002
228. Rothenberg ME, Hogan SP. The eosinophil. *Annu Rev Immunol*. 2006;24:147-174. doi:10.1146/annurev.immunol.24.021605.090720
229. Collins PD, Marleau S, Griffiths-Johnson DA, Jose PJ, Williams TJ. Cooperation between interleukin-5 and the chemokine eotaxin to induce eosinophil accumulation in vivo. *J Exp Med*. 1995;182(4):1169-1174. doi:10.1084/jem.182.4.1169

6 References

230. Lavinskiene S, Bajoriuniene I, Malakauskas K, Jeroch J, Sakalauskas R. Sputum neutrophil count after bronchial allergen challenge is related to peripheral blood neutrophil chemotaxis in asthma patients. *Inflamm Res.* 2014;63(11):951-959. doi:10.1007/s00011-014-0770-0
231. Wiechmann AF, Ceresa BP, Howard EW. Diurnal Variation of Tight Junction Integrity Associates Inversely with Matrix Metalloproteinase Expression in *Xenopus laevis* Corneal Epithelium: Implications for Circadian Regulation of Homeostatic Surface Cell Desquamation. *PLOS ONE.* 2014;9(11):e113810. doi:10.1371/journal.pone.0113810
232. Silver AC, Arjona A, Walker WE, Fikrig E. The circadian clock controls toll-like receptor 9-mediated innate and adaptive immunity. *Immunity.* 2012;36(2):251. doi:10.1016/j.immuni.2011.12.017
233. Clark T. Diurnal rhythm of asthma. *Chest.* 1987;91(6):137-141. doi:10.1378/chest.91.6_supplement.137s
234. Kaur M, Singh D. Neutrophil Chemotaxis Caused by Chronic Obstructive Pulmonary Disease Alveolar Macrophages: The Role of CXCL8 and the Receptors CXCR1/CXCR2. *J Pharmacol Exp Ther.* 2013;347(1):173-180. doi:10.1124/jpet.112.201855
235. Oster H, Damerow S, Kiessling S, et al. The circadian rhythm of glucocorticoids is regulated by a gating mechanism residing in the adrenal cortical clock. *Cell.* 2006;4(2):163-173. doi:10.1016/j.cmet.2006.07.002
236. Son GH, Chung S, Choe HK, et al. Adrenal peripheral clock controls the autonomous circadian rhythm of glucocorticoid by causing rhythmic steroid production. *Proc Natl Acad Sci.* 2008;105(52):20970-20975. doi:10.1073/pnas.0806962106
237. Dimitrov S, Benedict C, Heutling D, Westermann J, Born J, Lange T. Cortisol and epinephrine control opposing circadian rhythms in T cell subsets. *Blood.* 2009;113(21):5134. doi:10.1182/blood-2008-11-190769
238. Downton P, Early JO, Gibbs JE. Circadian rhythms in adaptive immunity. *Immunology.* Published online December 14, 2019. doi:10.1111/imm.13167
239. Yu X, Rollins D, Ruhn KA, et al. Th17 cell differentiation is regulated by the circadian clock. *Science.* 2013;342(6159):727-730. doi:10.1126/science.1243884

6 References

240. Hemmers S, Rudensky AY. The cell-intrinsic Circadian Clock is Dispensable for Lymphocyte Differentiation and Function. *Cell Rep.* 2015;11(9):1339. doi:10.1016/j.celrep.2015.04.058
241. Harb H, Chatila T. Mechanisms of Dupilumab. *Clin Exp Allergy J Br Soc Allergy Clin Immunol.* 2020;50(1):5-14. doi:10.1111/cea.13491
242. Matsunaga K, Katoh N, Fujieda S, Izuhara K, Oishi K. Dupilumab: Basic aspects and applications to allergic diseases. *Allergol Int Off J Jpn Soc Allergol.* 2020;69(2):187-196. doi:10.1016/j.alit.2020.01.002
243. Cheng F-L, An Y-F, Han Z-Q, et al. Period2 gene regulates diurnal changes of nasal symptoms in an allergic rhinitis mouse model. *Int Forum Allergy Rhinol.* 2020;10(11):1236-1248. doi:10.1002/alr.22607
244. Bollinger T, Leutz A, Leliavski A, et al. Circadian Clocks in Mouse and Human CD4+ T Cells. *PLoS ONE.* 2011;6(12). doi:10.1371/journal.pone.0029801
245. Motomura Y, Kitamura H, Hijikata A, et al. The transcription factor E4BP4 regulates the production of IL-10 and IL-13 in CD4+ T cells. *Nat Immunol.* 2011;12(5):ni.2020. doi:10.1038/ni.2020
246. Bollinger T, Bollinger A, Naujoks J, Lange T, Solbach W. The influence of regulatory T cells and diurnal hormone rhythms on T helper cell activity. *Immunology.* 2010;131(4):488-500. doi:10.1111/j.1365-2567.2010.03320.x
247. Bollinger T, Bollinger A, Skrum L, Dimitrov S, Lange T, Solbach W. Sleep-dependent activity of T cells and regulatory T cells. *Clin Exp Immunol.* 2009;155(2):231. doi:10.1111/j.1365-2249.2008.03822.x
248. Erhardt W, Hebestedt A, Aschenbrenner G, Pichotka B, Blümel G. A comparative study with various anesthetics in mice (pentobarbitone, ketamine-xylazine, carfentanyl-etomidate). *Res Exp Med Z Gesamte Exp Med Einschl Exp Chir.* 1984;184(3):159-169. doi:10.1007/BF01852390
249. Arras M, Autenried P, Rettich A, Spaeni D, Rüllicke T. Optimization of Intraperitoneal Injection Anesthesia in Mice: Drugs, Dosages, Adverse Effects, and Anesthesia Depth. *Comp Med.* 2001;51(5):443-456.
250. Mihara T, Kikuchi T, Kamiya Y, et al. Day or Night Administration of Ketamine and Pentobarbital Differentially Affect Circadian Rhythms of Pineal Melatonin Secretion and Locomotor Activity in Rats. *Anesth*

6 References

- Analg.* 2012;115(4):805-813.
doi:10.1213/ANE.0b013e3182632bcb
251. Shochat T, Haimov I, Lavie P. Melatonin - the key to the gate of sleep. *Ann Med.* 2009;Vol. 30(No. 1):109-114.
doi:10.3109/07853899808999392
252. Hohlbaum K, Bert B, Dietze S, Palme R, Fink H, Thöne-Reineke C. Impact of repeated anesthesia with ketamine and xylazine on the well-being of C57BL/6JRj mice. *PLoS ONE.* 2018;13(9).
doi:10.1371/journal.pone.0203559
253. Koinis-Mitchell D, Kopel S, Boergers K, et al. Asthma, allergic rhinitis, and sleep problems in urban children. *J Clin Sleep Med.* 2015;11(2):101-110. doi:10.5664/jcsm.4450.
254. Stores G, Ellis A, Wiggs L, Crawford C, Thomsom A. Sleep and psychological disturbance in nocturnal asthma. *Arch Dis Child.* 1998;78(5):413-419. doi:10.1136/adc.78.5.413
255. Oztürk L, Pelin Z, Karadeniz D, Kaynak H, Cakar L, Gözükmizi E. Effects of 48 hours sleep deprivation on human immune profile. *Sleep Res Online.* 1999;2(4):107-111.
256. Diette G, Marskon L, Skinner E, Nguyen T, Algatt-Bergstrom P, Wu A. Nocturnal asthma in children affects school attendance, school performance, and parents' work attendance. *Arch Pediatr Adolesc Med.* 2000;154(9):923-928. doi:10.1001/archpedi.154.9.923
257. Hartwig C, Munder A, Glage S, et al. The histamine H4-receptor (H4 R) regulates eosinophilic inflammation in ovalbumin-induced experimental allergic asthma in mice. *Eur J Immunol.* 2015;45(4):1129-1140. doi:10.1002/eji.201445179
258. Rozov S, Porkka-Heiskanen T, Panula P. On the Role of Histamine Receptors in the Regulation of Circadian Rhythms. *PLoS ONE.* 2015;10(12). doi:10.1371/journal.pone.0144694
259. Takahashi K, Lin J, Sakai K. Neuronal activity of histaminergic tuberomammillary neurons during wake-sleep states in the mouse. *J Neurosci.* 2006;26(40):10292-10298.
doi:10.1523/JNEUROSCI.2341-06.2006
260. Koinis-Mitchell D, Craig T, Esteban C, Klein R. Sleep and allergic disease: A summary of the literature and future directions for research. *J Allergy Clin Immunol.* 2012;130(6):1275-1281.
doi:10.1016/j.jaci.2012.06.026

7 Appendix

7.1 Supplementary material

Table 7-1: Detailed overview about statistical tests - Comparison of two groups with one independent variable

Graph	Title	Shapiro-Wilk test	t(df)=t-value	U=U-statistic	p-value	Significance level
4-5A	Light off	0.921	t(8)=0.363		0.726	ns
4-6B	Light on	0.364	t(8)=0.579		0.578	ns
4-20A	IL-13	ZT3: 0.3842 ZT15: 0.0088		U=29.00	0.0009	***
4-20B	IL-17	ZT3: 0.2377 ZT15: 0.4294	t(18)=3.317		0.0057	**
4-20C	IFN- γ	ZT3: 0.1578 ZT15: 0.0120		U=22.00	0.0329	*
4-22B	%PAS ⁺	ZT3: 0.0545 ZT15: 0.3202	t(16)=1.460		0.1636	ns
4-22D	%mucus area	ZT3: 0.2471 ZT15: 0.6793	t(16)=2.722		0.0151	*

7 Appendix

Table 7-2: Detailed overview about statistical tests - Comparison of more than two groups with one independent variable

Graph	Title	one-way ANOVA			Tukey's post-hoc multiple comparison test			
		F(df _{numerator} ,df _{denominator}) =F-value	p-value	Significance level	Compared parameters	Mean difference	95%-confidence interval	Sign. level
4-2A	BALF C5aR1 ^{+/+}	F(3,31)=1.132	0.3512	ns				
4-2B	Alveolar macrophages C5aR1 ^{+/+}	F(3,31)=0.793	0.5073	ns				
Not shown	Total cell numbers lung C5aR ^{+/+}	F(3,28)=2.388	0.0901	ns				
4-3A	Pulmonary macrophages C5aR1 ^{+/+}	F(3,29)=3.885	0.0189	*	CT9 vs. CT15	-851500	-1570459 to -132541	*
4-3B	CD11b ⁺ cDCs C5aR1 ^{+/+}	F(3,29)=4.489	0.0105	*	CT3 vs. CT15	88050	8809 to 167300	*
					CT3 vs. CT21	81810	10940 to 152700	*
4-3C	Eosinophils C5aR1 ^{+/+}	F(3,29)=2.529	0.0767	ns				
4-3D	CD103 ⁺ cDCs C5aR1 ^{+/+}	F(3,29)=2.688	0.0648	ns				
Not shown	BALF C5aR1 ^{-/-}	F(3,32)=0.303	0.8227	ns				
Not shown	Total cell numbers lung C5aR1 ^{-/-}	F(3,32)=0.170	0.9160	ns				
Not shown	Alveolar macrophages C5aR1 ^{-/-}	F(3,32)=0.547	0.6536	ns				
4-6A	Pulmonary macrophages C5aR1 ^{-/-}	F(3,32)=0.311	0.8176	ns				
4-6B	CD11b ⁺ cDCs C5aR1 ^{-/-}	F(3,32)=5.653	0.0032	**	CT3 vs. CT15	63800	9078 to 118522	*
					CT9 vs. CT15	72183	17461 to 126906	**
4-6C	Eosinophils C5aR1 ^{-/-}	F(3,32)=5.417	0.0040	**	CT3 vs. CT15	126590	16193 to 236987	*
					CT9 vs. CT15	137810	27413 to 248207	**
4-6D	CD103 ⁺ cDCs C5aR1 ^{-/-}	F(3,32)=0.415	0.7436	ns				
4-8A	Alveolar Macrophages	F(3,36)=4.869	0.0059	**	ZT3 (PBS) vs. ZT15 (HDM)	48450	8842 to 88060	*

7 Appendix

					ZT3 (HDM) vs. ZT15 (HDM)	39190	3762 to 74620	*
4-8B	Alveolar Eosinophils	F(3,35)=2.008	0.1308	ns				
4-8C	Alveolar Neutrophils	F(3,36)=5.723	0.0026	**	ZT3(PBS) vs. ZT15(HDM)	-30670	-53510 to -7827	**
					ZT15 (PBS) vs. ZT15 (HDM)	-27480	-50320 to -4643	*
4-8D	Alveolar T cells	F(3,36)=2.770	0.0556	ns				
4-9A	VEGF	F(3,13)=7.501	0.0037	**	ZT3 (PBS) vs. ZT3 (HDM)	-14.98	-29.27 to -0.6895	*
					ZT3 (PBS) vs. ZT15 (HDM)	-17.77	-32.41 to -3.129	*
					ZT3 (HDM) vs. ZT15 (PBS)	11.65	0.3518 to 22.95	*
					ZT15 (PBS) vs. ZT15 (HDM)	-14.44	-26.18 to -2.701	*
4-9B	CXCL1	F(3,19)=7.388	0.0018	**	ZT3 (PBS) vs. ZT3 (HDM)	-86.53	-145.2 to -27.90	**
					ZT3 (HDM) vs. ZT15 (PBS)	67.96	13.19 to 122.7	*
4-9C	IL-5	F(3,13)=6.099	0.0080	**	ZT3 (PBS) vs. ZT3 (HDM)	-1.252	-2.348 to -0.1565	*
					ZT3 (HDM) vs. ZT15 (PBS)	1.135	0.1858 to 2.083	*
4-9D	IL-6	F(3,19)=1.138	0.3590	ns				
4-9E	TNF- α	F(3,19)=9.855	0.0004	***	ZT3 (PBS) vs. ZT3 (HDM)	-55.96	-91.71 to -20.21	**
					ZT3 (PBS) vs. ZT15 (HDM)	-45.92	-81.67 to -10.17	**
					ZT3 (HDM) vs. ZT15 (PBS)	47.25	13.85 to 80.65	**
					ZT15 (PBS) vs. ZT15 (HDM)	-37.21	-70.61 to -3.815	*
4-10A	Lung Macrophages	F(3,36)=0.6056	0.6157	ns				
4-10B	Lung Eosinophils	F(3,36)=8.859	0.0002	***	ZT3 (PBS) vs. ZT15 (PBS)	143200	16910 to 269500	*
					ZT3 (PBS) vs. ZT15 (HDM)	131900	16610 to 247200	*
					ZT3 (HDM) vs. ZT15 (PBS)	168400	53110 to 283700	**

7 Appendix

					ZT3 (HDM) vs. ZT15 (HDM)	157100	53970 to 260200	**
4-10C	Lung Neutrophils	F(3,36)=5.468	0.0033	**	ZT3 (PBS) vs. ZT3 (HDM)	-1501000	-3002000 to -563,2	*
					ZT3 (HDM) vs. ZT15 (PBS)	1767000	266300 to 3268000	*
					ZT15 (PBS) vs. ZT15 (HDM)	-1664000	-3165000 to -163700	*
4-10D	Lung CD11b ⁺ cDCs	F(3,31)=10.60	<0.001	***	ZT3 (HDM) vs. ZT15 (PBS)	178400	92200 to 264600	***
					ZT15 (PBS) vs. ZT15 (HDM)	-104500	-185400 to -23490	**
4-10E	Lung CD103 ⁺ cDCs	F(3,31)=0.1204	0.9474	ns				
4-10F	Lung moDC	F(3,31)=11.39	<0.0001	***	ZT3 (PBS) vs. ZT15 (HDM)	-146500	-252300 to -40740	**
					ZT3 (HDM) vs. ZT15 (PBS)	147100	44300 to 249900	**
					ZT15 (PBS) vs. ZT15 (HDM)	-185300	-281800 to -88720	***
4-10G	Lung naïve T cells	F(3,36)=4.706	0.0071	**	ZT3 (HDM) vs. ZT15 (HDM)	1085000	195000 to 1975000	*
4-10H	Lung effector T cells	F(3,36)=3.430	0.0271	*	ZT3 (HDM) vs ZT15 (PBS)	122300	11870 to 232700	*
4-10I	Lung memory T cells	F(3,36)=4.600	0.0080	**	ZT3 (HDM) vs ZT15 (PBS)	266400	25070 to 507700	*
					ZT3 (HDM) vs ZT15 (HDM)	243000	27130 to 458800	*
Not shown	Lymph node naïve T cells	F(3,35)=0.2867	0.8346	ns				
Not shown	Lymph node effector T cells	F(3,35)=0.6308	0.6001	ns				
Not shown	Lymph node memory T cells	F(3,35)=0.1526	0.9273	ns				
4-15A	BALF Macrophages	F(3,29)=7.650	0.0006	***	ZT3 (PBS) vs. ZT3 (HDM)	-173791	-306563 to -41018	**
					ZT3 (PBS) vs. ZT15 (HDM)	-136400	-266236 to -6564	*
					ZT3 (HDM) vs. ZT15 (PBS)	186406	53633 to 319179	**
					ZT15 (PBS) vs. ZT15 (HDM)	-149015	-278851 to -19180	*
4-15B	BALF Eosinophils	F(3,29)=16.76	<0.0001	****	ZT3 (PBS) vs. ZT3 (HDM)	-287284	-420907 to -153660	****

7 Appendix

					ZT3 (PBS) vs. ZT15 (HDM)	-170877	-301545 to -40210	**
					ZT3 (HDM) vs. ZT15 (PBS)	287454	153831 to 421078	****
					ZT15 (PBS) vs. ZT15 (HDM)	-171048	-301716 to -40381	**
4-15C	BALF T cells	F(3,29)=13.43	<0.0001	****	ZT3 (PBS) vs. ZT3 (HDM)	-6346	-9741 to -2950	***
					ZT3 (PBS) vs. ZT15 (HDM)	-4470	-7791 to -1150	**
					ZT3 (HDM) vs. ZT15 (PBS)	6306	2911 to 9702	***
					ZT15 (PBS) vs. ZT15 (HDM)	-4431	-7752 to -1110	**
4-15D	BALF Neutrophils	F(3,29)=9.878	0.0001	***	ZT3 (PBS) vs. ZT3 (HDM)	-38005	-61065 to -14944	***
					ZT3 (HDM) vs. ZT15 (PBS)	39310	16250 to 62371	***
4-16C	Lung Macrophages	F(3,29)=9.233	0.0002	***	ZT3 (PBS) vs. ZT3 (HDM)	-924932	-1498232 to -351631	***
					ZT3 (PBS) vs. ZT15 (PBS)	-730886	-1352717 to -109054	*
					ZT3 (PBS) vs. ZT15 (HDM)	-1053496	-1639764 to -467227	***
4-16D	Lung Eosinophils	F(3,29)=2.032	0.1313	ns				
4-16E	Lung iEOS	F(3,29)=11.72	<0.0001	****	ZT3 (PBS) vs. ZT3 (HDM)	-2069320	-3522473 to -616167	**
					ZT3 (PBS) vs. ZT15 (HDM)	-2441369	-3927392 to -955345	***
					ZT3 (HDM) vs. ZT15 (PBS)	2063655	610502 to 3516808	**
					ZT15 (PBS) vs. ZT15 (HDM)	-2435704	-3921728 to -949681	***
4-16F	Lung Neutrophils	F(3,30)=3.395	0.0305	*	ZT3 (PBS) vs. ZT3 (HDM)	-1426423	-2723509 to -129336	*
4-16G	Lung CD11b ⁺ cDC	F(3,29)=9.855	0.0001	***	ZT3 (PBS) vs. ZT3 (HDM)	-192567	-316987 to -68146	**
					ZT3 (PBS) vs. ZT15 (HDM)	-170475	-297711 to -43240	**
					ZT3 (HDM) vs. ZT15 (PBS)	181385	56964 to 305806	**
					ZT15 (PBS) vs. ZT15 (HDM)	-159294	-286529 to -32059	**

7 Appendix

4-16H	Lung CD103 ⁺ cDC	F(3,29)=9.828	0.0001	***	ZT3 (PBS) vs.	-74345	-121963 to -26727	**
					ZT3 (HDM)			
					ZT3 (PBS) vs.	-83616	-132312 to -34921	***
					ZT15 (HDM)			
					ZT15 (PBS) vs.	-56080	-104775 to -7385	*
					ZT15 (HDM)			
4-16I	Lung moDC	F(3,29)=10.67	<0.0001	****	ZT3 (PBS) vs.	-181903	-308283 to -55524	**
					ZT3 (HDM)			
					ZT3 (PBS) vs.	-195513	-324751 to -66275	**
					ZT15 (HDM)			
					ZT3 (HDM) vs.	179741	53362 to 306121	**
					ZT15 (PBS)			
					ZT15 (PBS) vs.	-193351	-322589 to -64113	**
					ZT15 (HDM)			
					ZT3 (PBS) vs.	-1634972	-3147644 to -122301	*
4-18A	Lung naïve T cells	F(3,30)=3.176	0.0383	*	ZT3 (HDM)			
					ZT3 (HDM)			
4-18B	Lung effector T cells	F(3,30)=13.92	<0.0001	****	ZT3 (PBS) vs.	-1590683	-2474267 to -707099	***
					ZT3 (HDM)			
					ZT3 (PBS) vs.	-1557869	-2441453 to -674285	***
					ZT15 (HDM)			
					ZT3 (HDM) vs.	1401113	517529 to 2284697	***
					ZT15 (PBS)			
					ZT15 (PBS) vs.	-1368299	-2251883 to -484715	**
					ZT15 (HDM)			
					ZT3 (PBS) vs.	-460875	-789590 to -132160	**
4-18C	Lung memory T cells	F(3,30)=8.814	0.0004	***	ZT3 (HDM)			
					ZT3 (HDM)			
					ZT3 (PBS) vs.	-374124	-702839 to -45409	*
					ZT15 (HDM)			
					ZT3 (HDM) vs.	462126	133412 to 790841	**
					ZT15 (PBS)			
					ZT15 (PBS) vs.	-375375	-704090 to -46661	*
					ZT15 (HDM)			
4-18D	LN naïve T cells	F(3,28)=6.361	0.0020	**	ZT3 (PBS) vs.	-1000003	-1942794 to -57213	*
					ZT3 (HDM)			
					ZT3 (HDM) vs.	1150887	302625 to 1999149	**
					ZT15 (PBS)			
					ZT3 (HDM) vs.	986313	216528 to 1756098	**
					ZT15 (HDM)			
					ZT3 (PBS) vs.	-148722	-288727 to -8717	*
4-18E	LN effector T cells	F(3,28)=6.201	0.0023	**	ZT3 (HDM)			
					ZT3 (HDM)			
					ZT3 (HDM) vs.	176746	50778 to 302713	**
					ZT15 (PBS)			
					ZT3 (HDM) vs.	132032	17718 to 246345	*
					ZT15 (HDM)			
					ZT15 (HDM)			

7 Appendix

4-18F	LN memory T cells	F(3,28)=4.948	0.0070	**	ZT3 (PBS) vs.	-54727	-104164 to -5290	*
					ZT3 (HDM)			
					ZT3 (HDM) vs.	52763	8282 to 97243	*
					ZT15 (PBS)			
Not shown	effector T cells for ICS	F(3,8)=1.249	0.2719	ns				
4-22A	VEGF	F(3,19)=2.265	0.1138	ns				
4-22B	CXCL1	F(3,19)=23.01	<0.0001	****	ZT3 (PBS) vs.	-141.7	-200.3 to -83.14	***
					ZT3 (HDM)			
					ZT3 (PBS) vs.	-94.66	-153.3 to -36.07	**
					ZT15 (HDM)			
					ZT3 (HDM) vs.	147.0	84.32 to 209.8	***
					ZT15 (PBS)			
					ZT15 (PBS) vs.	-99.98	-162.7 to -37.26	**
					ZT15 (HDM)			
4-22C	IL-5	F(3,19)=9.534	0.0005	***	ZT3 (PBS) vs.	-3.638	-6.108 to -1.168	**
					ZT3 (HDM)			
					ZT3 (PBS) vs.	-3.224	-5.694 to -0.7542	**
					ZT15 (HDM)			
					ZT3 (HDM) vs.	3.594	0.9502 to 6.238	**
					ZT15 (PBS)			
					ZT15 (PBS) vs.	-3.180	-5.824 to -0.5363	*
					ZT15 (HDM)			
4-22D	IL-10	F(3,19)=7.039	0.0023	**	ZT3 (PBS) vs.	-4.400	-7.676 to -1.125	**
					ZT3 (HDM)			
					ZT3 (HDM) vs.	4.791	1.284 to 8.297	**
					ZT15 (PBS)			
					ZT3 (HDM) vs.	2.996	0.006383 to 5.986	*
					ZT15 (HDM)			
4-22E	TNF- α	F(3,19)=4.154	0.0202	*	ZT3 (HDM) vs.	2.323	0.4572 to 4.189	*
					ZT15 (PBS)			

7 Appendix

Table 7-3: Detailed overview about statistical tests - Comparison of more than two groups with two independent variables

Graph	Title	Mixed ANOVA: one within-subjects (W) and one between-subjects variable (B) two-way ANOVA: two between-subjects variables (B1 and B2)			Tukey's post-hoc multiple comparison test # Bonferroni posttest			
		F(df _{numerator} ,df _{denominator}) =F-value	p-value	Sign. level	Compared parameters	Mean difference	95%-confidence interval	Sign. level
Not shown	BALF C5aR1 ^{+/+} vs C5aR1 ^{-/-}	B1: genetic background F (1, 63) = 2,538 B2: time F (3, 63) = 1,023	0.1161 0.3887	ns ns				
Not shown	Alveolar Macrophages C5aR1 ^{+/+} vs C5aR1 ^{-/-}	B1: genetic background F (1, 63) = 1,446 B2: time F (3, 63) = 1,059	0.2336 0.3731	ns ns				
Not shown	Total lung cells C5aR1 ^{+/+} vs C5aR1 ^{-/-}	B1: genetic background F (1, 60) = 0,5068 B2: time F (3, 60) = 0,8528	0.4793 0.4706	ns ns				
4-7A	Macrophages C5aR1 ^{+/+} vs C5aR1 ^{-/-}	B1: genetic background F (1, 61) = 16,10 B2: time F (3, 61) = 2,229	0.0002 0.0938	*** ns	CT15# C5aR1 ^{+/+} vs. C5aR1 ^{-/-} CT21# C5aR1 ^{+/+} vs. C5aR1 ^{-/-}	857393 640043	222506 to 1492281 72182 to 1207904	** *
4-7B	Eosinophils C5aR1 ^{+/+} vs C5aR1 ^{-/-}	B1: genetic background F (1, 61) = 0,5486 B2: time F (3, 61) = 5,072	0.4617 0.0034	ns **				
4-7C	CD11b ⁺ cDCs C5aR1 ^{+/+} vs C5aR1 ^{-/-}	B1: genetic background F (1, 61) = 1,404 B2: time F (3, 61) = 7,995	0.2406 0.0001	ns ***				
4-7D	CD103 ⁺ cDCs C5aR1 ^{+/+} vs C5aR1 ^{-/-}	B1: genetic background F (1, 61) = 16,09 B2: time F (3, 61) = 1,885	0.0002 0.1416	*** ns	CT21# C5aR1 ^{+/+} vs. C5aR1 ^{-/-}	17268	6707 to 27828	***
4-12A	Total activity (24h)	W: treatment F (3, 7) = 4,815 B: time F (2,835, 19,84) = 14,44	0.0399 <0.001	* ****	PBS ZT3 Pre-Treatment vs. Week 1 Week 2 vs. Week 3 HDM ZT3 Week 1 vs. Week 4 Week 2 vs. Week 4 HDM ZT15	-0,6697 0,1514 0,4554 0,5427	-0,7151 to -0,6244 0,1403 to 0,1626 0,08318 to 0,8276 0,1517 to 0,9337	* * * *

7 Appendix

					Pre-Treatment vs. Week 2	-0,7757	-1,504 to -0,04756	*
4-12B	Light activity (rest phase)	W: treatment			PBS ZT3			
		F (3, 7) = 0,3962	0.7600	ns	Pre-Treatment vs. Week 1	-0,09726	-0,1755 to -0,01905	*
		B: time			HDM ZT3	0,09782	0,07228 to 0,1234	**
		F (1,564, 10,95) = 13,46	0.0017	**	Week 3 vs. Week 4			
					PBS ZT15			*
					Pre-Treatment vs. Week 1	-0,06223	-0,1080 to -0,01645	
4-12C	Pre-Treatment ZT3	W: treatment						
		F (1, 33) = 0,0001597	0.9900	ns				
		B: time						
		F (7,422, 2,449) = 53,82	<0.0001	****				
4-12D	Pre-Treatment ZT15	W: treatment						
		F (1, 27) = 0,01255	0.9116	ns				
		B: time						
		F (7,244, 195,6) = 62,04	<0.0001	****				
4-12E	Week1 ZT3	W: treatment			PBS vs HDM			
		F (1, 40) = 10,19	0.0027	**	ZT17	0,1115	0,05134 to 0,1716	
		B: time			ZT4	0,08420	0,02111 to 0,1473	***
		F (5,589, 223,6) = 102,7	<0.0001	****				**
4-12F	Week1 ZT15	W: treatment						
		F (1, 33) = 0,5922	0.4470	ns				
		B: time						
		F (5,168, 170,6) = 68,93	<0.0001	****				
4-12G	Week2 ZT3	W: treatment			PBS vs. HDM			
		F (1, 40) = 15,60	0.0003	***	ZT17	0,08749	0,02100 to 0,1540	**
		B: time			ZT4	0,07463	0,005138 to 0,1441	*
		F (6,565, 262,6) = 67,17	<0.0001	****				
4-12H	Week2 ZT15	W: treatment			PBS vs. HDM			
		F (1, 33) = 5,371	0.0268	*	ZT18	-0,1042	-0,1762 to -0,03221	**
		B: time			ZT19	-0,1035	-0,1653 to -0,04178	***
		F (7,714, 254,6) = 53,19	<0.0001	****	ZT20	-0,1125	-0,1719 to -0,05309	***
4-12I	Week3 ZT3	W: treatment			PBS vs. HDM			
		F (1, 40) = 19,58	<0.0001	****	ZT5	0,07380	0,03723 to 0,1104	***
		B: time			ZT17	0,07902	0,007533 to 0,1505	*
		F (5,928, 237,1) = 36,34	<0.0001	****	ZT4	0,08779	0,002485 to 0,1731	*
4-12J	Week3 ZT15	W: treatment			PBS vs. HDM			
		F (1, 33) = 20,79	<0.0001	****	ZT5	0,05674	0,003289 to 0,1102	*
		B: time			ZT17	-0,09961	-0,1695 to -0,02968	***
		F (7,921, 261,4) = 30,07	<0.0001	****	ZT18	-0,1518	-0,2235 to -0,08008	***
					ZT19	-0,1667	-0,2378 to -0,09566	***

7 Appendix

				ZT20	-0,1114	-0,1954 to -0,02748	**	
				ZT21	-0,1283	-0,2260 to -0,03059	**	
				ZT22	-0,09633	-0,1750 to -0,01767	**	
4-12K	Week4 ZT3	W: treatment F (1, 16) = 9,038 B: time F (5,227, 83,63) = 15,67	0.0084 <0.0001	** ****				
4-12L	Week4 ZT15	W: treatment F (1, 13) = 5,561 B: time F (5,473, 71,15) = 7,991	0.0347 <0.0001	* ****	PBS vs. HDM ZT17 ZT18 ZT19	-0,1177 -0,1826 -0,1617	-0,2225 to -0,01292 -0,2704 to -0,09483 -0,2854 to -0,03796	* *** **
4-13	Total activity ZT12-17	W: treatment F (1, 54) = 12,11 B: time F (2,637, 105,5) = 24,82	0.0010 <0.0001	*** ****	HDM ZT3 vs. HDM ZT15 Week 2 Week 3 Week 4	-292850 -697407 -649861	-567323 to -18377 -1040960 to -353854 -1145006 to -154716	* *** **
4-14A	Airway Resistance*	W: dose F (2,292, 61,89) = 35,07 B: treatment F (3, 30) = 6,945	<0.0001 0.0011	**** **	5 mg/mL HDM ZT3 vs. PBS ZT3 10 mg/mL HDM ZT15 vs. PBS ZT3 25 mg/mL HDM ZT3 vs. PBS ZT3 HDM ZT15 vs. PBS ZT3 50 mg/mL HDM ZT3 vs. PBS ZT3 HDM ZT15 vs. PBS ZT3 W: treatment F (3, 30) = 6,945 B: dose F (2,292, 61,89) = 35,07	1.882 9.414 11.98 9.030 10.10 10.13	0.2899 to 3.473 0.7345 to 18.09 3.008 to 20.96 2.325 to 15.74 0.2920 to 19.90 3.278 to 16.98	* * * ** * ** * * * * * * * *
				HDM ZT3 0 vs. 2.5 mg/ml 0 vs. 5 mg/mL 2.5 vs. 25 mg/mL 2.5 vs. 50 mg/mL 2.5 vs. 10 mg/mL 2.5 vs. 25 mg/mL 2.5 vs. 50 mg/mL 5 vs. 25 mg/mL 5 vs. 50 mg/mL	-0.6204 -2.722 -14.82 -15.31 -10.06 -14.20 -14.69 -12.10 -12.59	-1.149 to -0.09197 -4.581 to -0.8632 -24.83 to -4.814 -25.70 to -4.929 -18.49 to -1.639 -23.30 to -5.097 -28.94 to -0.4449 -22.94 to -1.260 -23.61 to -1.570	* ** ** ** * ** * * *	
				HDM ZT15 0 vs. 2.5 mg/ml	-0.5977	-1.116 to -0.07953	*	

7 Appendix

					0 vs. 5 mg/mL	-2.752	-4.979 to -0.5252	*
					0 vs. 10 mg/mL	-11.41	-21.09 to -1.721	*
					0 vs. 25 mg/mL	-11.97	-19.60 to -4.337	**
					0 vs. 50 mg/mL	-15.45	-22.19 to -8.705	***
					2.5 vs. 10 mg/mL	-10.81	-19.79 to -1.828	*
					2.5 vs. 25 mg/mL	-11.37	-18.26 to -4.478	**
					2.5 vs. 50 mg/mL	-14.85	-22.00 to -7.704	**
					5 vs. 25 mg/mL	-9.217	-17.50 to -0.9339	*
					5 vs. 50 mg/mL	-12.70	-19.95 to -5.444	**
					PBS ZT3			
					0 vs. 5 mg/mL	-0.9471	-1.624 to -0.2699	*
					0 vs. 10 mg/mL	-1.997	-3.648 to -0.3463	*
					0 vs. 25 mg/mL	-2.942	-4.922 to -0.9624	**
					PBS ZT15			
					0 vs. 10 mg/ml	-3.449	-5.450 to -1.447	**
					0 vs. 25 mg/mL	-7.521	-14.97 to -0.07502	*
					0 vs. 50 mg/mL	-9.344	-18.50 to -0.1861	*
					2.5 vs. 10 mg/mL	-2.906	-4.931 to -0.8808	*
					5 vs. 10 mg/mL	-1.747	-3.282 to -0.2124	*
4-14B	Relative Resistance*	W: treatment			HDM ZT3			
		F (1, 18) = 6,594	0.0194	*	0 vs. 25 mg/mL	-290.4	-544.6 to -36.16	*
		B: dose			0 vs. 50 mg/mL	-148.4	-292.5 to -4.291	*
		F (1,548, 25,07) = 8,517	0.0029	**	2.5 vs. 10 mg/mL	-278.1	-543.3 to -12.76	*
					2.5 vs. 25 mg/mL	-289.6	-505.8 to -73.48	*
		W: dose			25 mg/mL #			
		F (1,548, 25,07) = 8,517	0.0029	**	HDM ZT3 vs.	247.9	4.727 to 491.0	*
		B: treatment			HDM ZT15			
		F (1, 18) = 6,594	0.0194	*				

7.2 List of abbreviations

AHR	Airway Hyperresponsiveness
AP1	Activator protein 1
ARNTL	Aryl hydrocarbon receptor nuclear translocator-like protein 1
BALF	Bronchoalveolar lavage fluid
BMAL1	Brain and Muscle ARNT-like 1
BNC	Basonuclin
C5L2	C5a receptor-like 2
CCL	Chemokine (C-C motif) ligand
cDC	Conventional dendritic cell
cDC1	CD103 ⁺ cDC
cDC2	CD11b ⁺ cDC
CET	Central European Time
CLOCK	Circadian Locomotor Output Cycles Kaput
CRP	C-reactive protein
CRY	Cryptochrome gene
CT	Circadian time
CTLA	Cytotoxic T-lymphocyte-associated protein
CXCL	C-X-C motif ligand
DAMP	Danger-associated molecular pattern
DC	Dendritic cell
E4BP4	E4 binding protein 4

7 Appendix

EAE	Experimental autoimmune encephalomyelitis
EEG	Electroencephalogram
EMG	Submental electromyogram
EOG	Electro-oculogram
EPO	Erythropoietin
Flt3L	FMS-like tyrosine kinase 3 ligand
FMO	Fluorescence minus one
FOXO	Forkhead box protein O
FoxP3	Forkhead box P3
GM-CSF	Granulocyte-macrophage colony-stimulating factor
HDM	House dust mite
ICS	Intra-cellular staining
iEOS	inflammatory eosinophils
IL	Interleukin
ILC2	Type 2 innate lymphoid cells
Ig	Immunoglobulin
INF	Interferon
<i>i.p.</i>	Intra peritoneal
<i>i.t.</i>	Intra tracheal
KC/GRO	Keratinocyte chemoattractant/human growth-regulated oncogene
KLRC2	killer cell lectin-like receptor subfamily C, member 2
KO	Knock-out (here: CX3CR1 ^{GFP/+} C5aR1 ^{-/-} mouse strain)
LD	Light-dark

7 Appendix

LPS	Lipopolysaccharides
MAC	Membrane attack complex
MASP	MBL-associated serine protease
MBL	Mannose-binding lectin
MCP	Monocyte attracting proteins
MD2	Myeloid differentiation protein
MDP	Macrophage DC progenitor
MHC	Major histocompatibility complex
miR	Micro-RNA
MMP	matrix metalloproteinase
moDC	Monocytic origin dendritic cell
NF- κ B	nuclear factor 'kappa-light-chain-enhancer' of activated B-cells
p.	page
PAMP	Pathogen associated molecular pattern
PAR-2	Protease-activated receptor-2
PMA	Phorbol 12-myristate 13-acetate
PPAR- γ	Peroxisome proliferator-activated receptor gamma
PRM	Pattern recognition molecule
PRR	Pattern recognition receptor
qPCR	Quantitative PCR
resp.	respectively
ROR α	RAR-related orphan receptor alpha
ROR γ t	RAR-related orphan receptor gamma isoform 2
ROS	Reactive oxygen species

7 Appendix

RT-PCR	Real time polymerase chain reaction
SCN	Suprachiasmatic nucleus
SD	Standard deviation
sog.	sogenannten
ST	Synchronization time
SEM	Standard error of mean
Stat	Signal transducer and activator of transcription
T-bet	T-box transcription factor TBX21
TCR	T cell receptor
TGF- β	Transforming growth factor beta
TIMP	Tissue inhibitor of metalloproteinase 3
TLR	Toll-like receptor
TNF	Tumor necrosis factor
TSLP	thymic stromal lymphopoietin
UVB	ultraviolet light type B
VEGF-A	vascular endothelial growth-factor A
VIP	Vasoactive intestinal peptide
Wk	Weeks
WT	Wild type
ZT	Zeitgeber Time

7.3 List of figures

Figure 2-1: Immunopathology of allergic asthma	12
Figure 2-2: Differentiation of CD4⁺ T cells	15
Figure 2-3: Distribution of pulmonary APCs	21
Figure 2-4: The complement cascade	25
Figure 2-5: The mammalian molecular clock.	29
Figure 2-6: The molecular clock in asthma development.	33
Figure 3-1: Steady-state analysis of circadian rhythms in pulmonary APCs	50
Figure 3-2: Reading an actogram	51
Figure 3-3: Immunization of mice	52
Figure 3-4: One-step immunization model	53
Figure 3-5: Four-step immunization model	54
Figure 3-6: Bronchoalveolar lavage, lymph node and lung removal	56
Figure 3-7: Gating strategies for lung cell and BALF suspensions	61
Figure 3-8: Gating strategy for intracellular stained T cells	66
Figure 3-9: Calculation of mucus area in lung histological slides	70
Figure 3-10: Overview about statistical methods	71
Figure 4-1: Activity levels of C5aR1^{+/+} WT mice	73
Figure 4-2: Alveolar macrophages do not fluctuate in a circadian manner.	74
Figure 4-3: Pulmonary macrophages and cDC2 cells fluctuate over 24h in C5aR1^{+/+} WT mice.	75

Figure 4-4: Activity levels in C5aR1^{-/-} mice.....	76
Figure 4-5: C5ar1^{+/+} and C5ar1^{-/-} mice exert a similar circadian activity.....	76
Figure 4-6: Pulmonary cDC2 cells and eosinophils fluctuate in C5aR1^{-/-} mice over 24h.	78
Figure 4-7: Macrophage and cDC1 numbers differ between C5aR1^{+/+} and C5aR1^{-/-} mice.	79
Figure 4-8: Strong increase in neutrophil numbers after HDM immunization during the activity phase at ZT15	81
Figure 4-9: HDM stimulation during the activity or resting phase results in increased levels of proinflammatory cytokines in the airways	82
Figure 4-10: Pulmonary cell distribution in response to HDM immunization during the activity or the resting phase.....	85
Figure 4-11: Repeated HDM administration alters the sleep-wake cycle	87
Figure 4-12: Opposing effects of HDM-treatment during the activity or resting phase on the overall activity level.....	91
Figure 4-13: Higher total activity during the activity phase in mice treated with HDM at ZT15 compared with ZT3.....	92
Figure 4-14: The relative increase in airway resistance is higher after immunization at ZT3 than at ZT15	94
Figure 4-15: Airway immune cell distribution after repeated HDM immunization at ZT3 or ZT15.....	95
Figure 4-16: Recruitment of myeloid effector cells to the lung at ZT3 and ZT15	98
Figure 4-17: Gating strategy to define the different T cell subsets recruited to the lung and the draining lymph nodes at ZT3 and ZT15	100

Figure 4-18: Quantification of the different T cell subsets in the lungs and the draining lymph nodes after HDM immunization at ZT3 and ZT15	101
Figure 4-19: Increased frequency of pulmonary Th2, Th17 and Treg cells in response to HDM treatment at ZT3 and/or ZT15.	103
Figure 4-20: HDM treatment at ZT3 results in higher IL-13, IL-17 and IFN-γ production from pulmonary immune cells than HDM treatment at ZT15	104
Figure 4-21: Proinflammatory mediators in the airways after HDM treatment at ZT3 and ZT15.....	105
Figure 4-22: Increased frequency of mucus positive areas in the alveoli at ZT3	107
Figure 5-1: Impact of the circadian rhythm on airway and pulmonary inflammation in steady state and after allergen exposure.....	108
Figure 5-2: Conceptual model of the relation between allergic asthma and sleep	130

7.4 List of tables

Table 2-1: Asthma phenotypes	10
Table 3-1: Chemicals	38
Table 3-2: Antibodies used in flow cytometry and cell sorting. .	40
Table 3-3: Kits.....	41
Table 3-4: Buffers, solutions and culture mediums.....	42
Table 3-5: Consumables	43
Table 3-6: Devices.....	44
Table 3-7: Used mouse strains	46

Table 3-8: Material for the mouse keeping	46
Table 3-9: Software used for analyses.....	48
Table 3-10: Antibodies used to stain BALF cells.....	59
Table 3-11: Antibodies used to stain T cells in lung- and lymph node suspensions.....	60
Table 3-12: Antibodies used to stain neutrophils in lung- and lymph node suspensions	60
Table 3-13: Antibodies used to stain DCs in lung- and lymph node suspensions	60
Table 3-14: Characterization of T cell subsets via extra- and intracellular cytokine staining	63
Table 3-15: Scheme for preparation of the stimulation mix	64
Table 3-16: Scheme I for intracellular cytokine staining of T cells	65
Table 3-17: Scheme II for intracellular cytokine staining of T cells	65
Table 3-18: Scheme III for intracellular cytokine staining of T cells	65
Table 3-19: Detection levels for multiplex cytokine analysis	68
Table 3-20: Overview about hypotheses, the related independent and dependent variables as well as performed statistical analysis	72
Table 7-1: Detailed overview about statistical tests - Comparison of two groups with one independent variable.....	155
Table 7-2: Detailed overview about statistical tests - Comparison of more than two groups with one independent variable.....	156
Table 7-3: Detailed overview about statistical tests - Comparison of more than two groups with two independent variables	162

8 Acknowledgments

After a couple years of work, I thank all the people who support me and my dissertation project, from the first step of getting me started in the laboratory work to the final proofreading.

First, special thanks towards my supervisor Prof. Dr. Köhl, as he opened up the opportunity for me to realize my dissertation project in cooperation with his institute. I am grateful for his extraordinary support during the whole dissertation process, starting with finding a topic, through the experimental period, where I was allowed to use the laboratory's infrastructure, to reviewing my thesis.

Second, I want to thank my laboratory guide Dr. Anna Kordowski for her teaching and supervision in performing mouse experiments, analyzing and presenting data, and writing scientific reports. Thanks a lot for introducing me to research practice and guiding me through it.

Third, special thanks to Dr. Tillman Volbrandt, without whom the circadian studies would not have been possible. Dr. Volbrandt has supported me many nights in flow cytometry, conjured up cells in FlowJo, and especially for the earplugs, which made my life much easier.

Additional thanks go to the AG Chronobiology, especially to Prof. Dr. Henrik Oster. In cooperation with his institute, my dissertation project first became reality and I am grateful for all his support in the field of chronobiology. Further, I want to acknowledge Dr. Christiane Koch and Dr. Anthony Tsung here, for organizing time slots for my experiments, supporting me with activity analyses and giving me advice at any time.

I also thank the great allergic asthma team, especially Dr. Yves Laumonnier, Dr. Inken Schmudde, PhD Fanny Ender, and Anna-Valeska Wiese for the excellent collaboration. They were very supportive during my dissertation project and were always willing to help me in analyzing protocols or shared helpful tricks in the laboratory. Here, I also want to

8 Acknowledgments

thank Gabriele Köhl, Denise Theil and Esther Strerath for their excellent laboratory support.

Special thanks go to Joschka Dunkel, my 'MD buddy', who decided at the same time as me to go for an experimental dissertation project. Thanks for the daily motivational coffee break, your encouraging smile and the good morning story when entering the FACS room. I am very happy to have found a close friend in you.

I also want to thank the staff at the GTH Lübeck for mice keeping; and the anatomy institute for supporting me with the histological analysis of lung samples.

Moreover, this work would not have been possible without the financial support of the German Academic Scholarship Foundation and the German Research Foundation.

Finally, I want to thank my parents, as they supported my decision to perform an extended laboratory medical thesis from the beginning, and listened to all the challenges from the last years, even though they did not fully understand what I was talking about. A big thank goes to my sister Carolin for her great support in performing statistics, proof-reading as well as supporting me mentally during the whole process; and, of course, to my dear boyfriend Philipp and our lovely daughter Frida.

9 Curriculum vitæ



Name Julia Kilian
Date and place of birth 02.01.1992
 Altdöbern, Germany
Nationality German

Education

since 09/2020 Assistant physician in general medicine
 Medical practice Stationslægerne
 Glostrup, Denmark
 10/2014 – 06/2019 Medical study
 University of Lübeck, Germany
 Medical approbation (final grade 2,83)
 08/2016 – 06/2017 Exchange semester
 Aarhus University, Denmark
 10/2011 – 09/2014 Medical study
 University of Leipzig, Germany
 02/2012 – 06/2019 Fellow of the German National Academic
 Foundation
 06/2011 Higher education entrance qualification
 (Abitur, Final grade 1.0)
 Max-Steenbeck-Gymnasium, Cottbus, Germany

Scientific Career

04/2015 – 03/2016 Experimental MD Project at the Institute for
 Systemic Inflammation Research (ISEF), Lübeck
 about: „*The influence of the circadian rhythm on
 the development of experimental allergic asthma*“
 04/2015 – 03/2016 Fellow of the German Research Foundation (DFG)
 of the *International Research Training Group
 (IRTG) 1911*

Languages

German mother tongue
 English fluently
 Danish fluently
 French good command

Congress Contributions

Poster presentations

1. **Kilian J**, Czabanska A, Laumonnier Y, Oster H, Köhl J. The role of complement in the circadian fluctuation of pulmonary immune cells and its impact on the development of allergic asthma. *Student Retreat 'Life Sciences'*, Kiel; 2015.
2. **Kilian J**, Czabanska A, Laumonnier Y, Oster H, Köhl J. The role of complement in the circadian fluctuation of pulmonary immune cells and its impact on the development of allergic asthma. *International Symposium on Immunoregulation in Allergy and Infection*, Lübeck; 2015.
3. **Kilian J**, Czabanska A, Oster H, Köhl J. Circadian regulation of alveolar immune cells in allergic asthma. *Lower Saxony International Summer Academy in Immunology*, Hannover; 2015.
4. **Kilian J**, Kordowski A, Oster H, Köhl J. The circadian rhythm regulates pulmonary immune cell composition and the development of experimental allergic asthma. *IRTG1911 Renewal*, Lübeck; 2017.

Talks

1. **Kilian J**, Czabanska A, Laumonnier Y, Oster H, Köhl J. A strong impact of the circadian rhythm on the development of experimental allergic asthma. *Mainzer Allergy Workshop, Spring Meeting of the DGAKI*, Mainz; 2016.

Abstract

1. **Kilian J**, Czabanska A, Laumonnier Y, Köhl J, Koch C, Tsang A. C3a and C5a control central and peripheral circadian rhythms. *Immunobiology*. 2016;221:1195.

Paper

1. **Kilian J**, Kordowski A, Laumonnier Y, Oster H, Köhl J. Impact of the circadian rhythm on the development of allergic asthma. (manuscript in preparation).